NTNU

Norwegian University of
Science and Technology

Synthesis of conjugated unsaturated Amino Acids

Vanja Buvik

Chemistry
Submission date: May 2016
Supervisor: Vassilia Partali, IKJ
Co-supervisor: Hans-Richard Sliwka, IKJ

Norwegian University of Science and Technology
Department of Chemistry

Abstract

Of the three main groups of biomolecules - lipids, carbohydrates and proteins - lipids and carbohydrates containing polyene functionalities have already been investigated. This thesis describes a first approach to the synthesis of polyene amino acids. Conjugated unsaturated amino acids could be interesting building blocks for the making of novel peptides and proteins with rigid structural elements and chromophoric properties. The first L-polyene amino acid was synthesized by a Wittig reaction between a protected glutamic acid aldehyde and a triphenylphosphonium salt of a C15:3-polyene compound.

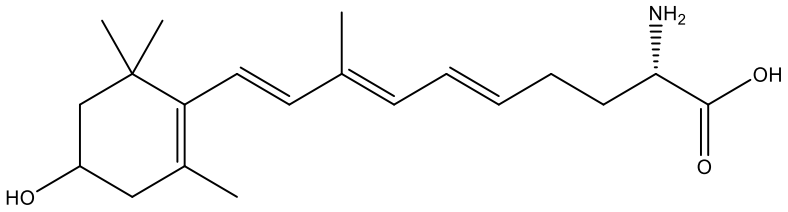

Sammendrag

Av de tre hovedgruppene av biomolekyler – lipider, karbohydrater og proteiner – har både polyen-karbohydrater og polyen-lipider allerede blitt undersøkt. Denne oppgaven beskriver en første tilnærming til syntese av en konjugert, polyenisk aminosyre. Konjugerte umettede aminosyrer er interessante med tanke på framstilling av nye peptider og proteiner med rigide strukturelementer og kromoforiske egenskaper. Den første L-polyen-aminosyren ble framstilt ved en Wittig-reaksjon mellom et beskyttet glutaminsyrealdehyd og et trifenylfosfoniumsalt av et C15:3-polyen.

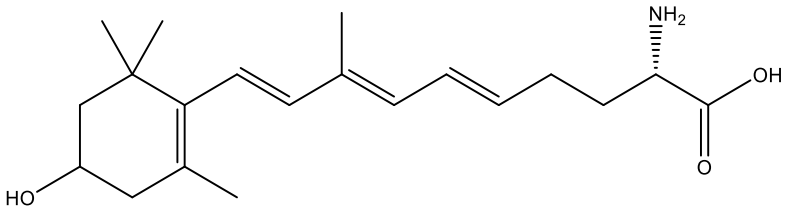

Acknowledgements

First of all I want to thank my supervisor Vassilia Partali, for giving me the opportunity to work on this thesis, but also for always having time for me, for all that she has taught me and for all the interesting conversations we had during the two years. I am equally grateful for the help from my co-supervisor, Hans-Richard Sliwka. His ability to always find solutions to problems that occur along the way has been a great help during the work for, and the writing of this thesis.

For all good advice, for teaching me techniques both regarding NMR, IR and laboratory work, I thank Melanie Siah, the best colleague and friend I could wish for. Thank you to Susana Villa Gonzales and Julie Asmussen for running my MS-samples and always patiently answering my emails and many questions. I want to thank Torun Margareta Melø for all good advice and instructions about running NMR. Thanks also to Claire Katja Peterson, for helping me in the writing process and to Josip Zecevic for helping me in the lab on long afternoons and evenings.

Thank you to all the great people in my life who support me and who make Trondheim the greatest place in the world. My family: my parents and my brother, being an inspiration in so many ways, and Mormor, who has taught me and still teaches me so much about life. Torunn who maybe knows me better than I know myself and always cheers me on. Julie, with whom I can always have a rewarding conversation or a good laugh, and all the rest of the amazing people I know here.

Table of contents

List of figures

Abbreviations

APCI	Atmospheric Pressure Chemical Ionization
aq.	aqueous
ASAP	Atmospheric Solids Analysis Probe
Boc	*tert*-Butyloxycarbonyl
CC	Column Chromatography
CD	Circular Dichroism
conc.	concentrated
DCM	Dichloromethane
DIBAL-H	Diisobutylaluminium hydride
DMS	Dimethyl sulfide
DMSO	Dimethylsulfoxide
DNA	Deoxyribonucleic acid
ESI	Electron Spray Ionization
Et_3N	Triethylamine
Et_2O	Diethyl ether
EtOAc	Ethyl acetate
EtOH	Ethanol
HSQC	Heteronuclear Single Quantum Coherence
$KN(TMS)_2$	Potassium bis(trimethylsilyl)amide
λ_{max}	wavelength of maximum absorption
M	mol per liter
MeOH	Methanol

Me_2S	Dimethylsulfide
MS	Mass Spectrometry
m/z	mass to charge ratio
NaOMe	Sodium methoxide
NBS	N-bromosuccinimide
nBuOH	n-butanol/1-butanol
NMR	Nuclear Magnetic Resonance
PG	Protective Group
Q-TOF	Quadrupole Time Of Flight mass analyser
RNA	Ribonucleic acid
sat.	Saturated
tBuOH	*tert*-butyl alcohol
THF	Tetrahydrofurane
TLC	Thin layer chromatography
UV	Ultra Violet
vis	visible

1 Introduction

Lipids, carbohydrates and proteins are the fundamental constituents of life. Lipids = fats, carbohydrates = sugars and proteins = polyamides of amino acids, are essential parts of the human diet. The emergence of amino acids from extra-terrestrial sources or by spontaneous synthesis from CO_2, CH_4, N_2 and lightning with subsequent chiral resolution by polarized sunlight (quartz or other crystals), provided the first L-amino acid enantiomer. Since the L-amino acid enantiomer is only infinitesimally more stable than the D-enantiomer[1], resolution took a historically long time. Once substantial amounts of the L-amino acid molecules were present, spontaneous assembly in amides took place, giving linear dipeptides (di-amino acid amides), tripeptides, oligopeptides and polypeptides, and finally resulted in folded and helical 3D proteins. In another primordial synthetic reaction, fragments of amino acids combined with sugars creating nucleic acids, of which DNA and RNA are well known gene carrying molecules.[2]

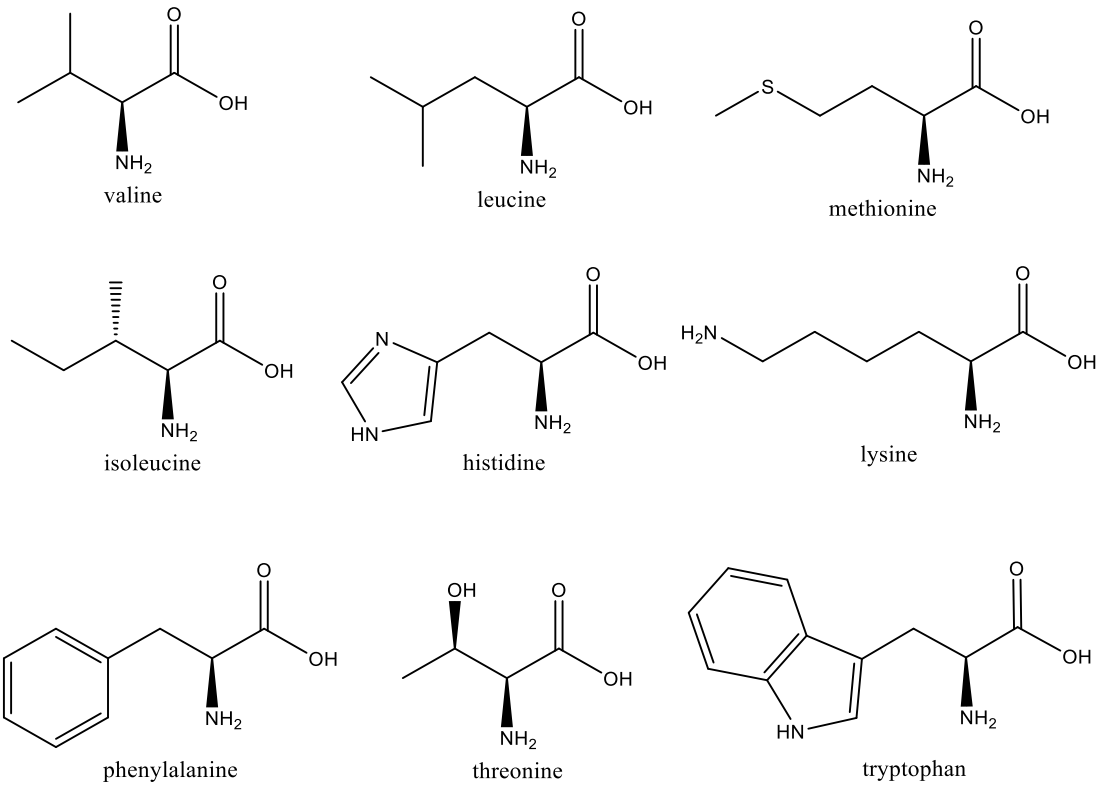

Figure 1.1: The nine essential amino acids.

Both the nine essential (Figure 1.1), the twelve non-essential (Figure 1.2) and more than 500 listed other natural amino acids[3-5] (Figure 1.3) occur as saturated amino acids, i.e. there is no

C=C double bond in the carbon chain (the C=C bonds in histidine phenylalanine, tryptophan, and tyrosine are found in ring structures).

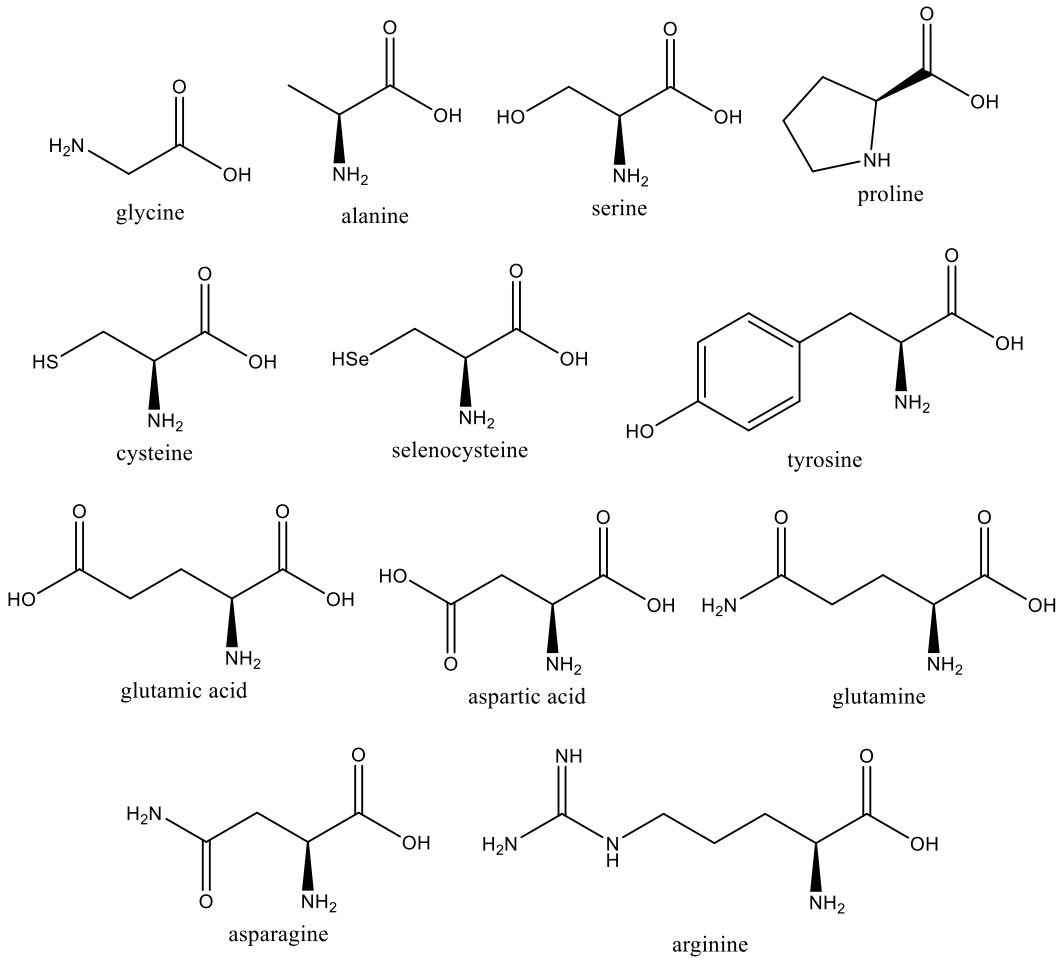

Figure 1.2: The twelve non-essential amino acids.

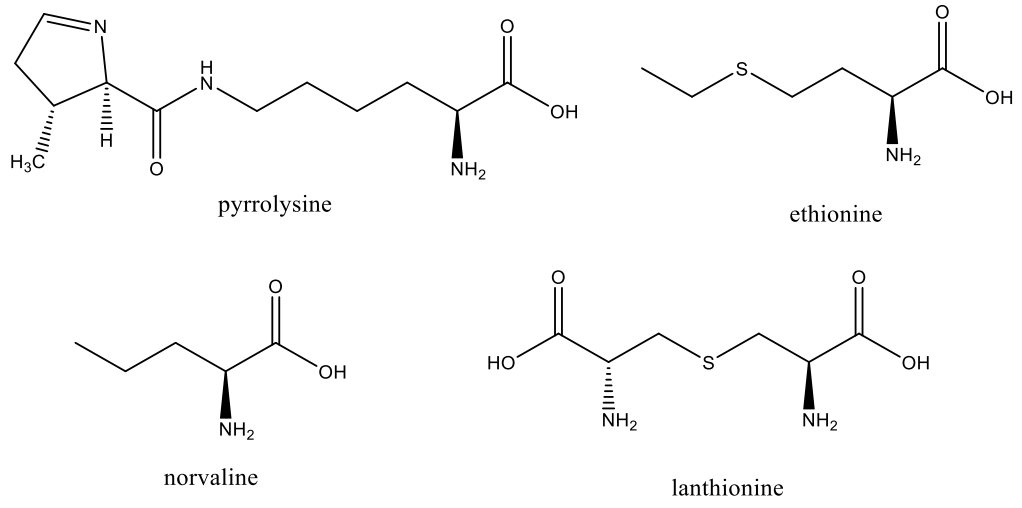

Figure 1.3: Examples of naturally occurring, non-proteinogenic amino acids.

Minimal change in amino acids can have important physiological effects. Whereas the L-enantiomer of glutamic acid (an important molecule in this thesis) is known as a flavour enhancer, the corresponding D-enantiomer shows no such effect.[6] Small structural changes in amino acids can result in novel peptides, inducing changes in proteins, enhancing or silencing physiological processes. This effect can be used in the treatment of cancer, rheumatism, cataract, arteriosclerosis and other medical conditions.[7-9]

The topic of this master thesis can be shortly expressed as "modification of an amino acid by introducing conjugated double bonds". Chains of C-C bonds are flexible, at least from a certain length, whereas conjugated poly(C=C)-chains are rigid. Peptides from polyene amino acids will maintain the rigid structures, and the corresponding proteins will contain rigid segments. It is therefore expected that polyene moieties in peptides and proteins affect the physiological impact of amino acids, peptides and proteins. Such effects can be illustrated with a lobster. In the actual world of saturated amino acids, a living lobster is dark bluish green - the colour arising from the protein complex crustacyanin, which encloses non-covalently bound astaxanthin. Boiling the lobster decomposes crustacyanin; astaxanthin (**F**, Figure 1.10) is released; and the colour of the lobster changes to orange (Figure 1.4). A lobster in a world of polyene proteins would keep the colour after cooking (Figure 1.5).[10]

Combining polyenic carotenoids and their antioxidative properties with amino acids would possibly combine the physiological effects of both compound classes.

Figure 1.4: A living lobster: dark blue, and a cooked lobster: orange.[11]

Figure 1.5: Hypothetical lobster with yellow polyene proteins; alive and cooked.[12]

Polyene amino acids are further expected to facilitate structural analyses. The optical activity of amino acids is predominantly measured by polarimetry, recording the different deviation of polarized light to $\alpha = +x^{\circ}$ or $\alpha = -x^{\circ}$. Optical investigations of saturated amino acids and proteins with circularly polarized light is only possible with expensive dichrographs, allowing measurement in the difficult to access vacuum short wavelength (UV) light[13-15] or synchrotron radiation[16, 17]. Polyene amino acids will give CD spectra in the visual absorption scale, thus facilitating determination of optical activity.

Another aspect of polyene amino acids, namely their colour, should not be underestimated for practical laboratory work. Amino acid solutions are colourless, and peptides and proteins are white. Chromatographic procedures with saturated amino acids are literally deprived of "chrome"; so detection must rely on additives or instruments. Polyene amino acids are coloured and will donate their colours to peptides and proteins. As a matter of course, visual detection facilitates handling of amino acids, peptides and proteins.

A similar effect of visual detectability was recently demonstrated by gene delivery to cancer cells with polyene modified cationic phospholipids.[18]

1.1 Amino acids

The amino acids in naturally occurring proteins are chiral compounds with identical stereochemical L-configuration. Some D-amino acids have been found in nature, but they do not form proteins. Although the “Laevus”- and “Dexter”-assignment of chirality has been mostly replaced by the R/S-system, the L/D-system still applies for sugars and amino acids (Figure 1.6). Amino acids are zwitterions, containing dual neutralizing charge at the isoelectric point (Figure 1.7).[19]

L-alanine (S) D-alanine (R)

Figure 1.6: Alanine-enantiomers.

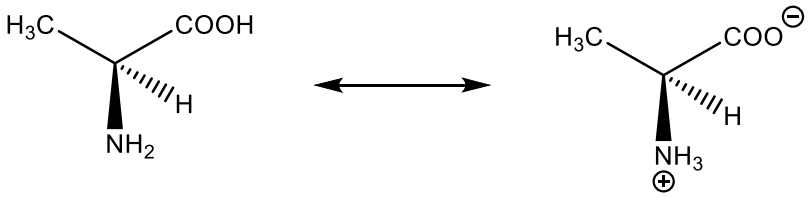

Figure 1.7: The two possible states of an amino acid at its isoelectric point.

1.2 Unsaturated amino acids

Some α,β-dehydroamino acids, deprived of a chiral C-atom, have been found in peptides of microbial origin and in some proteins (**A**, Figure 1.8).[3] Unsaturated β,γ-, γ,δ- etc. amino acids with α-chirality have been synthesized before (**B**/**C**, Figure 1.8).[20, 21] Polyunsaturated, non-conjugated L-NHBoc amino acids have also been described (**D**, Figure 1.9).[22]

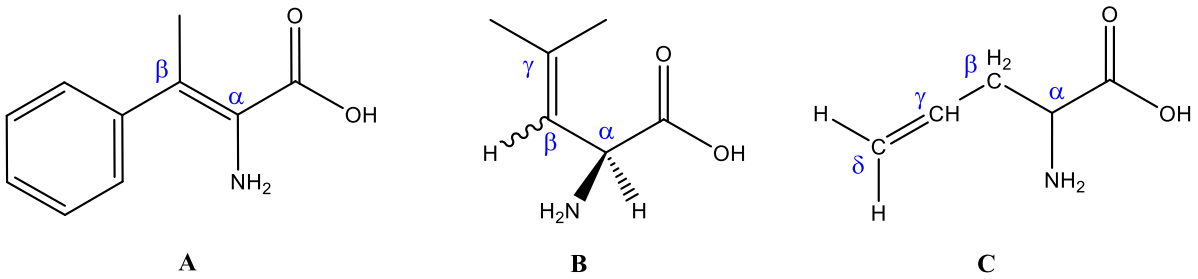

A **B** **C**

Figure 1.8: A: α,β-, B: β,γ- and C: γ,δ-unsaturated amino acid.

Polyene amino acids could be interesting building blocks in new peptides, where they could induce "β-turns", allowing modification of secondary peptide structure.[7, 23, 24]

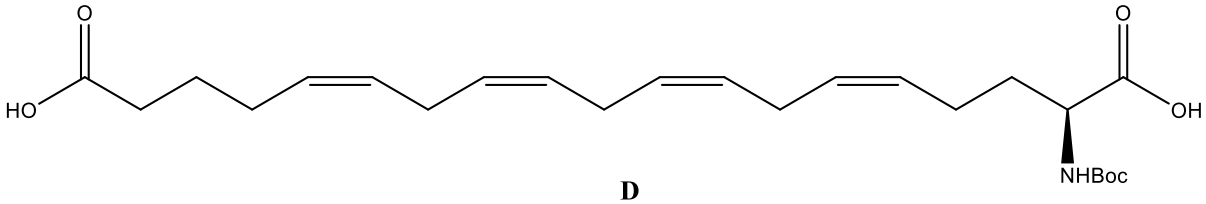

D

Figure 1.9: Unsaturated, non-conjugated tetraenic L-amino acid.

Polyene moieties in amino acids are promising biocompatible chromophore tags for structural studies using circular dichroism (CD). CD investigations have so far been mostly restricted to aromatic amino acids such as histidine, phenylalanine and tryptophan (Figure 1.1).[25, 26] CD spectra of amino acids without chromophoric groups can only be recorded at $\lambda_{max} < 190$ nm with vacuum CD-instruments.[13, 14, 27]

1.3 Carotenoids

Carotenoids are stable, naturally occurring polyenes, with β-carotene (**E**, Figure 1.10) being the name-giving compound for this series of natural products. Many carotenoids are abundantly found as pigments in fruits, vegetables, crustaceans and bird feathers, and they are produced by bacteria, plants and fungi.

β-Apo-15-carotenoids, better known as retinoids (e.g. retinol: **G**, Figure 1.10), consist of four isoprene units with 5 double bonds. Retinoids and carotenoids enhance communication between cells by inducing gap junction formation (connexin 43), they induce transmembrane transport as light-sensitive proteins in bacteria and are also essential for the proper function of most body organs.[28-32]

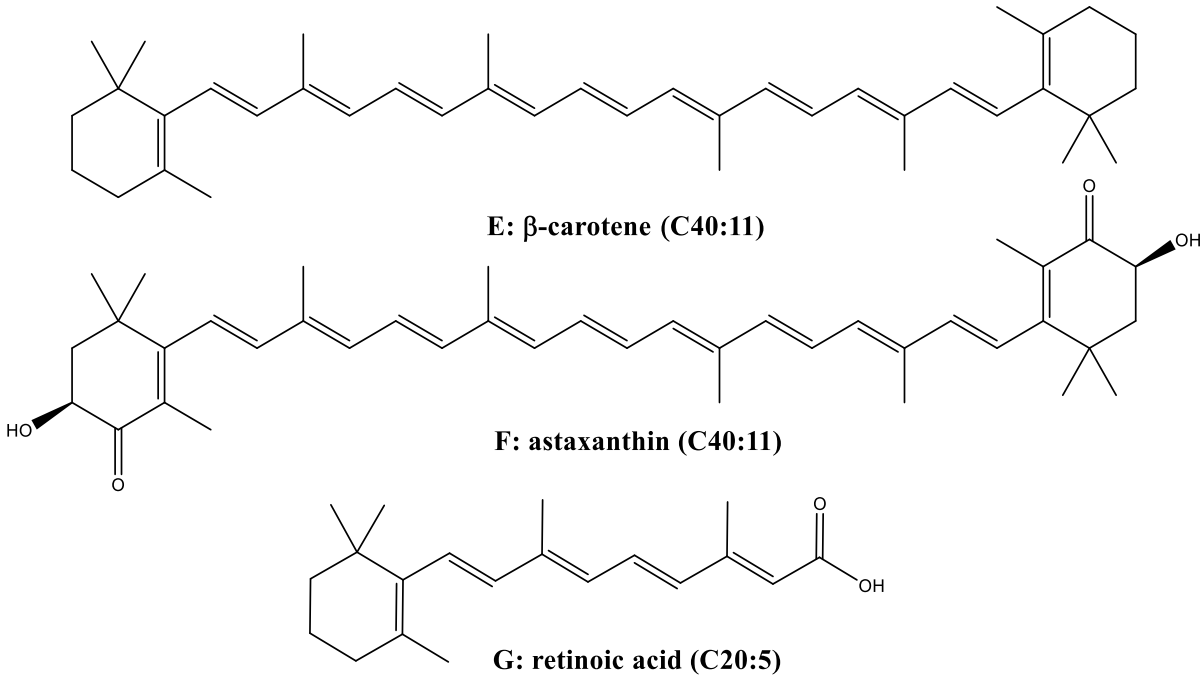

Figure 1.10: Polyenes mentioned in this thesis.

Since methyl branched stabilized polyenes such as carotenoids are available, it appeared evident to rely on carotenoids the synthesis of polyene amino acids.

1.4 Key biological compounds, polyene modified

Carbohydrates naturally occur with polyenes. Crocin (**H**, Figure 1.11) from saffron is the most sold polyene sugar.[33]

Carotenoid modified lipids have so far not been detected in nature. Carotenoid diglycerides (**I**, Figure 1.11) and carotenoid phospholipids[18, 34] have been synthesized.[35]

Polyene modified amino acid and subsequent peptides and proteins have not been found in nature.

The synthesis of the first polyene amino acid (**G**, Figure 1.11) is the topic of this thesis.

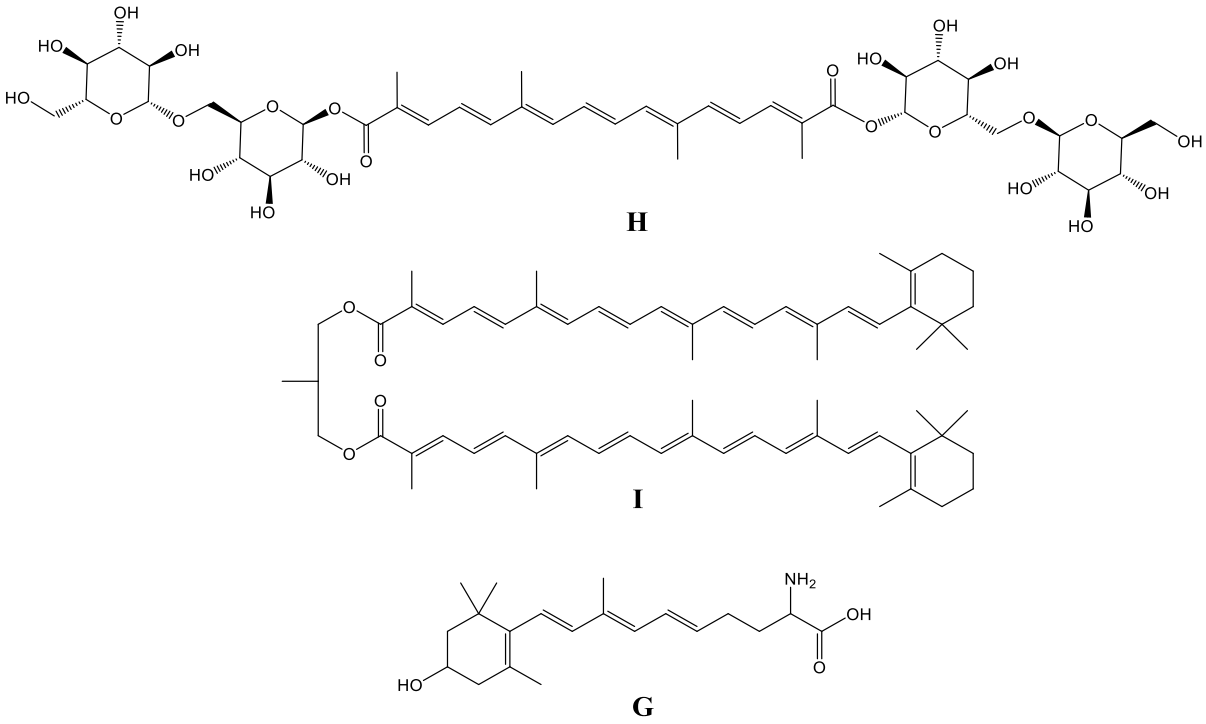

Figure 1.11: Key biological compounds, polyene modified. Crocin H, polyene diglyceride I and polyene amino acid G (this work).

2 Results and discussion

2.1 Strategies

An established method for synthesizing α-amino acids is the Strecker-reaction[36, 37], developed by Adolph Strecker in Kristiania 1854.[38] It requires a rather acidic milieu for the hydrolysis of the α-aminonitrile intermediate - conditions that were likely to affect the π-bonds of unsaturated compounds. The Strecker reaction was therefore not regarded as a realistic option. Two obvious approaches lend themselves for the synthesis of polyene amino acids:

1. Adding an amino acid function to a polyene.

   Polyene + N-functionality → polyene-N-acid

2. Adding a polyene chain to an amino acid.

   N-acid + polyene → polyene-N-acid

2.2 Addition of amino acid function to a polyene

The prominent example for this approach is the Bucherer-Bergs reaction[39], in which:

1. An aldehyde is reacted with HCN to a cyanohydrin.
2. The cyanohydrin reacts with ammonium carbonate to a hydantoin[40]. The hydantoin is hydrolysed with K_2CO_3/H_2O to the α-amino acid salt, which after acidifying delivers the amino acid.

The Bucherer-Berg reaction is used by Evonik in the industrial synthesis of L-methionine with yields over 90%.[19, 41, 42] It was therefore apparent to apply this well-tried method for the synthesis of polyene amino acids. Before launching the method with a polyenic aldehyde, the synthesis was tested with a saturated aldehyde.

Dodecanal (**1**) was reacted in a Bucherer-Bergs reaction as described by Tellier et al.[43] and Šmit et al.[41]. 5-Undecylimidazolidine-2,4-dione (**2**) was obtained, purified by recrystallization to a white powder in 23% yield and characterized by NMR and MS (Scheme 2.1).

Undecylhydantoin **2** was then hydrolysed with $Ba(OH)_2$ resulting in racemic amino acid **3** giving a positive ninhydrin test upon neutralization.[44] High hygroscopicity of the amino acid prevented characterization of the compound by routine NMR methods, but MS studies confirmed the presence of 2-aminotridecanoic acid (**3**) in 55% yield (Scheme 2.2).

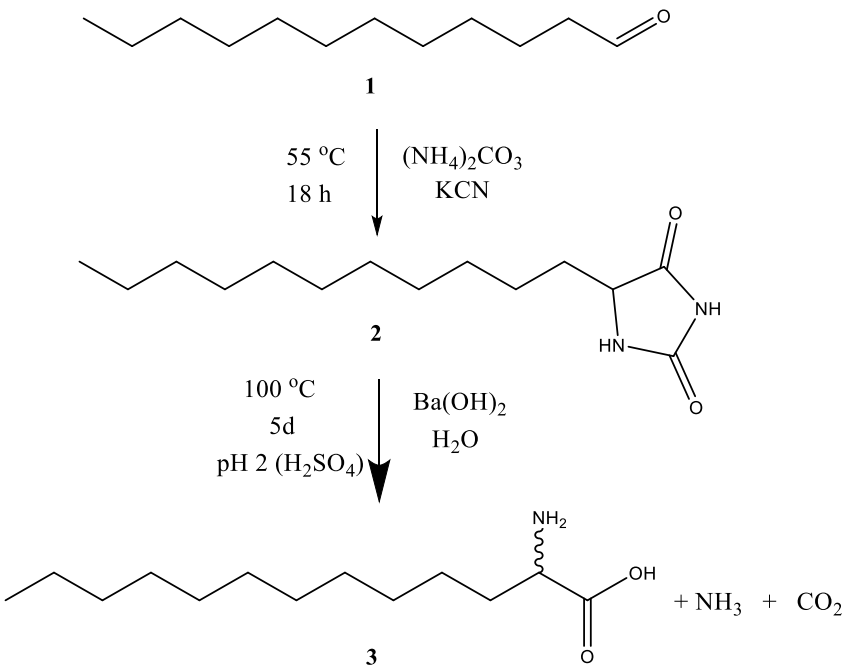

Scheme 2.1: Test reaction with a saturated aldehyde to hydantoin and amino acid.

Based on the successful synthesis with a saturated aldehyde, dodecanal (**1**) was replaced with carotenal **4** (C30:9 apocarotenal, BASF) and treated with KCN and $(NH_4)_2CO_3$ (Scheme 2.2).

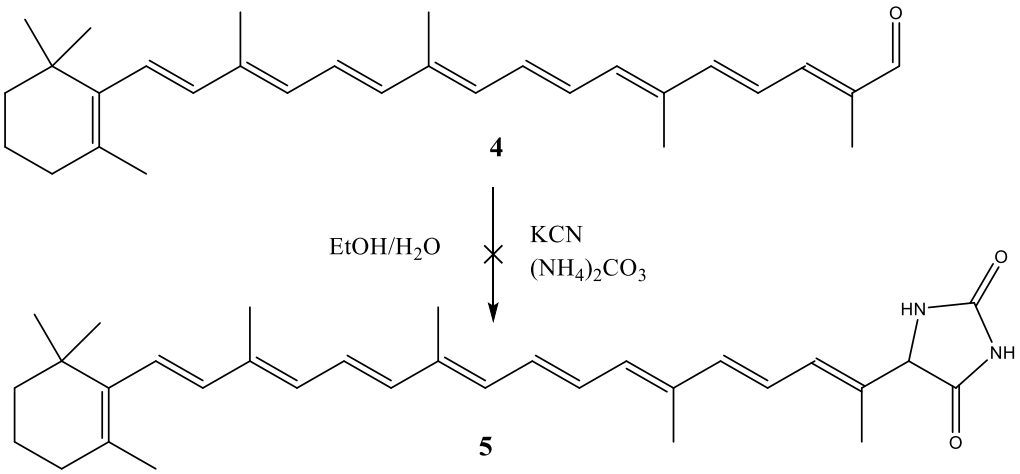

Scheme 2.2: Attempted Bucherer-Berg reaction with polyene aldehyde.

No hydantoin **5** was formed and synthetic strategy 1 (polyene + N-acid → polyene-N-acid) was therefore abandoned.

2.3 Addition of the polyene to an amino acid

Synthetic strategy 2 now became necessary. Although established (industrial) examples are missing, strategy 2 has the advantage of relying on a predefined enantiomeric amino acid fragment.

L-glutamic acid was selected as a starting compound. It was anticipated that the less hindered γ-acid group could be converted to an aldehyde function, which then would react with an appropriate polyenic Wittig salt to L-amino acid C35N:10 **6** (Figure 2.1).

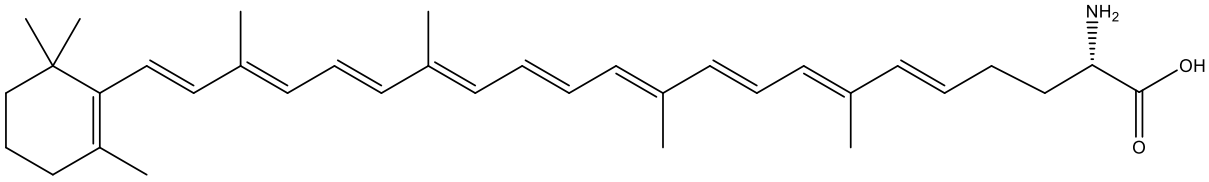

6

Figure 2.1: L-amino acid C35N:10

The challenges were:

1. Synthesis of an L-glutamic acid aldehyde **7**
2. Synthesis of a polyene Wittig salt **8**

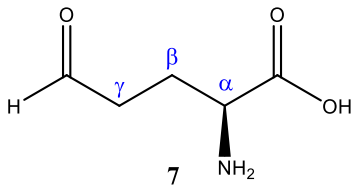

7

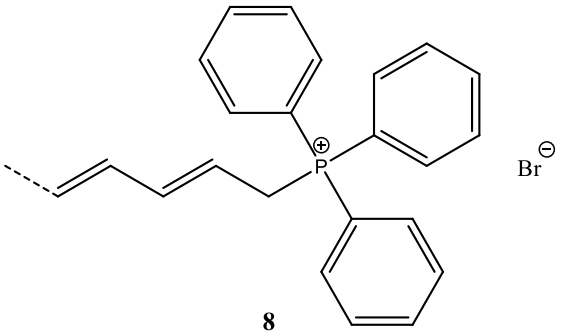

8

Figure 2.2: L-glutamic acid aldehyde 7 and polyene Wittig salt 8.

Working with amino acids requires protection of the functional units that are not desired to participate in the reaction.[45] All reactive functions of glutamic acid can be protected in a one-pot synthesis with benzyl (Bn) bromide, analogical to the method of Rodriquez et al.[46]. One site would then be deprotected and reduced to the aldehyde. As Bn-deprotection did not work as expected, methyl ester- and *tert*-butyloxycarbonyl were employed with good results. Selective reduction of the γ-ester group gave the desired aldehyde **15** in good yields.

2.3.1 Synthesis of L-glutamic acid aldehyde

1. Protection
2. Reduction and oxidation

2.3.1.1 Synthesis of dibenzyl N,N-dibenzyl-L-glutamate

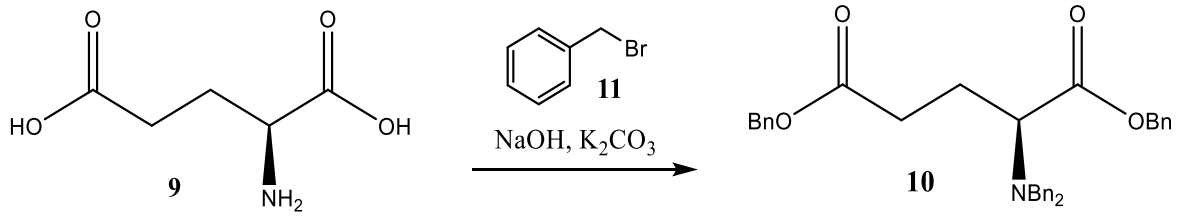

Scheme 2.3: One-pot benzyl-protection of L-glutamic acid.

The reactive OH and NH_2 groups of L-glutamic acid were reacted with benzyl bromide.[46] Compared with methods with several steps and different protective groups, this seemed like an easy approach. In the method analogous to of Rodriquez et al. tetrabenzyl glutamate **10** was isolated as a yellow oil in 57% yield and characterized by NMR and MS.

2.3.1.2 Attempted synthesis of benzyl (*S*) 2-(dibenzylamino)-5-hydroxypentanoate

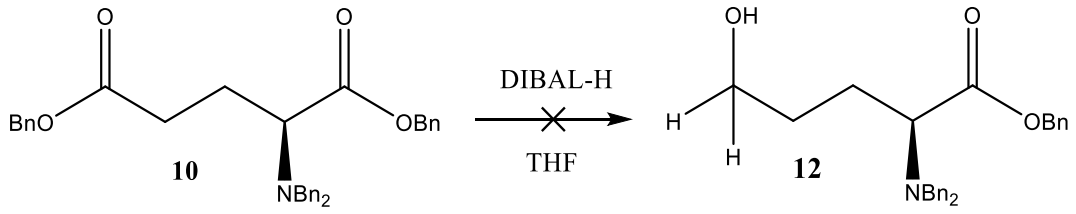

Scheme 2.4: Attempted deprotection of γ-ester group with DIBAL-H.

Attempts to reduce the less sterically hindered site of benzyl ester **10** to the alcohol **12** failed regardless when performed at -78 ^{0}C, 0 ^{0}C and room temperature.

2.3.1.3 Synthesis of dimethyl (*tert*-butoxycarbonyl)-L-glutamate

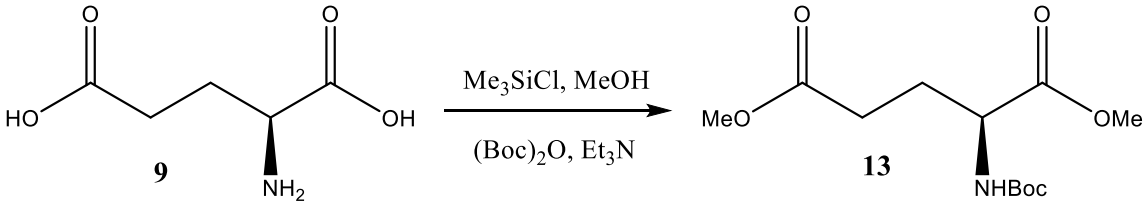

Scheme 2.5: Partial protection of L-glutamic acid with methyl ester- and Boc-PG.

The amino group in L-glutamic acid (**9**) was selectively reacted with *tert*-butyloxycarbonyl-(Boc) and the carboxylic acid group with methyl ester-PG, analogous to Padrón et al.[47] Dimethyl mono-Boc glutamate **13** was isolated as a light yellow oil in 70% yield. The product was characterized by NMR and MS.

2.3.1.4 Synthesis of dimethyl di(tert-butoxycarbonyl)-L-glutamate

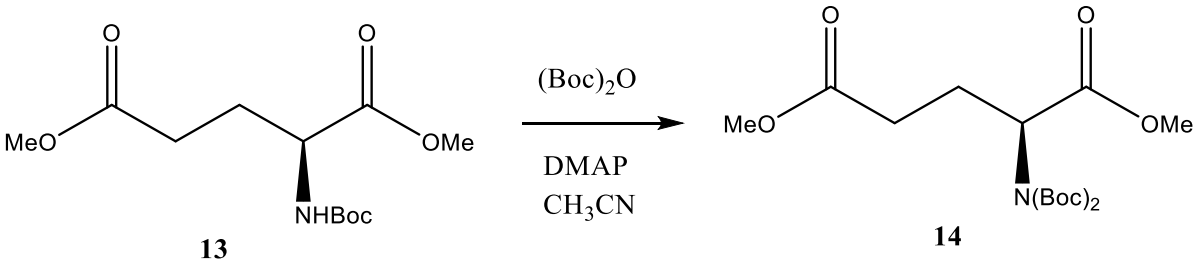

Scheme 2.6: Protection of mono-Boc 13 to di-Boc 14.

Dimethyl mono-Boc glutamate **13** was reacted with $(Boc)_2O$ and DMAP to catalyse the reaction. Dimethyl di-Boc-glutamate **14** was isolated as a light yellow oil in 86% yield followed by characterization by NMR and MS.[47]

2.3.1.5 Reduction of dimethyl di(*tert*-butoxycarbonyl)-L-glutamate

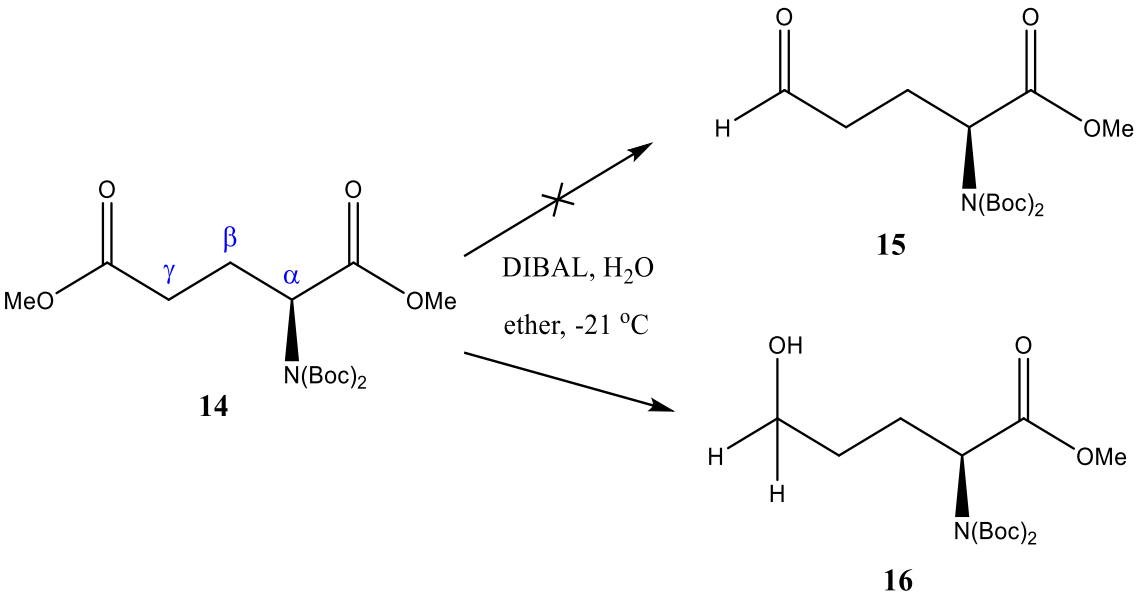

Scheme 2.7: Reduction of one ester unit of fully protected L-glutamic acid.

A selective reduction of the γ-ester group of **14** to aldehyde **15** was not possible. The reduction with diisobutyl aluminium hydride (DIBAL-H) hardly stopped at the aldehyde stage even with short reaction time, in variance with a previously described procedure.[47] Alcohol **16** was always obtained regardless of the reaction conditions of -78 ^{0}C, -10 ^{0}C and reaction times varying between 5 min and 24 h (see Table 1). Three compounds were isolated at the end of reduction in most cases: non-converted educt, an alcohol as a main product and small amounts of aldehyde. The products were characterized by MS and NMR.

The direct reduction to **15** turned out to be impractical. Therefore, **14** was selectively reduced to alcohol **16**, as described by Rodriquez et al.[46], using higher temperature and different reaction times. **16** was isolated as a colourless oil.

	Temperature [^{0}C]	Reaction time	Alcohol (%)	Aldehyde (%)
1	-78	5 min	33	17
2	-78	24 h	40	0
3	-78-rt	5 h	54	0
4	-21	5 min	47	0
5	-10	1 h	69	0

Table 2.1: Alcohol 16 and aldehyde 15 relation after reduction of 14.

2.3.1.6 Synthesis of methyl (2*S*)-2-[bis(*tert*-butoxycarbonyl)amino]-5-oxopentanoate

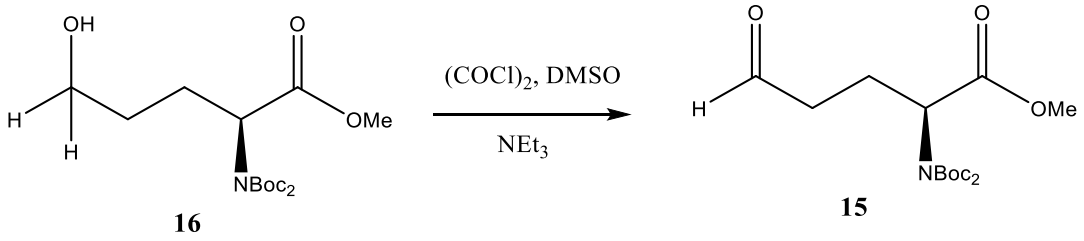

Scheme 2.8: Oxidation of glutamic acid alcohol to its aldehyde.

A Swern oxidation[48] was performed with alcohol **16** according to Rodriquez et al.[46] Aldehyde **15** was obtained as a white solid in 58% yield, characterized by NMR and MS.

2.3.2 Synthesis of polyene Wittig salt

1. Reduction to –OH
2. Replacement of –OH with –Br
3. Formation of triphenylphosphonium salt

2.3.2.1 Synthesis of 8'-apo-β-caroten-8'-ol

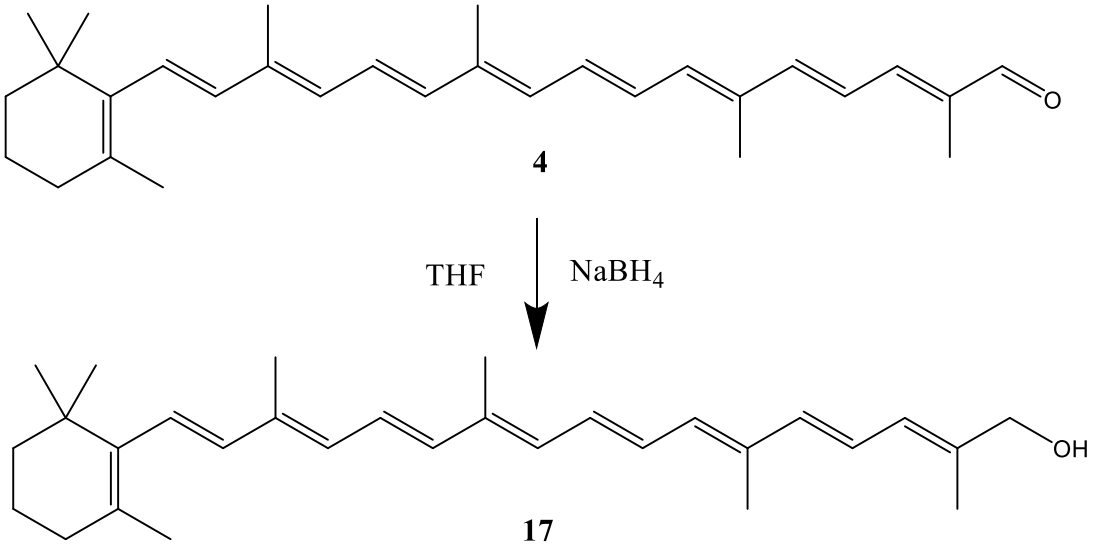

Scheme 2.9: Reduction of carotenal 4 to carotenol 17.

Carotenal **4** was reduced to carotenal **17** according to Haugan.[49] Alcohol **17** resulted as a lighter red powder than aldehyde **4**, in 55% yield. The product was characterized by UV/vis, MS and NMR. The first attempts to perform the reduction using non-dry THF or MeOH were not successful. The use of a dry solvent appeared to be crucial.

2.3.2.2 Attempted synthesis of β-apo-8'-bromocarotene and 8'-apo-β-caroten-8'-triphenylphosphine bromide

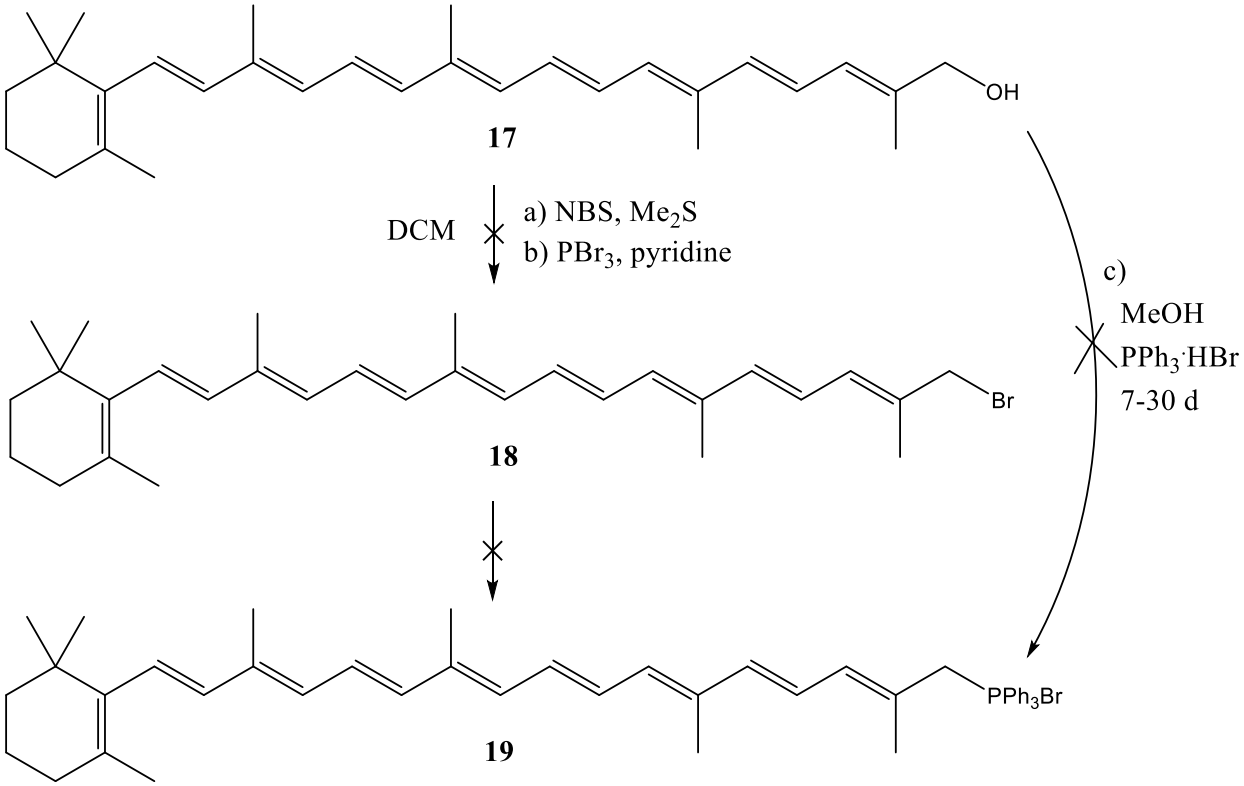

Scheme 2.10: Attempted synthesis of a polyene Wittig salt.

When alcohol **17** was brominated according to reactions a)[49] and b)[50], bromide **18** was not obtained, in accordance with observations in a previous master thesis[51]. Likewise, the direct one-pot reaction c)[50] of carotenol **17** to phosphonium salt **19** with $PPh_3 \cdot HBr$ failed.

Since the preparation of polyene bromide **18** was not possible and consequently triphenylphosphonium salt **19** could not be obtained, the synthesis of a long polyene amino acid with ten double bonds was abandoned. The reaction with a triene Wittig salt was envisaged.

2.3.3 Wittig reaction with a triene phosphonium salt

When the Wittig reaction between protected glutamic aldehyde acid **15** and Wittig salt C15Zea-P **22** (BASF) was performed, the amino acid L-C20N:4 **25** was obtained.

2.3.3.1 Synthesis of C20:4-N-diBoc-methylester 25

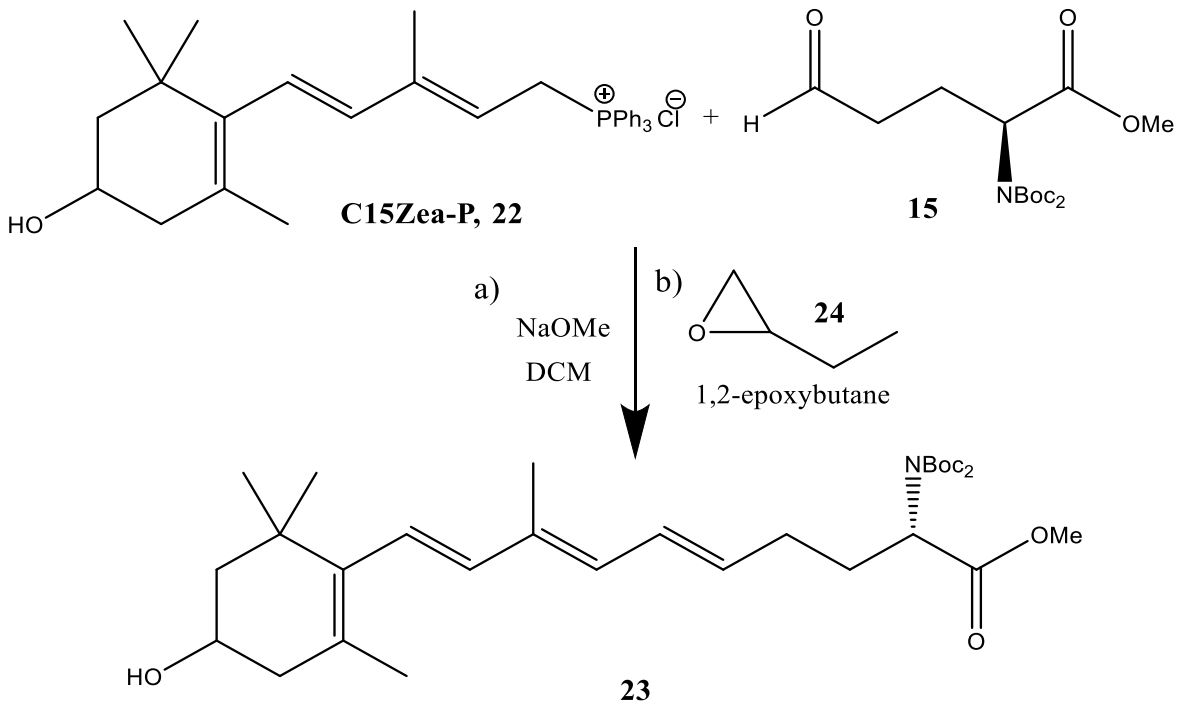

Scheme 2.11: Wittig reaction between C15Zea-P and aldehyde 15.

The Wittig salt C15Zea-P **22** (provided by BASF) was coupled to aldehyde **15** using sodium methoxide in reaction a), analogous to Yamano et al.[52], giving di-Boc methyl ester **23** as a yellow oil in 61% yield. Reaction b) with 1,2-epoxybutane[53] gave **23** in 51% yield.

23 was characterized by NMR and MS.

2.3.3.2 Synthesis of L-C20N:4 by deprotection of di-Boc methylester 23

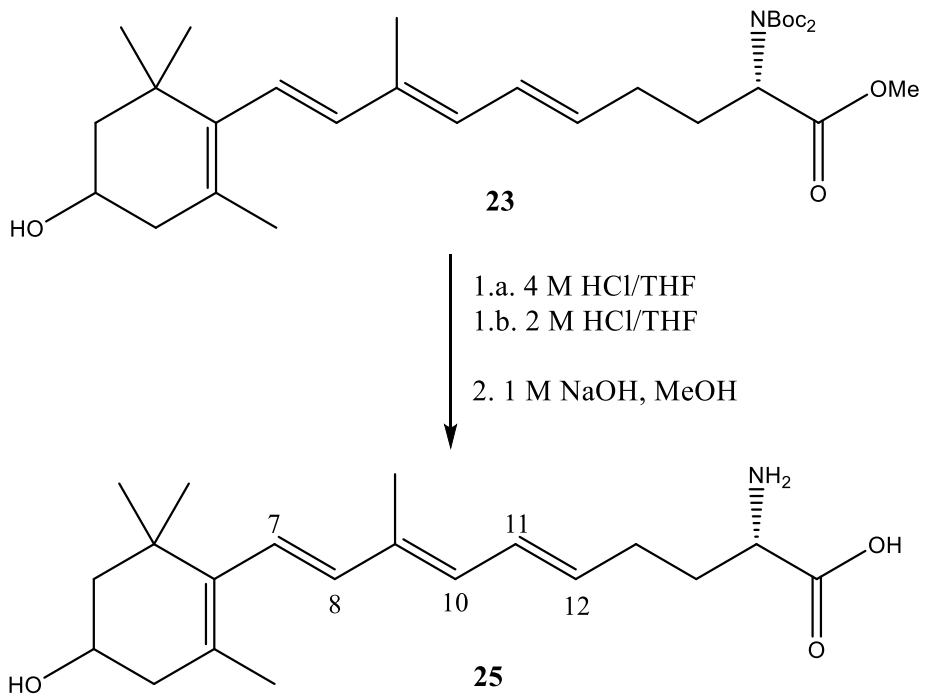

Scheme 2.12: Synthesis of polyene amino acid by removal of protective groups from amino acid moiety.

Deprotection of di-Boc methylester **23** was assumed to be the crucial step because of acidic conditions that could disrupt the polyene moiety.[47] However, both 4 M and 2 M HCl in THF removed Boc, leaving the polyene chain intact. When 4 M HCl was used, 1 out of 4 experiments were successful, with 2 M 1 out of 3 experiments gave **25**.

A yellow powder precipitated upon neutralization. The presence of the amino unit in **25** was proven with the ninhydrin test. Purification by flash column chromatography or TLC led to considerable loss of product, reducing the yield to 0.002%. It was not possible to remove the contaminants from the precipitate with water. MS identified the characteristic m/z of C20 polyene amino acid **25** and NMR confirmed the presence of characteristic shifts of **25** despite of high hygroscopicity. UV/vis of **25** in DCM λ_{max} = 275 nm (Figure 2.3), confirmed the presence of conjugated double bonds. Although the absorption maximum is slightly lower than what could be expected, HSQC-NMR (Figure 2.4) confirms the presence of five protons coupling to carbon atoms in a conjugated system, indicating a triene chain.

Due to problems with the CD instrument, no CD could be recorded in the scope of this thesis.

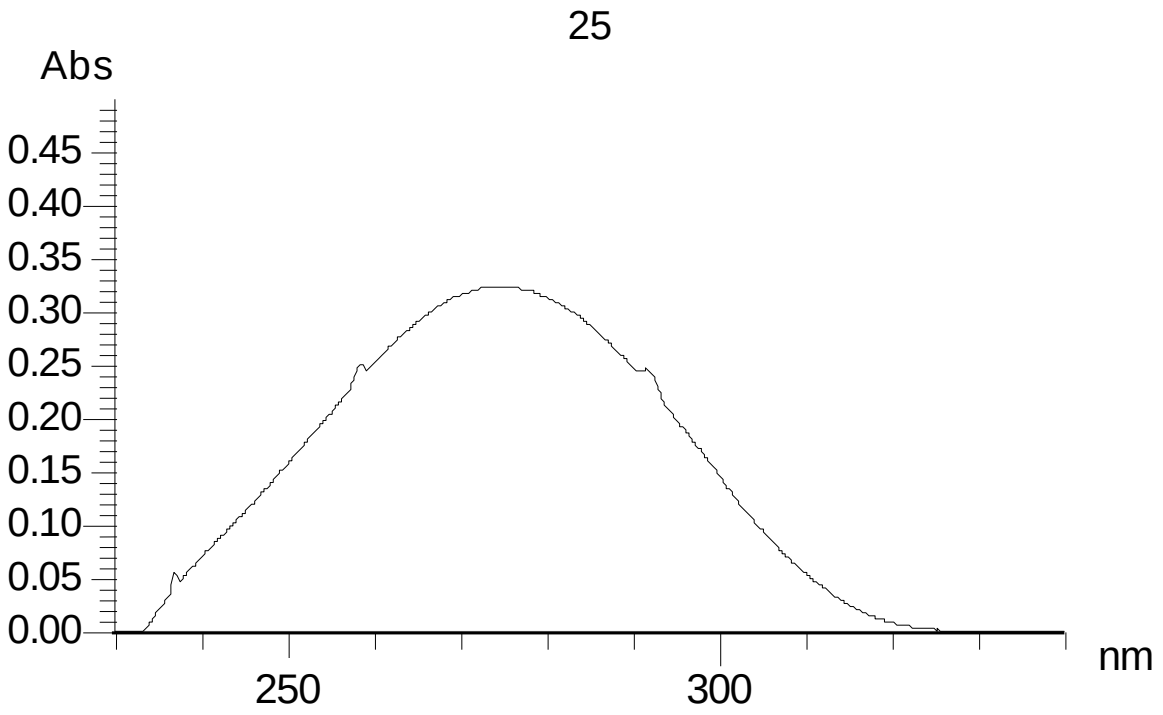

Figure 2.3: UV/vis absorption spectre of L-C20N:4

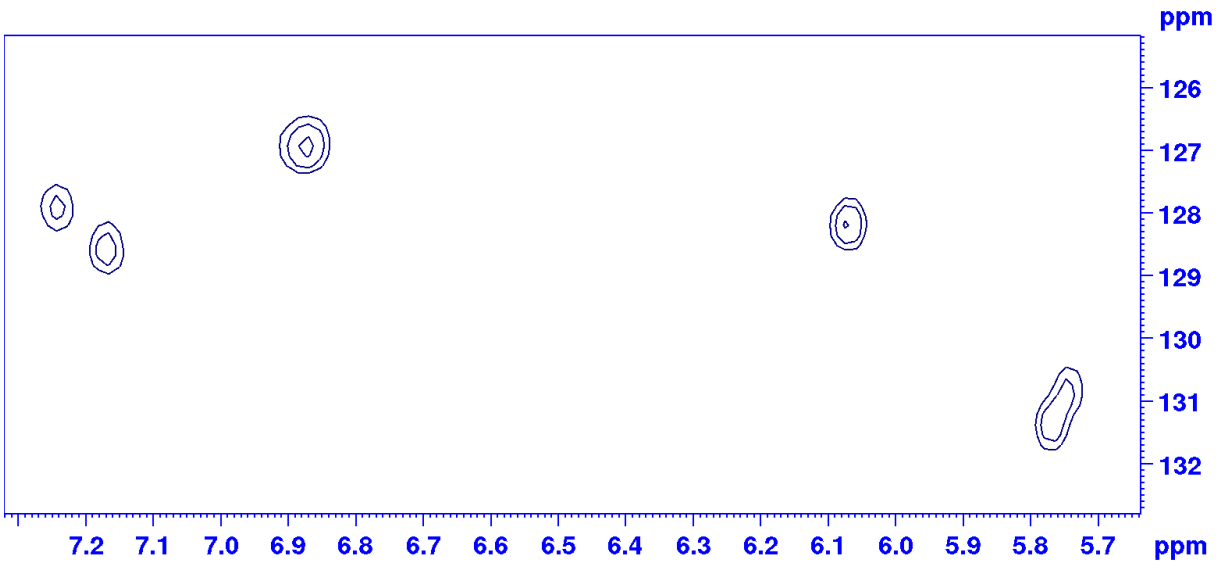

Figure 2.4: Excerpt of HSQC-NMR of 25, indicating olefinic proton signals from C7, C8, C10, C11 and C12.

3 Molecular models of L-20N:4

Like other amino acids, **25** can be present without (Figure 3.1) or with dual intrinsic charge (Figure 3.2) at its isoelectric point. The exchangeable protons of the amino and carboxylic acid group make the interpretation of NMR-spectra challenging.

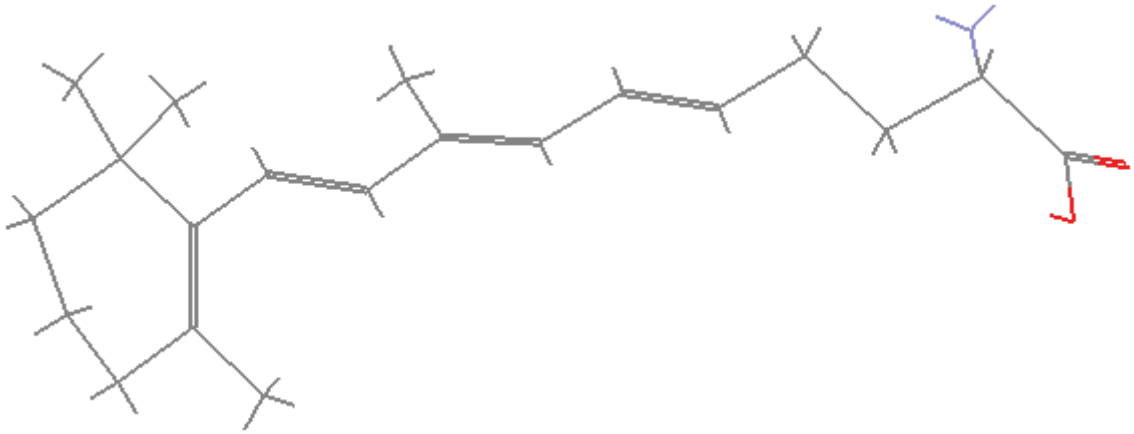

Figure 3.1: Molecular model of 25 at its isoelectric point without charge.

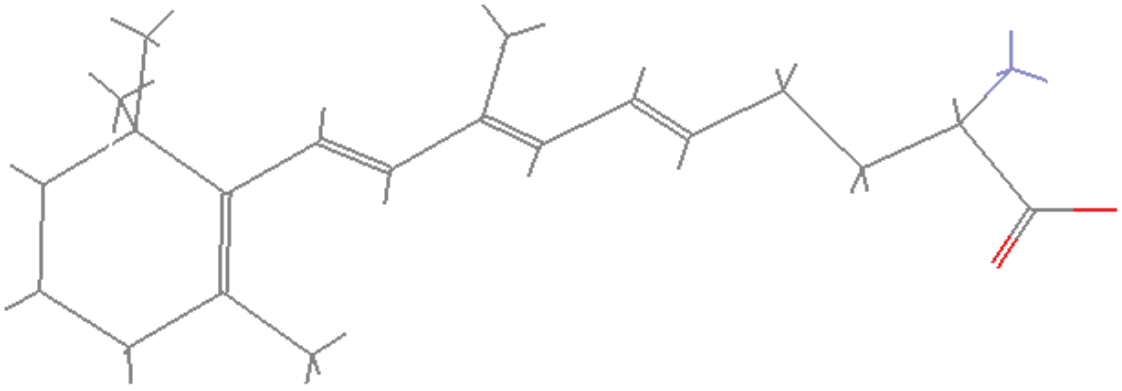

Figure 3.2: Molecular model of 25 at its isoelectric point with dual charge.

4 Future aspects

The synthesis of polyene amino acid **25** was based on the synthesized aldehyde di-Boc precursor **15**, which reacted with predefined Wittig salt **22**. The conditions for the Wittig reaction, using NaOMe or 1,2-epoxybutane, gave good yields and were compatible with the short polyene applied.

A challenge encountered in the work for this master thesis was the synthesis of a polyene triphenylphosphonium salt. Instead of preparing a polyene Wittig salt, a Wittig salt could be prepared from the amino acid that is then coupled to an available polyene aldehyde.

4.1 Triphenyl phosphonium salt of glutamic acid

In the future, the Wittig salt of the amino acid precursor **27** could be prepared from protected alcohol **16**, via bromide **26**, which then reacts with carotenal **4** from BASF. The synthesis of Wittig salt **27** from glutamic acid via bromide **26** is more likely to succeed than the unsuccessful synthesis of polyene Wittig salt **19** via bromide **18**. (Scheme 4.1)

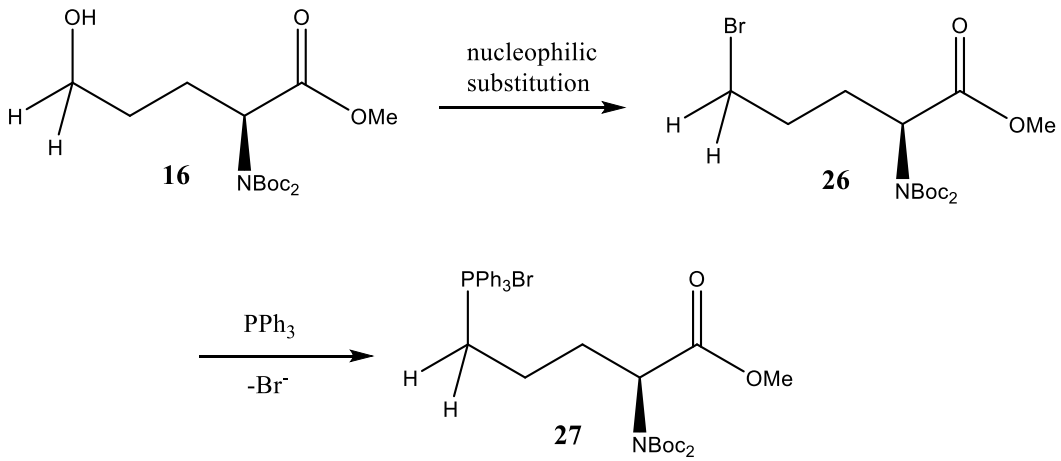

Scheme 4.1: Preparation of phosphonium salt.

The Wittig reaction between **4** and **27** to C35N:10-di-Boc **28** (Scheme 4.2) could be performed either using NaOMe, or 1,2-epoxybutane in analogy to Scheme 2.11. Deprotection conditions could rely on the tested reaction with 2 M HCl/THF (Scheme 2.12).

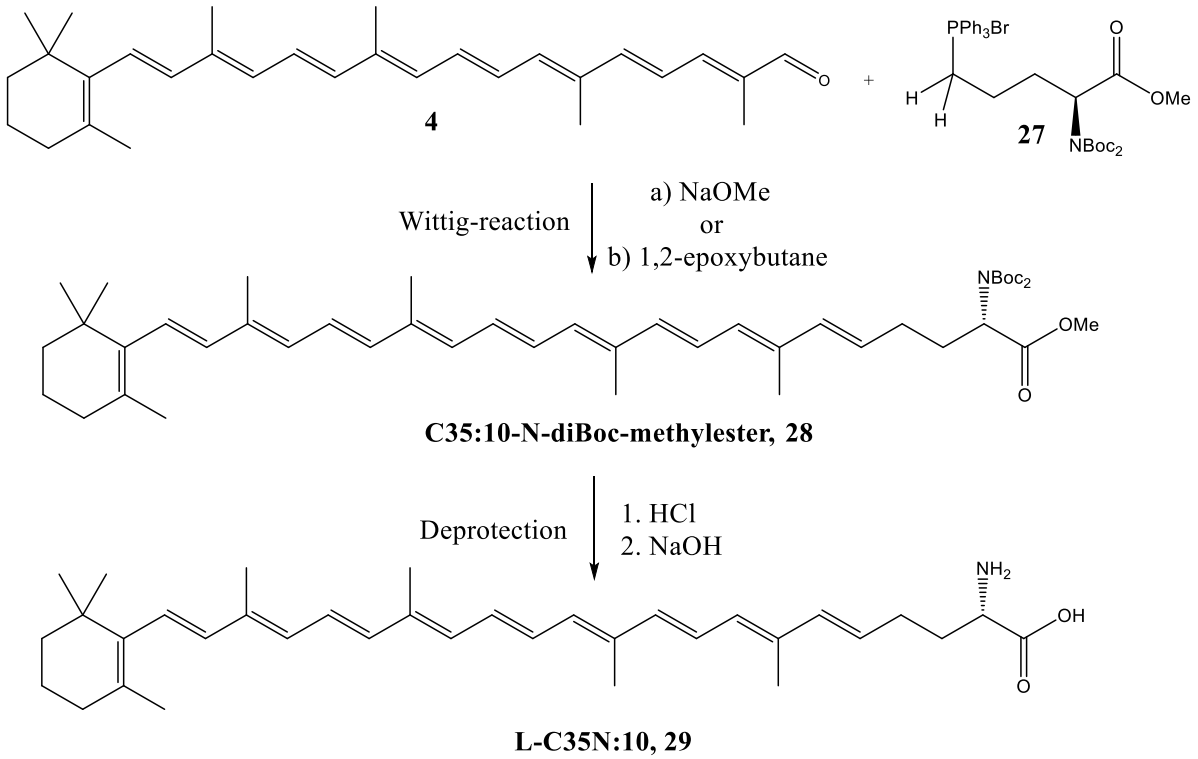

Scheme 4.2: Wittig reaction with glutamic acid phosphonium salt and 8'-apo-β-caroten-8'-al.

4.2 Deprotection of glutamic acid before Wittig reaction

Another suggestion for future studies would be to remove the protective groups before the Wittig reaction. The challenge of the deprotection without polyene disruption can thereby be avoided. Wittig salt **27** is synthesized as described and then deprotected under acidic followed by alkali conditions (Scheme 4.3).

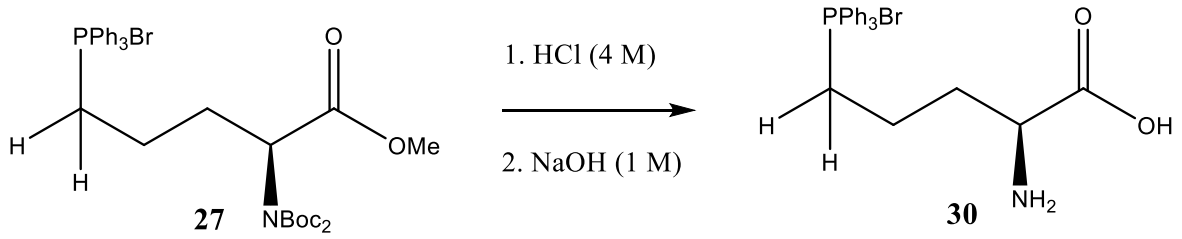

Scheme 4.3: Deprotection of aldehyde of L-glutamic acid 15 to L-glutamic acid aldehyde 7.

The Wittig coupling should occur selectively between the aldehyde unit of C30:9 aldehyde **4** and the triphenylphosphonium group of Wittig salt **30** (Scheme 4.4). The amino and carboxylic acid moieties should not react under the Wittig reaction conditions. Deprotection prior to the Wittig reaction eliminates the need for the polyene to sustain the acidic deprotection conditions and this is an advantage when the polyene chains get longer and contain higher numbers of conjugated double bonds, decreasing the stability of the polyenes.

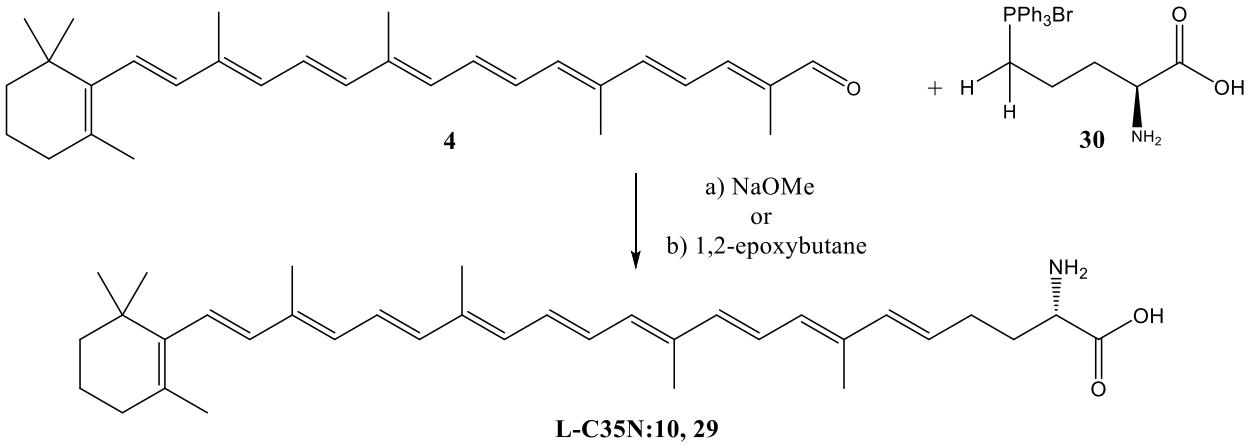

Scheme 4.4: Wittig reaction between C30:9 aldehyde 4 and Wittig salt of L-glutamic acid 30.

The proposed methods should be compatible also for other polyene aldehydes.

5 Experimental

5.1 Synthesis of 5-undecylimidazolidine-2,4-dione (2)

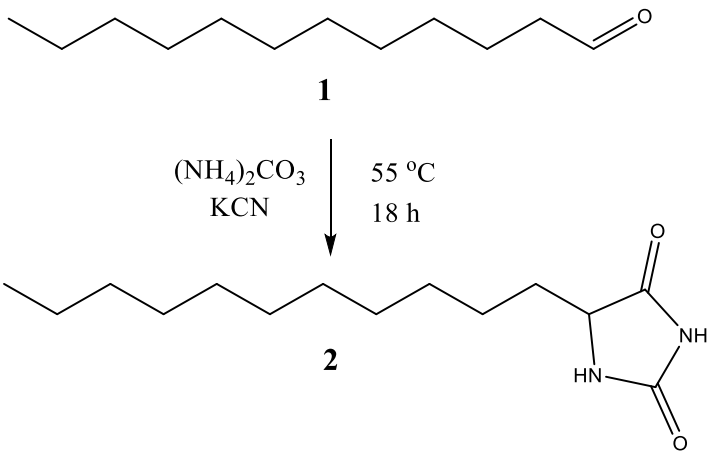

Dodecanal (**1**, 0.66 mL, 3.0 mmol) was dissolved in EtOH/H_2O (1:1, 12 mL), to which $(NH_4)_2CO_3$ (1.44 g, 15 mmol) and KCN (0.24 g, 3.6 mmol) were added. The mixture was stirred at 55 ^{0}C for 18 h after which the temperature was increased to 90 ^{0}C to eliminate excess ammonium carbonate. EtOH was evaporated and the solution acidified to pH 3 with HCl (conc.), then evaporated to dryness. The residue was extracted with EtOH, filtered and dried. The obtained light yellow needle formed crystals were recrystallized from EtOH (96 %), giving 0.19 g (0.7 mmol, 23%) of hydantoin **2** as a white powder.

^{1}H-NMR (600 MHz, 25 °C, d_6-DMSO): δ = 0.86 (t, 3H), 1.28 (m, 18H), 1.64 (dt, 2H), 3.97 (m, 1H), 6.07 (d, 1H), 7.93 (s, 1H)

^{13}C-NMR (600 MHz, 25 °C, d_6-DMSO): δ = 14.4, 22.6, 24.6, 29.1, 29.2, 29.3, 29.4, 29.5, 31.7, 31.8, 58.0, 157.9, 176.6

MS (ESI): *m/z* = 255.2073 $[M+H]^+$

5.2 Synthesis of 2-aminotridecanoic acid (3)

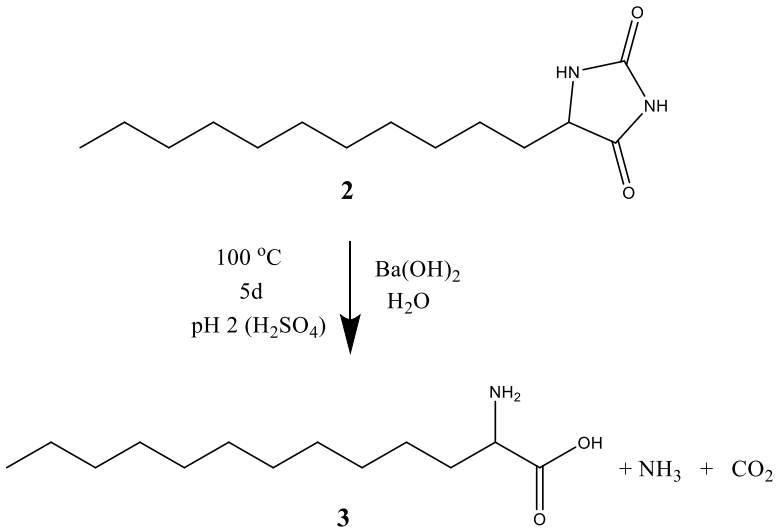

Undecylhydantoin **2** (190 mg, 0.7 mmol) was dissolved in H_2O (40 mL). BaO (6.2 g, 40 mmol) was added and the mixture stirred 96 h at 100 ^{0}C under reflux conditions. The reaction mixture was then acidified with H_2SO_4 (conc.) to pH 2. $BaSO_4$ precipitated immediately and was filtered off on a pad of celite. The solvent was removed under reduced pressure and the residue dried, giving 94 mg (0.4 mmol, 55%) of white, hygroscopic *2-aminotridecanoic acid* (**3**). A small amount of the product was dissolved in EtOH and the pH adjusted to 7-8 and with Et_3N. 1 mL of a ninhydrin-solution (0.1% in EtOH) was added and boiled for a short time, giving the characteristic Ruhemann purple, proving the presence of an amino acid.

MS (ESI): *m/z* = 230.9961 $[M+H]^+$

5.3 Attempted synthesis of β-apo-8'-carotene-5-imidazolidine-2,4-dione (5)

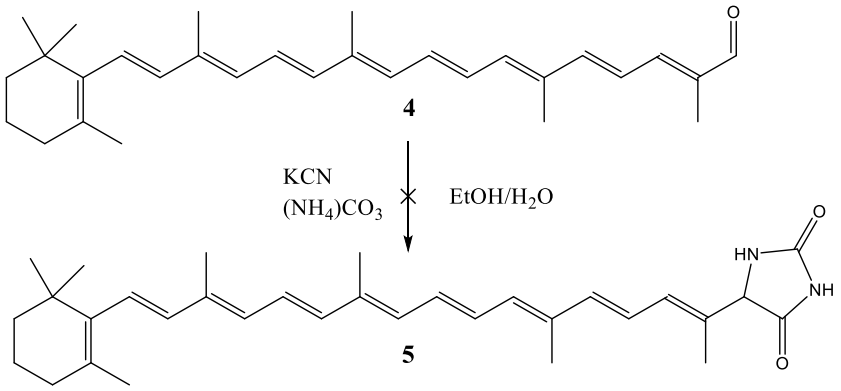

Carotenal **4** (200 mg 4.8 mmol) was dissolved in 20 mL of EtOH / H_2O (1:1). $(NH_4)_2CO_3$ (2.3 g, 23.9 mmol) and KCN (276 mg, 4.2 mmol) were successively added to the solution. After heating to 55 ^{0}C and stirring for 18 h. TLC (hexane/acetone, 7:3) did not show conversion of the educt. Therefore, the reaction was stirred for 4 d, checking the reaction by TLC regularly. After 4 d, signs of decomposition were detected. The temperature was raised to 90 ^{0}C to remove excess ammonium carbonate. EtOH was evaporated and the solution acidified to pH 6 with diluted HCl, then evaporated until dry. The residue was taken up in EtOH, filtered and dried. The desired hydantoin **5** could not be identified by MS (ESI).

5.4 Synthesis of dibenzyl N,N-dibenzyl-L-glutamate (10)

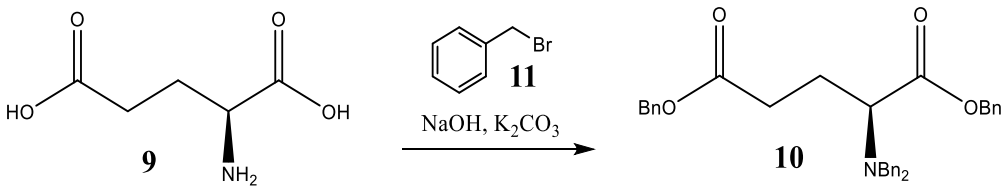

L-Glutamic acid (**9**, 5.00 g, 34 mmol) was dissolved in H_2O (60 mL) with K_2CO_3 (18.8 g, 7.3 mol) and NaOH (2.75 g, 69 mmol). The mixture was refluxed under stirring and benzyl bromide (**11**, 23.25 g, 136 mmol) was slowly added. When TLC (petroleum ether (60-80)/EtOAc, 6:1) showed absence of educt, the mixture was cooled to room temperature. An oily layer separated, which was extracted from the aq. phase with Et_2O. The collected organic phases were dried over Na_2SO_4 and the solvent removed under reduced pressure. The crude product (15.09 g) was purified by flash column chromatography (petroleum ether (60-80)/EtOAc, 20:1). 9.89 g (19 mmol, 57%) tetrabenzyl glutamate **10** was isolated as an oil.

^{1}H NMR (400 MHz, 25 °C, $CDCl_3$): δ = 2.05 (m, 2H), 2.40 (m, 2H), 3.40 (m, 1H), 3.49 (m, 2H), 3.87 (m, 2H), 4.95 (m, 2H), 5.18 (m, 2H), 7.18-7.40 (m, 20H)

^{13}C NMR (400 MHz, 25 °C, $CDCl_3$): δ = 24.3, 30.7, 54.5, 59.9 (4C), 65.2, 66.3, 127.0-129.0 (20C), 136.0 (2C), 139.3 (2C), 172.3, 173.0

MS (ESI): *m/z* = 508.2483 $(M+H)^+$

5.5 Attempted synthesis of benzyl (*S*)-2-(dibenzylamino)-5-hydroxypentanoate (12)

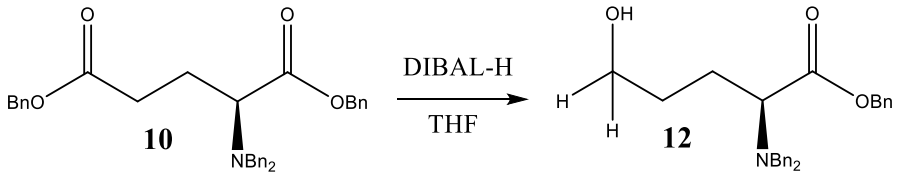

Tetrabenzyl glutamate **10** (200 mg, 0.4 mmol) was dissolved in dry THF (2 mL) and the mixture cooled under N_2 to -10 ^{0}C. DIBAL-H (1 M in toluene, 1.2 mL, 1.2 mmol) was slowly added under stirring. After the addition of DIBAL-H was ended, the temperature was increased to 0 ^{0}C. The reaction mixture was stirred and monitored by TLC (petroleum ether (60-80)/EtOAc, 6:1). As no reaction was observed, the reaction was stirred over night at room temperature. H_2O was added and the mixture stirred for 30 minutes. When signs of some conversion were observed, additional THF and Na_2SO_4 were added, and the mixture was again stirred for 30 minutes. The mixture was filtered over celite, and the filtrate was washed with THF. The solvent was removed at reduced pressure and the residue purified by flash column chromatography (petroleum ether (60-80)/EtOAc, 3:1). 126 mg of the educt was recovered; the rest of the educt had been decomposed, and alcohol **12** could not be obtained.

5.6 Synthesis of dimethyl (*tert*-butoxycarbonyl)-L-glutamate (13)

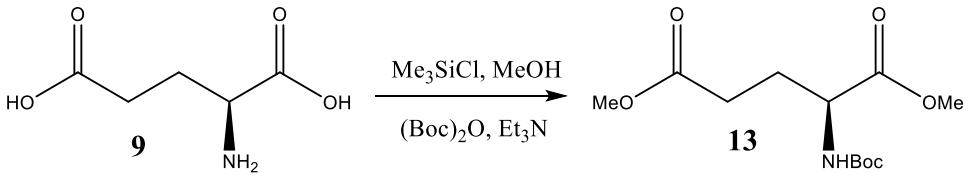

To a stirred ice cold suspension of L-glutamic acid (**9**, 147 mg, 1.0 mmol) in dry MeOH (3.3 mL), Me_3SiCl (0.56 mL, 4.4 mmol) was added under stirring. After addition, the reaction was heated to room temperature and stirred overnight under N_2-atmosphere. The following morning, TLC (nBuOH/acetic acid/H_2O, 3:1:1) showed complete conversion of the starting material. Et_3N (0.9 mL, 6.5 mmol) and $(Boc)_2O$ (240 mg, 1.1 mmol) were sequentially added. The reaction was stirred under N_2-atmosphere until TLC (nBuOH/acetic acid/H_2O, 3:1:1) showed the reaction was completed. The solvent was removed at reduced pressure and the dry residue triturated and washed with Et_2O (3x15 mL). The ether fractions were combined and the solvent removed at reduced pressure, leaving an oil, which was purified by flash column chromatography on a short silica column (n-pentane/EtOAc 4:1), giving 190 mg (0.7 mmol, 70%) of dimethyl mono Boc glutamate **13**.

^{1}H NMR (400 MHz, 25 °C, $CDCl_3$): δ = 1.44 (s, 9H), 1.97 (m, 1H), 2.18 (m, 1H), 2.41 (ddd, 2H), 3.68 (s, 3H), 3.75 (s, 3H), 4.34 (m, 1H), 5.17 (d, 1H)

^{13}C NMR (400 MHz, 25 °C, $CDCl_3$): δ = 27.7, 28.3 (3C), 30.0, 51.8, 52.4, 52.8, 80.0, 155.3, 172.7, 173.2

MS (ESI): *m/z* = 298.1270 $[M+Na]^+$

5.7 Synthesis of dimethyl di(*tert*-butoxycarbonyl)-L-glutamate (14)

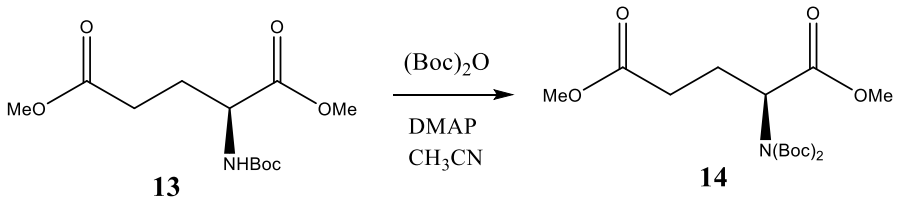

Mono Boc glutamate **13** (190 mg, 0.7 mmol) and DMAP (22 mg, 0.18 mmol) were dissolved in CH_3CN (3 mL) and stirred while $(Boc)_2O$ (220 mg, 1.0 mmol) was added. The reaction mixture was stirred overnight at room temperature. On the following day, TLC (n-pentane/EtOAc, 4:1) did not show complete conversion of the starting material. $(Boc)_2O$ (110 mg, 0.50 mmol) was added and the reaction stirred one more night. The following day, more $(Boc)_2O$ (100 mg, 0.46 mmol) was added and the reaction stirred until TLC showed full product formation. The solvent was evaporated and the residue purified by flash column chromatography (n-pentane/EtOAc, 5:1), resulting in 222 mg (0.59 mmol, 86%) of dimethyl di-Boc glutamate **14**.

^{1}H NMR (400 MHz, 25 °C, $CDCl_3$): δ = 1.50 (s, 18H), 2.20 m, 1H), 2.46 (m, 2H), 2.52 (m, 1H), 3.68 (s, 3H), 3.73 (s, 3H), 4.95 (dd, 1H)

^{13}C NMR (400 MHz, 25 °C, $CDCl_3$): δ = 25.2, 28.0 (6C), 30.6, 51.7, 52.2, 57.3, 83.3 (2C), 151.9, 170.8, 173.1

MS (ESI): *m/z* = 398.1793 $[M+Na]^+$

5.8 Synthesis of methyl (2*S*)-2-[bis(*tert*-butoxycarbonyl)amino]-5-hydroxypentanoate (16)

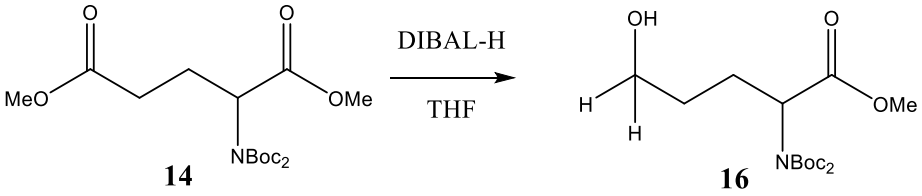

14 **16**

Dimethyl di-Boc glutamate **14** (900 mg, 2.66 mmol) was dissolved in dry THF (30 mL). Under N_2-atmosphere, the mixture was cooled to −10 ^{0}C; DIBAL-H (7.4 mL of a 1 M solution, 7.4 mmol) was slowly added and then stirred for 4 h, or until TLC (n-pentane/EtOAc, 3:1) showed full conversion of the starting material. The solution was allowed to reach room temperature, was then quenched with H_2O and stirred for 30 min. Additional THF (1.5 mL) and Na_2SO_4 (500 mg) were added and the mixture was again stirred for 30 min. The mixture was filtered over celite and the filtrate washed with THF. The solvent was removed under reduced pressure and the residue purified by flash column chromatography (petroleum ether (60-80)/EtOAc, 3:1), resulting in 573 mg (1.65 mmol, 62%) of methyl di-Boc alcohol **16**.

^{1}H-NMR (400 MHz, 25 °C, $CDCl_3$): δ = 1.50 (s, 18H), 1.52 (1H), 1.65 (m, 2H), 1.94 (m, 1H), 2.25 (m, 1H), 3.69 (t, 2H), 3.72 (s, 3H), 4.89 (dd, 1H)

^{13}C NMR (400 MHz, 25 °C, $CDCl_3$): δ = 26.4, 28.0 (6C), 29.4, 52.2, 57.9, 65.9, 83.2 (2C), 152.2, 171.4 (2C)

MS (ESI-TOF): *m/z* =370.1843 $[M+Na]^+$

5.9 Synthesis of methyl (2*S*)-2-[bis(*tert*-butoxycarbonyl)amino]-5-oxopentanoate (15)

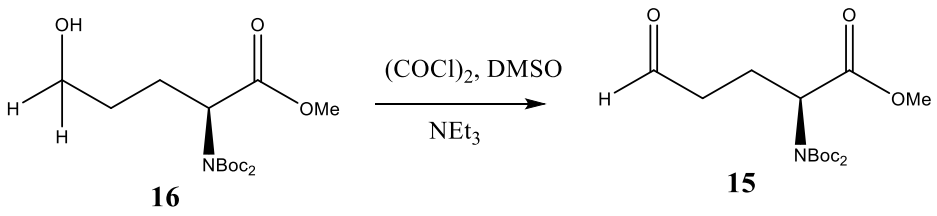

16 **15**

Under N_2-atmosphere, a solution of dry DMSO (120 µL) in dry DCM (810 µL) was added slowly to a flask cooled to -78 ^{0}C containing oxalyl chloride (78 µL) dissolved in dry DCM (1.67 mL). Stirring was maintained for 15 min, then a solution of alcohol **16** (250 mg, 0.72 mmol) in dry DCM (450 µL) was slowly added and stirred for 15 min. Et_3N (240 µL) was added and the mixture stirred for further 15 min, then additional Et_3N (200 µL) was added to ensure the end of the reaction. The flask was then cooled to 0 ^{0}C, stirred for 15 min, H_2O (3 mL) was added and the mixture heated. After reaching room temperature, the organic phase was separated and the aq. phase extracted with DCM. The collected organic phases were washed with HCl (1 M), $NaHCO_3$ solution (aq., sat.) and brine. The organic phases were then dried over Na_2SO_4 and the solvent removed under reduced pressure. The residue was purified by flash column chromatography (petroleum ether (60-80)/EtOAc, 3:1), resulting in 143 mg (0.41 mmol, 58%) aldehyde **15**.

^{1}H NMR (400 MHz, 25 °C, $CDCl_3$): δ = 1.50 (s, 18H), 2.48-2.61 (m, 4H), 3.73 (s, 3H), 4.89 (dd, 1H), 9.78 (s, 1H)

^{13}C NMR (400 MHz, 25 °C, $CDCl_3$): δ = 22.5, 28.0 (6C), 40.5, 52.3, 57.3, 83.5 (2C), 152.0, 170.7 (2C), 201.0

MS (ESI-TOF): *m/z* 368.1685 $[M+Na]^+$

5.10 Synthesis of 8'-apo-β-caroten-8'-ol (17)

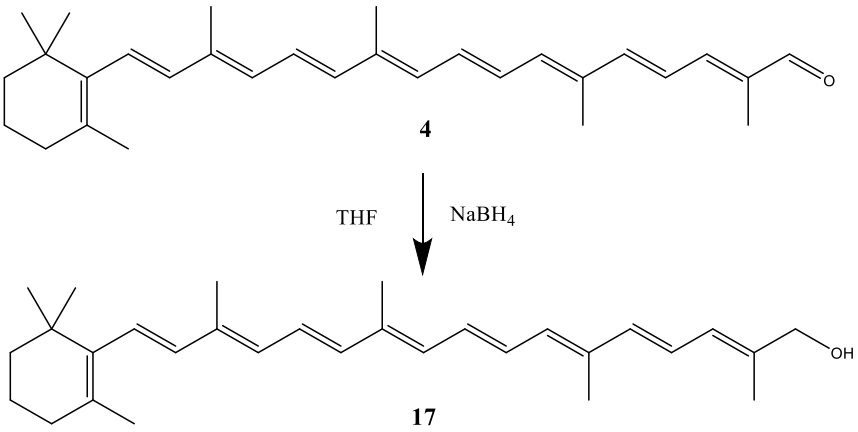

Carotenal **4** (500 mg, 1.2 mmol) and $NaBH_4$ (52 mg, 1.4 mmol) were dissolved under vigorous stirring in dry THF (40 mL). The reaction was monitored by TLC (hexane/acetone, 4:1) and showed no presence of aldehyde **4** after 4 h. The solvent was removed at reduced pressure. The obtained viscous, orange oil was purified by flash column chromatography, using a hexane/ EtOAc gradient. The fractions were controlled by TLC (EtOAc/hexane, 2:3). After removing the solvents at reduced pressure, 281 mg (0.67 mmol, 55%) carotenal **17** was obtained as a light red powder.

λ_{max} (DCM) = 458.0 nm, 432.5 nm

^{1}H-NMR (400 MHz, 25 °C, $CDCl_3$): δ = 1.03 (s, 6H), 1.47 (m, 4H), 1.72 (s, 3H), 1.76 (m, 1H), 1.80 (m, 1H), 1.96 (s, 3H), 1.97 (s, 6H), 4.12 (s, 2H), 6.01-6.71 (m, 12H)

MS (ESI): *m/z* = 418.3232 $[M+H]^+$

5.11 Attempted synthesis of β-apo-8'-bromocarotene (18) and 8'-apo-β-caroten-8'-triphenylphosphine bromide (19)

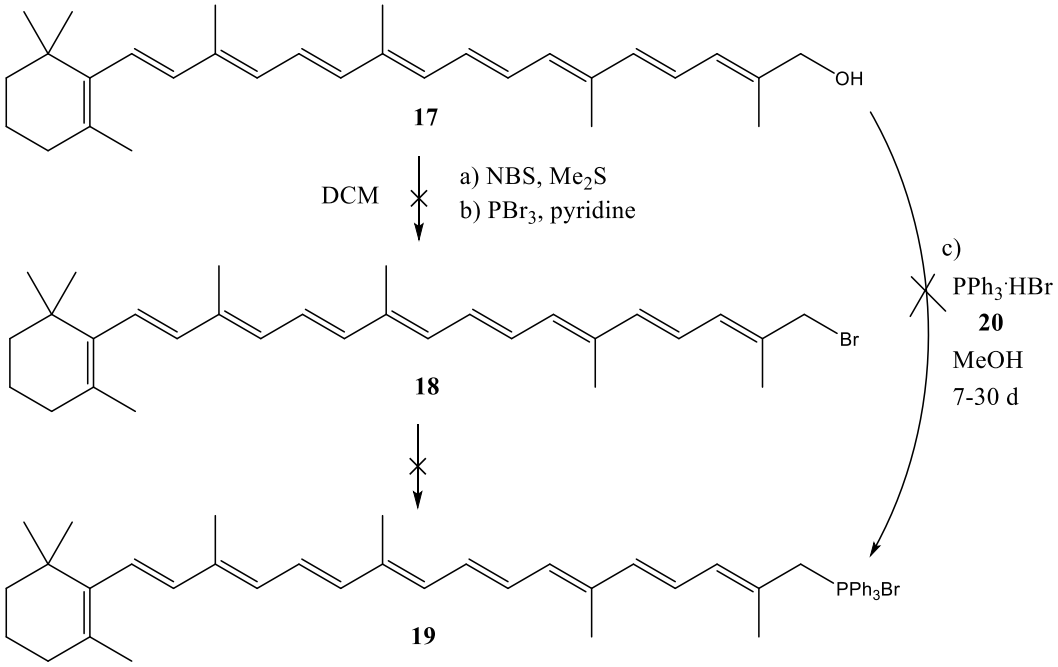

5.11.1 Reaction a)

NBS (150 mg, 0.8 mmol) was dissolved in DCM (3 mL) and cooled to 0 ^{0}C. Me_2S (57.2 mg, 0.9 mmol) was added dropwise under N_2-atmosphere under vigorous stirring. The mixture was cooled to -20 ^{0}C with an ice/salt-bath. Carotenol **17** (100 mg, 0.2 mmol) was dissolved in DCM (1 mL) and added dropwise to the solution of NBS and dimethyl sulfide under vigorous stirring. The mixture was stirred at 20 ^{0}C for 2.5 h and then poured over ice-cold brine. The product was extracted with Et_2O. The ether phase was washed with half sat. $NaHCO_3$ (aq.), followed by brine and finally H_2O. The ether extracts were dried over anhydrous Na_2SO_4 and the solvent removed under reduced pressure. The product was crystallized from diisopropyl ether and gave 384 mg of deep red crystals, which were not bromide **18** according to MS.

λ_{max} (DCM) = 325 nm

5.11.2 Reaction b)

Carotenol **17** (20 mg, 0.05 mmol) and pyridine (19 µL, 19 mg, 0.2 mmol) were dissolved in DCM (200 µL) and cooled to -10 ^{0}C. PBr_3 (4 µL, 11 mg, 0.04 mL), dissolved in of DCM (200 µL) was carefully added dropwise to the reaction mixture over a period of 15-20 min and stirred for 30 min at -10 ^{0}C. Aq. $NaHCO_3$ (sat., 300 µL) was added to the reaction mixture and the product extracted with Et_2O. The organic phase was washed with brine and H_2O, dried over $MgSO_4$ and filtered. The solvent was removed at reduced pressure. Recording of a UV/vis-spectre showed that the polyene was intact and that the absorption maximum had not shifted relative to carotenol **17**. Bromide **18** could not be identified by MS or NMR.

λ_{max} (DCM) = 458.5 nm, 433.0 nm

5.11.3 Reaction c)

Carotenol **17** (150 mg, 0.65 mmol) was dissolved in 30 mL of dry MeOH. $PPh_3{\cdot}HBr$ (**20**, 225 mg, 0.66 mmol) was added under stirring and the reaction mixture stirred at room temperature for 18 d in total darkness. The amount of precipitate was controlled regularly. MeOH was then evaporated. The residue was dissolved in a very small amount of DCM and precipitated in a vigorously stirred ice-cold mixture of Et_2O (150 mL) and hexane (20 mL). The precipitate was filtered and washed twice with ice-cold Et_2O. Phosphonium salt **19** could not be identified by MS or NMR, although the polyene chain was intact, according to UV/vis and NMR spectrometry.

λ_{max} (DCM) = 441.0 nm, 268.0 nm

5.12 Synthesis of L-C20N:4-diBoc-methylester (23)

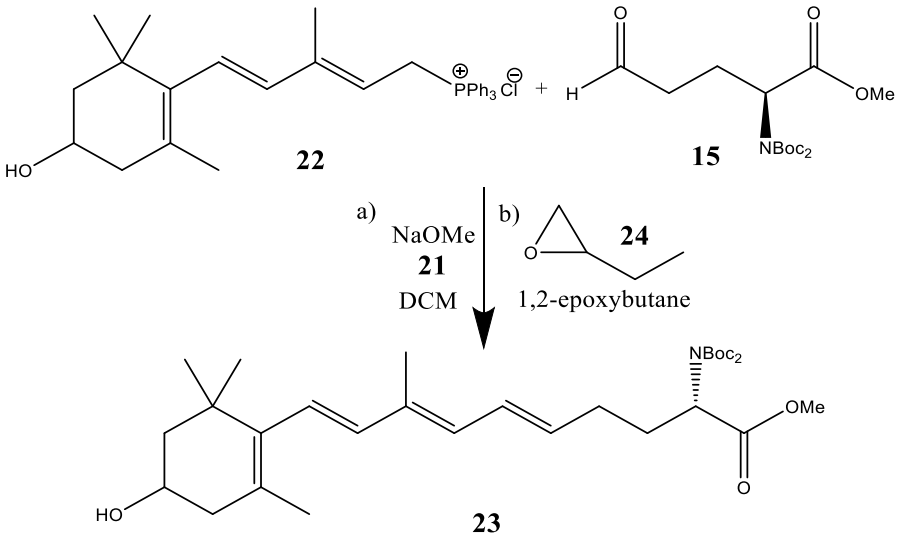

5.12.1 Reaction a)

Phosphonium salt **22** from BASF (416 mg, 0.8 mmol) and di-Boc aldehyde **15** (231 mg, 0.7 mmol) were suspended in DCM (5 mL). At room temperature, NaOMe **21** (25% in MeOH, 208 mg, 1.0 mmol) was added. The reaction was followed by TLC (n-pentane/EtOAc, 3:1). After 1.5 h, the reaction mixture was poured into aq. NH_4Cl (sat.) and extracted with EtOAc. The extracts were washed with brine, dried over Na_2SO_4 and the solvent removed at reduced pressure. The yellow residue was purified by flash column chromatography (n-pentane/acetone 5:1) to give 224 mg (0.4 mmol, 61%) of di-Boc methyl ester **23** as yellow oil.

5.12.2 Reaction b)

A mixture of C15-phosphonium salt **20** (621 mg 1.2 mmol) and aldehyde of glutamic acid **15** (345 mg, 1.0 mmol) in EtOH (5.0 mL) and 1,2-epoxybutane (**24**, 0.75 mL) was stirred for 20 h under N_2 and reflux conditions. The reaction was controlled by TLC (n-pentane/acetone, 5:2) until **15** had reacted. The reaction mixture was then cooled to 0 ^{0}C while continuously stirred for 1 h. The suspension was poured into aq. NH_4Cl-solution (sat.), extracted with Et_2O, washed

with brine and dried over Na_2SO_4. Solvents were removed at reduced pressure. The yellow residue was purified by flash column chromatography (n-pentane/acetone, 5:2), giving 282 mg (0.5 mmol, 51%) of di-Boc methyl ester **23** as a yellow oil.

^{1}H NMR (600 MHz, 25 °C, $CDCl_3$): δ = 1.05 (s, 3H), 1.06 (d, 3H), 1.47 (dd, 1H), 1.49 (s, 9H), 1.50 (s, 9H), 1.71 (d, 3H), 1.78 (ddd, 1H), 1.89 (d, 3H), 1.98-2.05 (m, 2H), 2.21-2.22 (m, 2H), 2.29 (m, 2H), 2.38 (dt, 1H), 3.71 (s, 3H), 4.02 (s, 1H), 4.89 (m, 1H), 5.60 (m, 1H), 5.39-6.38 (m, 4H)

^{13}C NMR (600 MHz, 25 °C, $CDCl_3$): δ = 12.4, 21.5, 24.5, 28.0 (6C), 29.9 (2C), 30.2, 37.1, 42.5, 48.4, 52.2, 57.6, 65.1, 83.1 (2C), 125.1, 125.7, 127.9, 130.1, 130.7, 133.5, 138.5, 138.7, 152.1 (2C), 171.3

MS (ESI): *m/z* = 570.3413 $[M+Na]^+$

5.13 Synthesis of L-C20N:4 (25)

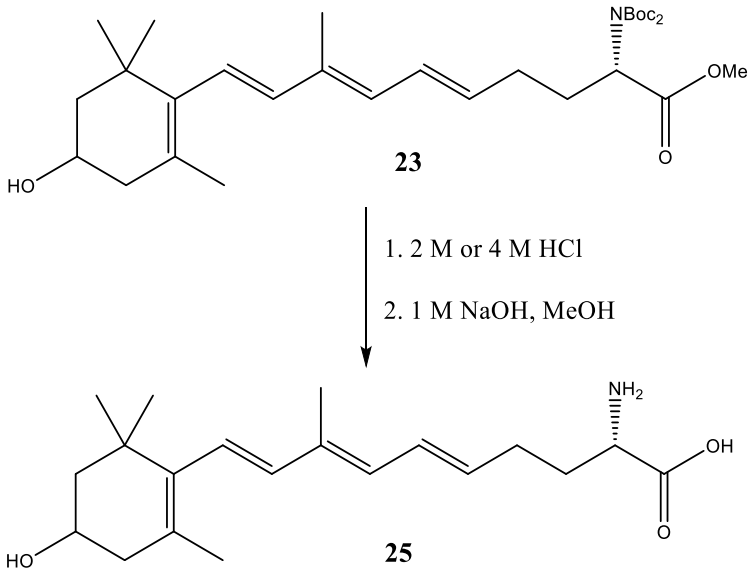

A solution of di-Boc methyl ester **23** (100 mg, 0.2 mmol) in HCl/THF (4 M/2 M, 4.56 mL) was stirred for 30 min at room temperature. Excess solvent and HCl were removed at reduced pressure. The residue was treated with THF and evaporated twice (2 x 1 mL). The solid mixture was dissolved in MeOH (0.40 mL) and an aq. solution of NaOH (1 M, 0.51 mL) was added. After vigorous stirring for 2 h, the organic solvent was removed and the aq. solution was carefully neutralized using HCl (1 M), precipitating 94 mg (4 M HCl/THF) or 68 mg (2 M HCl/THF) of a yellow powder. The amino acid **25** was filtered and washed with H_2O. Presence of the amino unit was ascertained by the ninhydrin test. Despite attempts to dry the product under vacuum, NMR showed high contents of H_2O in the product, explaining the high mass of the precipitate.

Purification of 68 mg amino acid **25** by flash chromatography over silica gel (nBuOH/acetic acid/H_2O, 3:1:1) resulted in 0.2 mg pure amino acid **25** as a yellow powder.

Interpretation of NMR-signals are based on the ^{1}H-^{13}C couplings seen in HSQC, combined with the shifts observed in the solvent suppressed ^{1}H-spectre. Small amounts (0.2 mg) of pure compound resulted in a lot of noise, causing inaccurate integrals of the signals. The number of protons listed in the following paragraphs are therefore assumed values based on the characteristic shifts. It was assumed, that the amino acid **25** is present as a zwitterion and that

the signals of the carboxylic acid and amino group therefore can be present with a varying number of protons attached.

^{1}H-NMR (d_6-DMSO, 25 °C, 600 MHz): δ = 1.04 (6H), 1.33 (1H), 1.34 (3H), 1.42 (2H) 1.65 (1H), 1.75 (2H), 1.87 (1H), 1.97 (3H) 2.20 (1H), 3.58/3.62 (1H) 3.81 (1H), 5.75 (1H), 6.07 (1H), 6.87 (1H), 7.17 (1H) 7.24 (1H), 7.28 (2/3H), 8.41 (0/1H)

^{13}C-NMR (d_6-DMSO, 25 °C, 600 MHz): δ = 15.7, 20.6, 28.9, 29.1, 30.1, 41.2, 48.0, 51.1/51.6, 62.6, 126.9, 127.8, 128.1, 128.5, 131.2

λ_{max} (DCM) = 275 nm

MS (ESI): *m/z* = 332.2232 $[M-H]^-$

5.14 General procedures and apparature

5.14.1 Chromatography

Silicagel 60, F_{254}, 0.2 mm TLC plates from Merck were used for TLC.

For colourless and non-aromatic compounds, a phosphomolybdic acid (10% in EtOH) stain was used.

Silicagel 60, 230-400 mesh, particle size 40-63 µm, from Fluka was used for flash column chromatography.

5.14.2 Molecular models

Molecular modelling with semi empirical AM1 in Spartan 08

5.14.3 Apparature

Accurate mass determination in positive and negative mode was performed on a "Synapt G2-S" Q-TOF instrument from Waters™. Samples were ionized by the use of ASAP probe (APCI) or ESI probe. No chromatographic separation was used previous to the mass analysis. Calculated exact mass and spectra processing was done by Waters™ Software Masslynx V4.1 SCN871.

NMR spectra were recorded on 400 MHz Bruker Avance™ III HD NMR spectrometer and 600 MHz Ultrashielded Bruker Avance™ III HD NMR spectrometer, both at 25 °C.

UV/vis spectra were recorded with a Hitachi U-1900 Spectrophotometer, 200V in DCM and at room temperature.

6 References

1. de Reyff, C., Deux enantiomeres, antipodes optiques, ont-ils meme energie? *Journal de Chimie Physique* **1983,** *80*, 563-571.
2. Meierhenrich, U. J., Amino acids and the asymmetry of life. *European Review* **2013,** *21*, 190-199.
3. Gupta, M.; Chauhan, V. S., De novo design of α,β-didehydrophenylalanine containing peptides: From models to applications. *Biopolymers* **2011,** *95*, 161-173.
4. Ng, P. C.; Henikoff, S., SIFT: predicting amino acid changes that affect protein function. *Nucleic Acids Research* **2003,** *31*, 3812-3814.
5. Wagner, I.; Musso, H., New naturally occurring amino acids. *Angewandte Chemie International Edition in English* **1983,** *22*, 816-828.
6. Ault, A., The monosodium glutamate story: The commercial production of MSG and other amino acids. *Journal of Chemical Education* **2004,** *81*, 347.
7. Zhuang, H.; Wang, Z.; Wang, J.; Zhang, H.; Xun, E.; Chen, G.; Yue, H.; Tang, N.; Wang, L., Synthesis of triptorelin lactate catalyzed by lipase in organic media. *International Journal of Molecular Sciences* **2012,** *13*, 9971-9.
8. Britton, G.; Liaaen-Jensen, S.; Pfander, H., *Carotenoids Volume 5: Nutrition and health*. Birkhäuser Verlag: Basel, Switzerland, 2009; Vol. 5.
9. Willett, W. C.; MacMahon, B., Diet and cancer - an overview. *New England Journal of Medicine* **1984,** *310*, 697-703.
10. Britton, G.; Liaaen-Jensen, S.; Pfander, H., *Carotenoids, Volume 4: Natural functions*. Birkhäuser Verlag: Basel, 2008; Vol. 4.
11. van Wijk, A. A. C.; Spaans, A.; Uzunbajakava, N.; Otto, C.; de Groot, H. J. M.; Lugtenburg, J.; Buda, F., Spectroscopy and quantum chemical modeling reveal a predominant contribution of excitonic interactions to the bathochromic shift in α-crustacyanin, the blue carotenoprotein in the carapace of the lobster *Homarus gammarus*. *Journal of the American Chemical Society* **2005,** *127*, 1438-1445.
12. The lobsterman's page. http://www.lobstermanspage.net/lobstrs/lfacts.jsp (07.05.16),
13. Meierhenrich, U. J.; Filippi, J. J.; Meinert, C.; Bredehöft, J. H.; Takahashi, J. i.; Nahon, L.; Jones, N. C.; Hoffmann, S. V., Circular dichroism of amino acids in the vacuum-ultraviolet region. *Angewandte Chemie International Edition* **2010,** *49*, 7799-7802.

14. Tanaka, M.; Yagi-Watanabe, K.; Kaneko, F.; Nakagawa, K., Chiroptical study of α-aliphatic amino acid films in the vacuum ultraviolet region. *The Journal of Physical Chemistry A* **2010,** *114*, 11928-11932.
15. Goto, T.; Ikehata, A.; Morisawa, Y.; Ozaki, Y., Electronic Transitions of Protonated and Deprotonated Amino Acids in Aqueous Solution in the Region 145–300 nm Studied by Attenuated Total Reflection Far-Ultraviolet Spectroscopy. *The Journal of Physical Chemistry A* **2013,** *117*, 2517-2528.
16. Tanaka, M.; Nakagawa, K.; Agui, A.; Fujii, K.; Yokoya, A., First observation of natural circular dichroism for biomolecules in soft X-ray region studied with a polarizing undulator. *Physica Scripta* **2005,** *2005*, 873.
17. Wallace, B. A., Protein characterisation by synchrotron radiation circular dichroism spectroscopy. *Quarterly Reviews of Biophysics* **2009,** *42*, 317-370.
18. Jubeli, E.; Raju, L.; Khalique, N. A.; Bilchuk, N.; Zegel, C.; Chen, A.; Lou, H. H.; Øpstad, C. L.; Zeeshan, M.; Sliwka, H.-R.; Partali, V.; Leopold, P. L.; Pungente, M. D., Polyene-based cationic lipids as visually traceable siRNA transfer reagents. *European Journal of Pharmaceutics and Biopharmaceutics* **2015,** *89*, 280-289.
19. Hoppe, B.; Martens, J., Aminosäuren – Herstellung und Gewinnung. *Chemie in unserer Zeit* **1984,** *18*, 73-86.
20. Baldwin, J. E.; Moloney, M. G.; North, M., Non-proteinogenic amino acid synthesis: Synthesis of β,γ-unsaturated α-amino acids from asparic acid. *Tetrahedron* **1989,** *45*, 6319-6330.
21. Shapira, J.; Dittmer, K., Unsaturated amino acids V. Microbiological properties of some halogenated olefinic amino acids. *Journal of Bacteriology* **1961,** *82*, 640-647.
22. Constantinou-Kokotou, V., Synthesis of optically active lipidic α-amino acids and lipidic 2-amino alcohols. *Amino Acids* **1999,** *16*, 273-285.
23. Rémond, E.; Bayardon, J.; Ondel-Eymin, M.-J.; Jugé, S., Stereoselective synthesis of unsaturated and functionalized L-NHBoc amino acids, using Wittig reaction under mild phase-transfer conditions. *The Journal of organic chemistry* **2012,** *77*, 7579-7587.
24. Duggan, H. M. E.; Hitchcock, P. B.; Young, D. W., Synthesis of 5/7-, 5/8- and 5/9-bicyclic lactam templates as constraints for external [small beta]-turns *Organic & Biomolecular Chemistry* **2005,** *3*, 2287-2295.

25. Kawai, M.; Nagai, U., A new sensitive method for determining absolute configuration of α-amino acids: CD spectra of N-2,4-dinitrophenyl-α-amino acylanilides. *Tetrahedron Letters* **1977,** *18*, 3889-3890.

26. Kawai, M.; Nagai, U.; Tanaka, A., Upon DNP-aromatic rule. Effect of introducing a methyl group to the .BETA.-position upon the CD spectra of DNP derivatives of aromatic .ALPHA.-amino acids. *Bull. Chem. Soc. Jpn.* **1982,** *55*, 1213-1215.

27. Greenfield, N. J., Using circular dichroism spectra to estimate protein secondary structure. *Nature Protocols* **2006,** *1*, 2876-2890.

28. Olson, J. A., Biochemistry of vitamin A and carotenoids. In *Vitamin A Deficiency: Health, Survival, and Vision*, Oxford University Press: New York, 1996; pp 221-250.

29. Hossain, M.; Zhang, L.-X.; Bertram, J., Mechanistic studies of cancer chemoprevention by retinoids and carotenoids. *Clinical Dermatology* **1993,** *5*, 361-361.

30. Mathies, R. A., From femtoseconds to biology: mechanism of bacteriorhodopsin's light-driven proton pump. *Proceedings of the Indian Academy of Sciences-Chemical Sciences* **1991,** *103*, 283-293.

31. Frank, H. A.; Violette, C.; Trautman, J.; Shreve, A.; Owens, T.; Albrecht, A., Carotenoids in photosynthesis: structure and photochemistry. *Pure and Applied Chemistry* **1991,** *63*, 109-114.

32. Willett, W. C., Goals for nutrition in the year 2000. *CA: A Cancer Journal for Clinicians* **1999,** *49*, 331-352.

33. Dhingra, V.; Seshadri, T.; Mukerjee, S., Carotenoid glycosides of *Nyctanthes arbor-tristis Linn*. *Indian Journal of Chemistry, Section B: Organic Chemistry Including Medicinal Chemistry* **1976,** *14*, 231-232.

34. Foss, B. J.; Sliwka, H. R.; Partali, V.; Köpsel, C.; Mayer, B.; Martin, H. D.; Zsila, F.; Bikadi, Z.; Simonyi, M., Optically active oligomer units in aggregates of a highly unsaturated, optically inactive carotenoid phospholipid. *Chemistry–A European Journal* **2005,** *11*, 4103-4108.

35. Partali, V.; Kvittingen, L.; Sliwka, H. R.; Anthonsen, T., Stable, highly unsaturated glycerides - enzymatic synthesis with a carotenoic acid. *Angewandte Chemie International Edition in English* **1996,** *35*, 329-330.

36. Greenlee, W., Synthesis of β,γ-unsaturated amino acids by the Strecker reaction. *The Journal of organic chemistry* **1984,** *49*, 2632-2634.

37. Clayden, J., *Organic chemistry*. Oxford University Press: Oxford, 2001.

38. Strecker, A., Ueber einen neuen aus Aldehyd-Ammoniak und Blausäure entstehenden Körper. *Justus Liebigs Annalen der Chemie* **1854,** *91*, 349-351.
39. Bucherer, H. T.; Steiner, W., Über Reaktionen der alpha-Oxy-Aminonitrile. Synthese von Hydantoinen. *J. prakt. Chem.* **1934,** *140*, 291-316.
40. Ware, E., The chemistry of the hydantoins. *Chemical reviews* **1950,** *46*, 403-470.
41. Šmit, B. M.; Pavlović, R. Z., Three-step synthetic pathway to fused bicyclic hydantoins involving a selenocyclization step. *Tetrahedron* **2015,** *71*, 1101-1108.
42. Schaefer, B., *Natural Products in the Chemical Industry*. Springer: Heidelberg, 2014.
43. Tellier, F.; Acher, F.; Brabet, I.; Pin, J.-P.; Azerad, R., Aminobicyclo [2.2. 1.] heptane dicarboxylic acids (ABHD), rigid analogs of ACPD and glutamic acid: synthesis and pharmacological activity on metabotropic receptors mGluR1 and mGluR2. *Bioorganic & Medicinal Chemistry* **1998,** *6*, 195-208.
44. Ruhemann, S., 138. Cyclic di- and tri-ketones. *Journal of the Chemical Society, Transactions* **1910,** *97*, 1438-1449.
45. Greene, T. W.; Wuts, P. G. M., *Protective groups in organic synthesis*. 2 ed.; Wiley: New York, 1991.
46. Rodriquez, M.; Taddei, M., A simple procedure for the transformation of L-glutamic acid into the corresponding γ-aldehyde. *Synthesis* **2005**, 493-495.
47. Padrón, J. M.; Kokotos, G.; Martín, T.; Markidis, T.; Gibbons, W. A.; Martín, V. c. S., Enantiospecific synthesis of α-amino acid semialdehydes: a key step for the synthesis of unnatural unsaturated and saturated α-amino acids. *Tetrahedron Asymmetry* **1998,** *9*, 3381-3394.
48. Marx, M.; Tidwell, T. T., Reactivity-selectivity in the Swern oxidation of alcohols using dimethyl sulfoxide-oxalyl chloride. *The Journal of organic chemistry* **1984,** *49*, 788-793.
49. Haugan, J. A., Total Synthesis of C31-Methyl Ketone Apocarotenoids: Sintaxanthin and (3*R*)-3-hydroxysintaxanthin. *Acta Chemica Scandinavica* **1994,** *48*, 657-664.
50. Häberli, A.; Pfander, H., Synthesis of bixin and three minor carotenoids from annatto (*Bixa orellana*). *Helvetica Chimica Acta* **1999,** *82*, 696-706.
51. Størseth, T. R. Synthesis and radical scavenging activity of two novel antioxidant combinations. Norwegian University of Science and Technology, Trondheim 2001.

52. Yamano, Y.; Chary, M. V.; Wada, A., Stereoselective total synthesis of the acetylenic carotenoids alloxanthin and triophaxanthin. *Organic & Biomolecular Chemistry* **2012,** *10*, 4103-4108.
53. Ernst, H.; Henrich, K. Verfahren und neue Zwischenprodukte zur Herstellung von 3,3'-Dihydroxyisorenieratin. WO/2008/003742, 2008.

Appendix A: Reaction mechanisms

Strecker Reaction

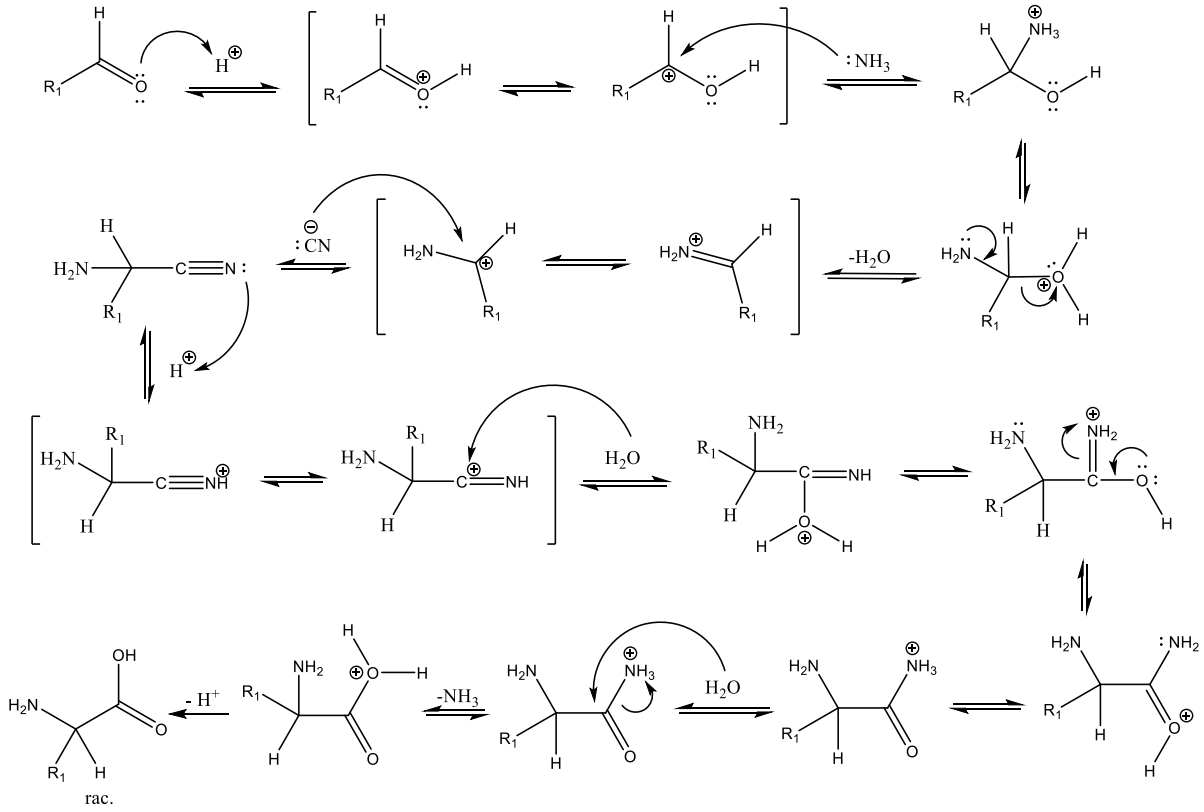

Scheme i: Mechanism of Strecker reaction

Bucherer-Bergs reaction

The Bucherer-Bergs reaction is a preparative method for imidazolidine-2,4-dione derivatives, more commonly known as hydantoins, developed in 1929 by Bergs and improved by Bucherer in 1934. Hydantoins are intermediates in the industrial synthesis of α-amino acids. The method uses potassium cyanide and ammonium carbonate to produce the hydantoin and alkali conditions for the conversion into α-amino acid.

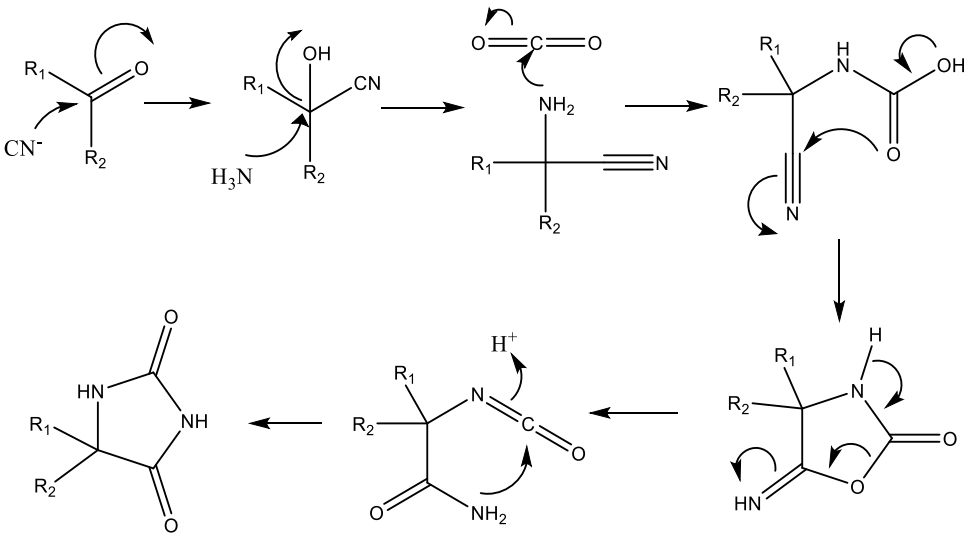

Scheme ii: Mechanism of the formation of hydantoin.

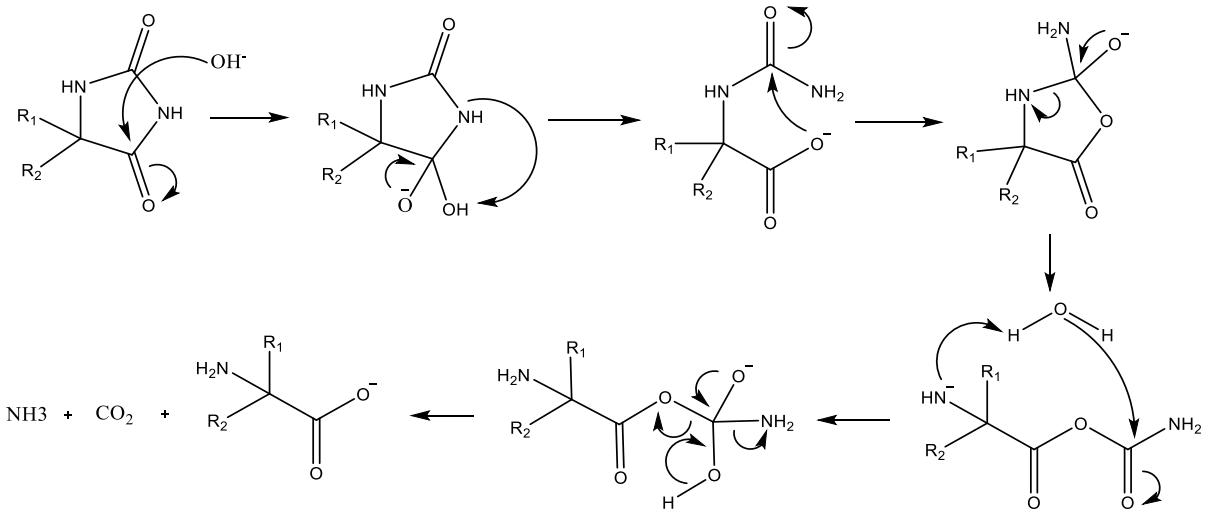

Scheme v: Mechanism for hydantoin-opening under elimination of ammonia and CO_2.

Wittig reaction

Wittig reactions are widely used in alkene synthesis, in which alkenes are formed in a reaction between a carbonyl and a triphenyl phosphonium ylide, giving a triphenylphosphonium oxide as side product. The method was developed by Georg Wittig in 1947.

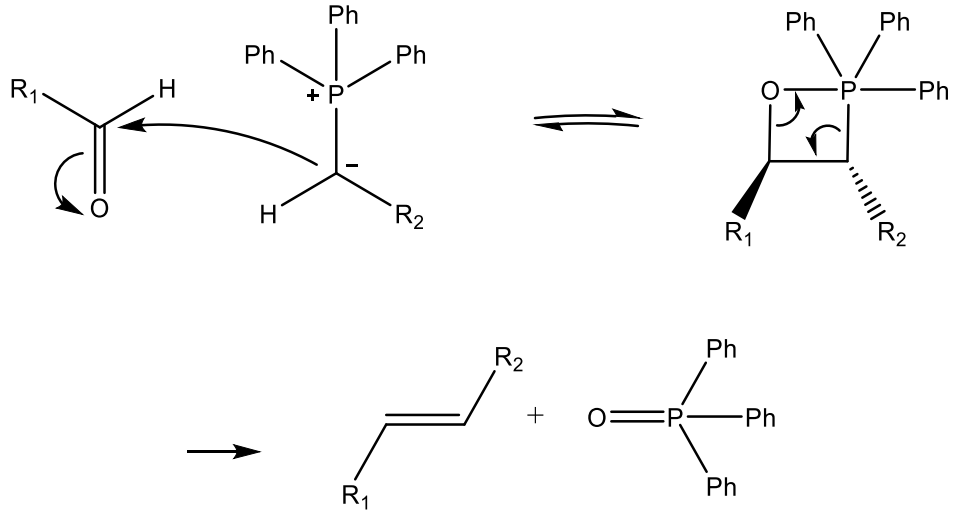

Scheme viv: Mechanism of the Wittig reaction.

Reduction with DIBAL-H

The reducing agent diisobutylaluminium hydride (DIBAL-H) is commonly used in organic synthesis to convert esters in alcohols.

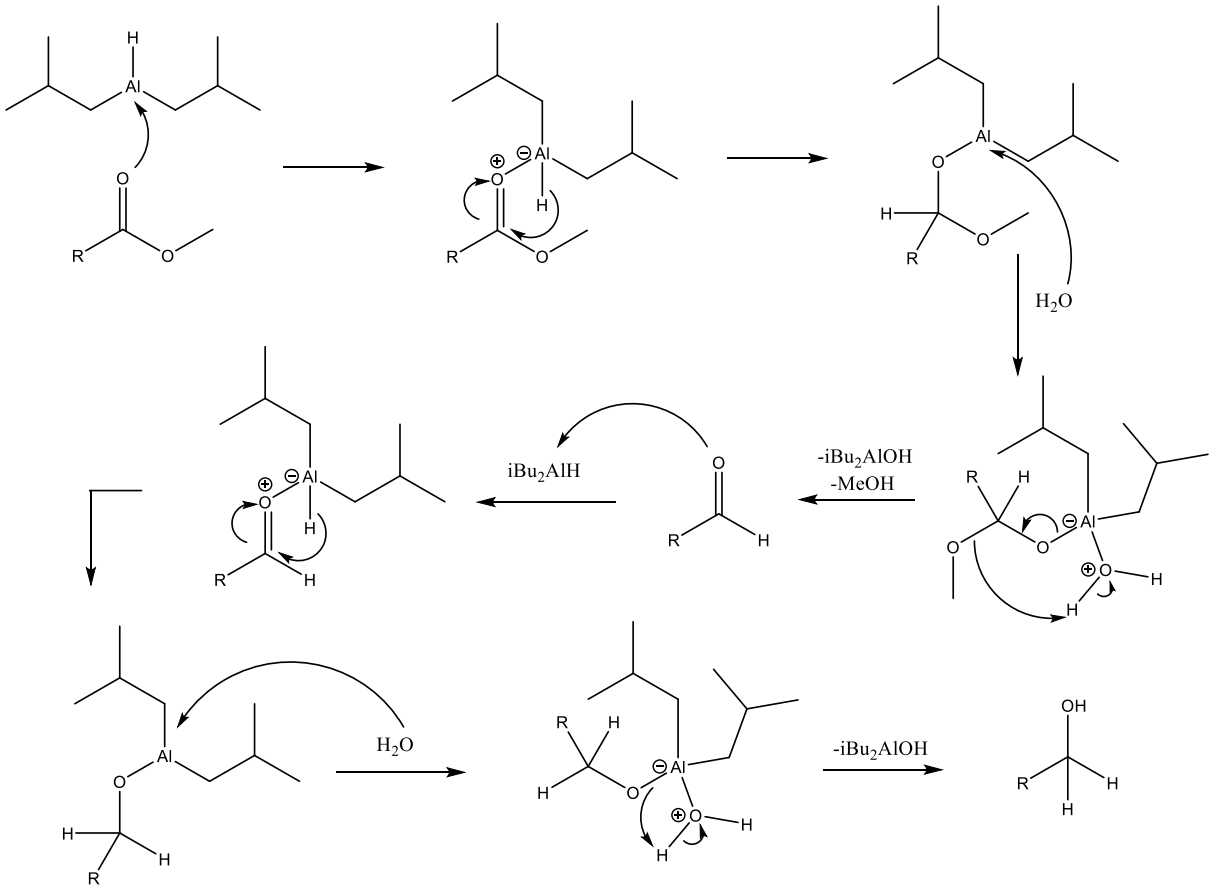

Scheme v: Mechanism of the reduction of an ester to an alcohol, via aldehyde using DIBAL-H as a reducing agent.

Swern oxidation

An oxidation technique developed by Daniel Swern in 1978, using chloro(dimethyl)sulfonium chloride, developed in situ from oxalyl chloride and DMSO, is a highly selective method for oxidizing alcohols to aldehydes. The reaction is performed at low temperatures and its by-products are volatile (CO, CO_2, Me_2S) and toxic (CO, Me_2S).

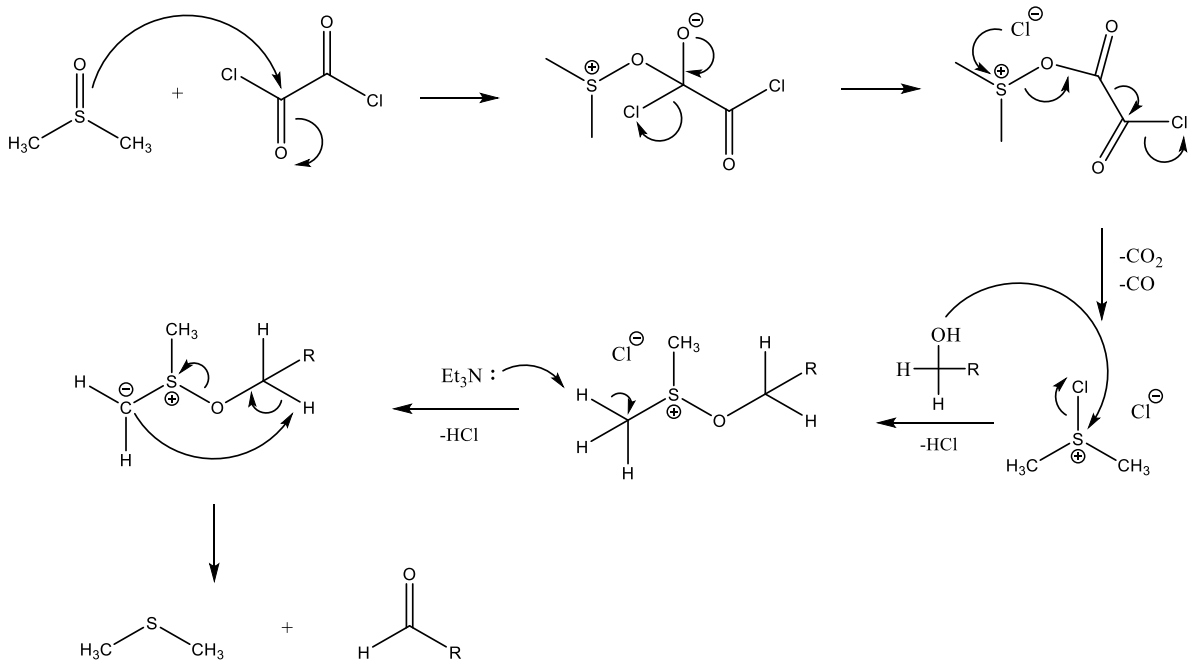

Scheme vi: Mechanism of the Swern oxidation.

Ninhydrin test

Ninhydrin, or 2,2-Dihydroxyindane-1,3-dione, is used in a simple test to check for presence of amino acids, invented by Siegfried Ruhemann in 1911. Through a reaction with a primary or secondary amine, the two ninhydrin molecules unite, creating a colour known as Ruhemann's purple. Ninhydrin is solid at room temperature and it is soluble in ethanol.

To investigate the presence of an amino acid, a small amount of the sample is dissolved in 1 mL of EtOH or MeOH and added 1 mL of a ninhydrin solution (0.1% in EtOH). The mixture is heated for a few minutes and will develop Ruhemann's purple if the sample contains an amino acid.

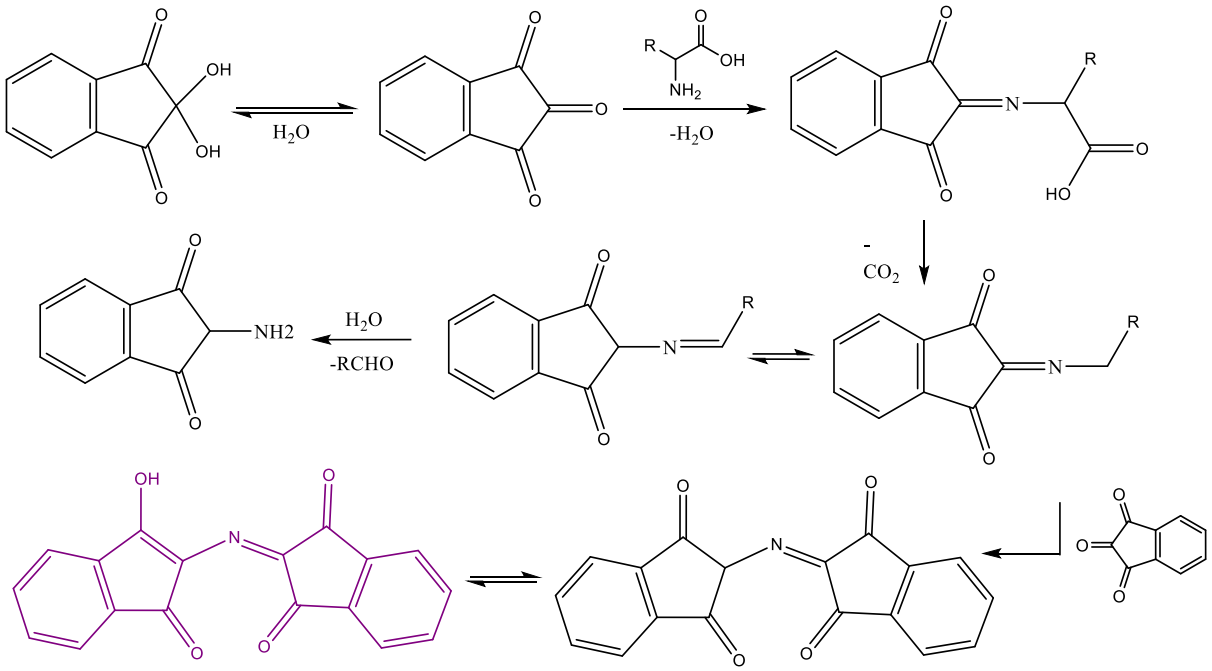

Scheme vii: Mechanism of the ninhydrin test.

Appendix B: Protective groups

In a molecule containing several reactive sites, the non-participating reactive groups must be temporarily protected, to prevent unwanted side-reactions. The right protective group has to be chosen considering both the stability during the reaction and the lability for unproblematic deprotection.

Amine and carboxylic acid groups are likely to undergo unwanted side reactions if not protected. The PGs used in this thesis are stable under the applied oxidative and reductive conditions, *tert*-butoxycarbonyl (Boc) can be removed in acidic conditions, methylester groups are hydrolysed with alkali conditions at room temperature.

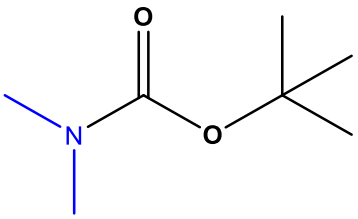

Figure i: *Tert*-butoxycarbonyl PG on an amino moiety

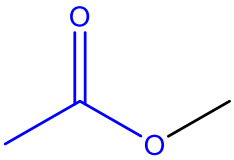

Figure ii: Methyl ester-PG on a carboxylic acid moiety

Appendix C: Spectra and data

Compound 2: 5-undecylimidazolidine-2,4-dione

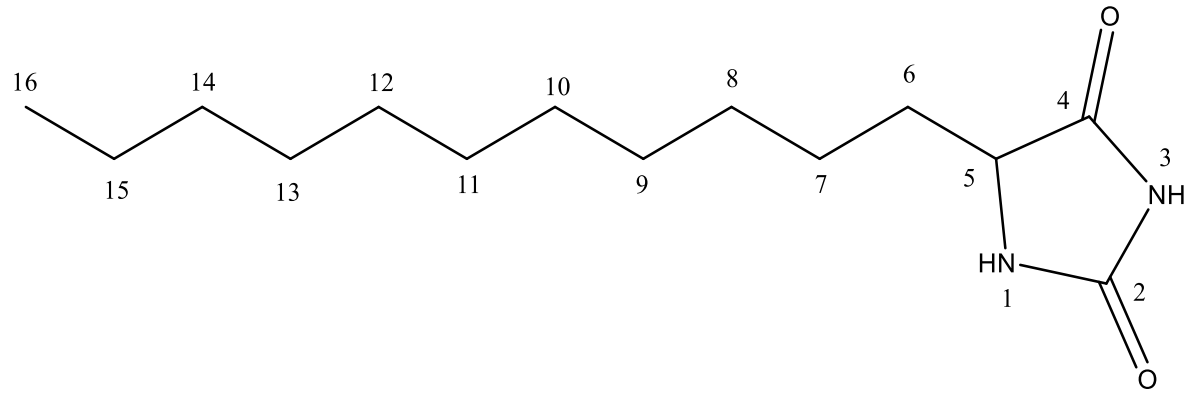

	Proton shift (ppm)	Carbon shift (ppm)
1	6.07	-
2	-	157.9
3	7.93	-
4	-	176.6
5	3.97	58.0
6	1.64	31.8
7-15	1.28	22.6-31.7
16	0.86	14.4

Table i: NMR data

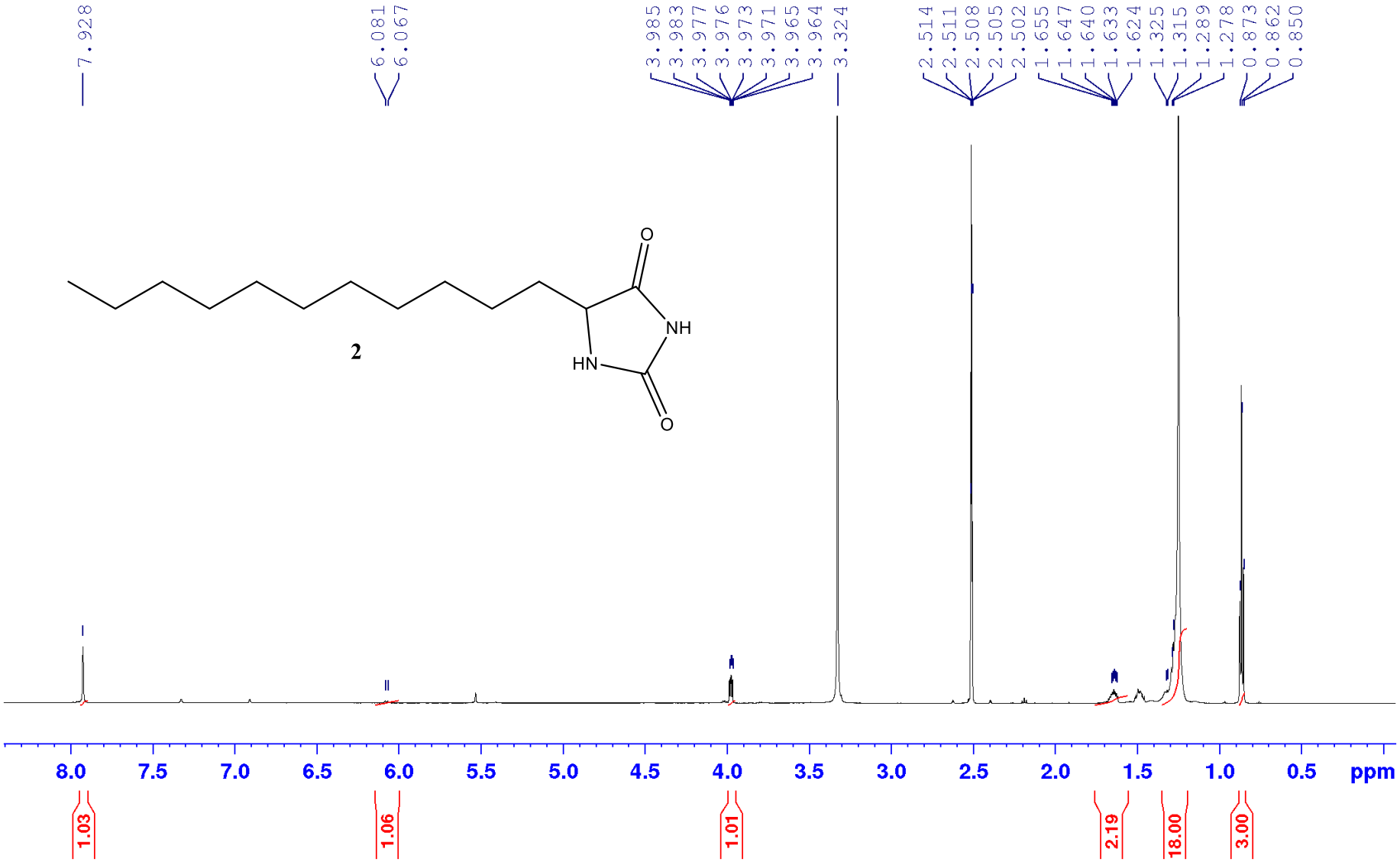

Figure iii: ^{1}H-NMR (600 MHz, $CDCl_3$)

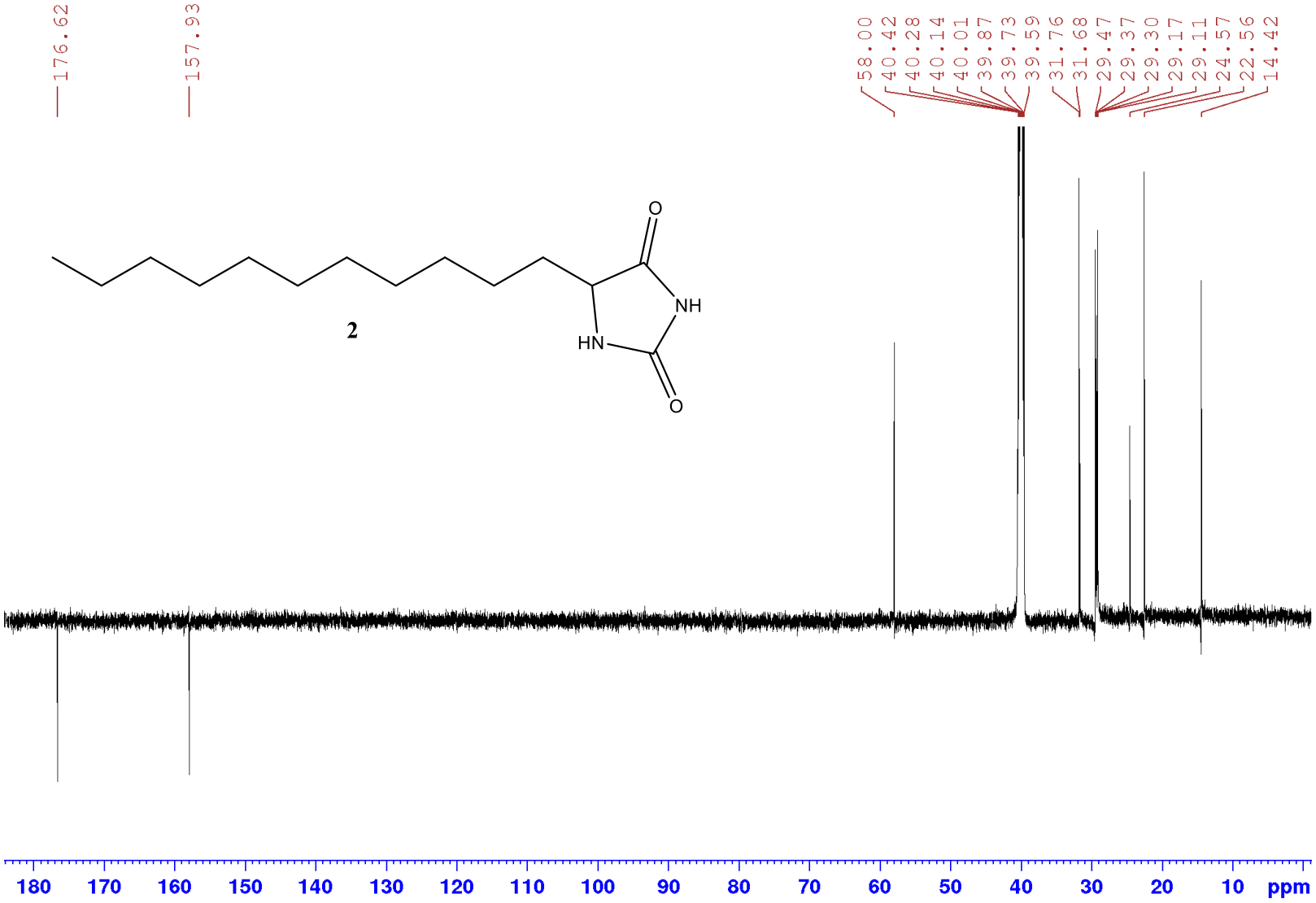

Figure iv: ^{13}C-NMR (600 MHz, $CDCl_3$)

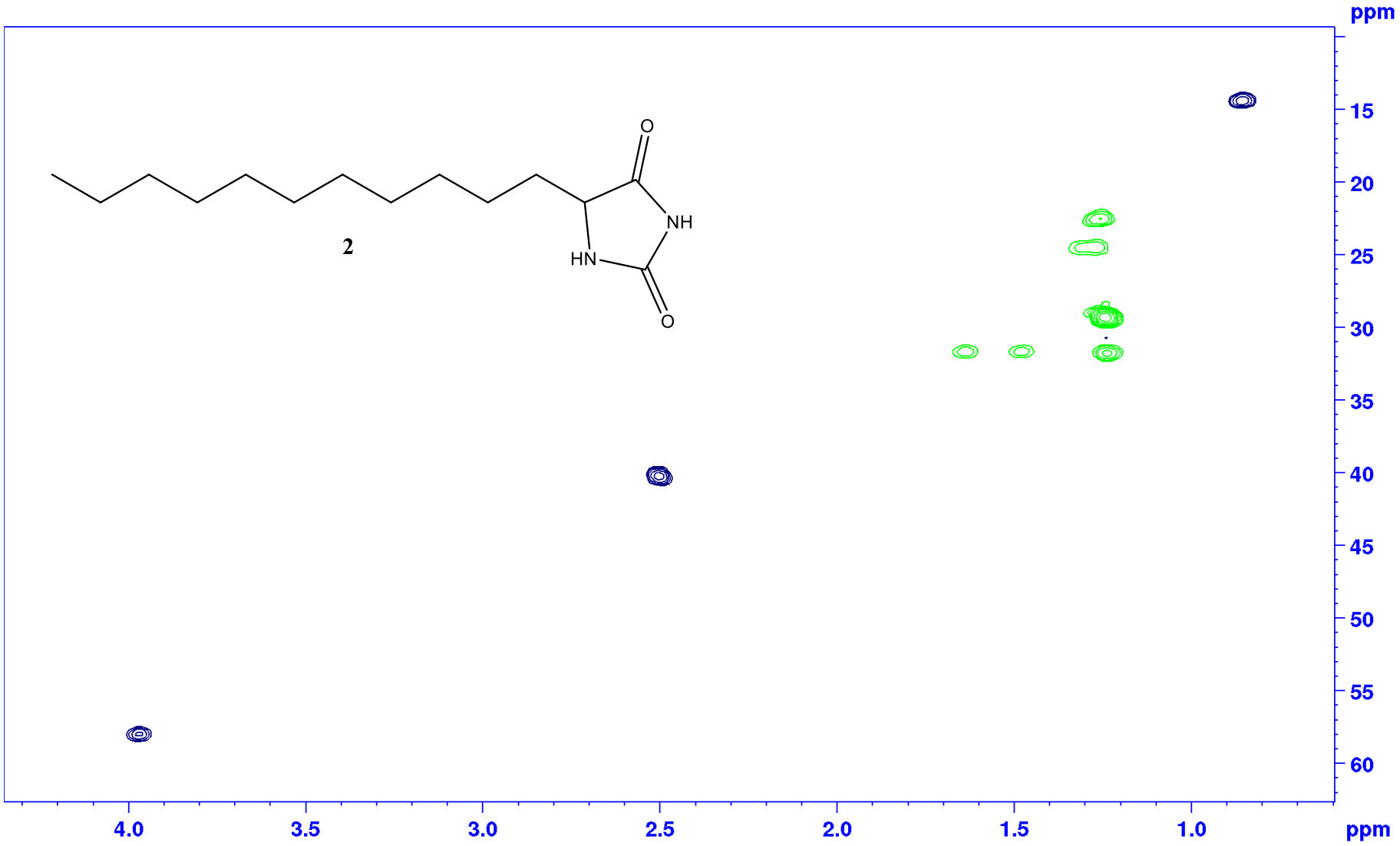

Figure v: HSQC (600 MHz, $CDCl_3$)

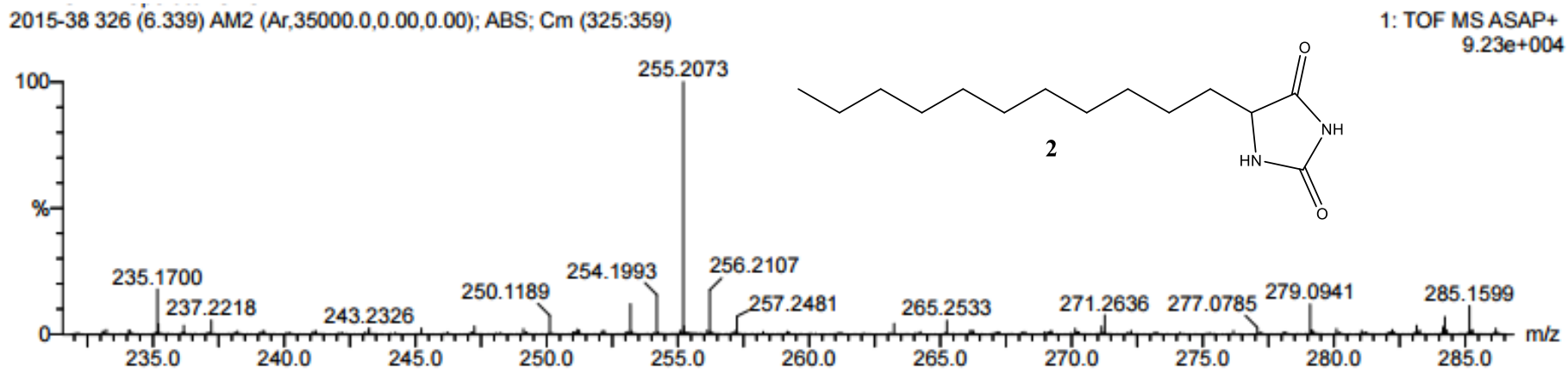

Minimum:				-1.5				
Maximum:		5.0	5.0	50.0				
Mass	Calc. Mass	mDa	PPM	DBE	i-FIT	Norm	Conf(%)	Formula
255.2073	255.2073	0.0	0.0	2.5	1027.6	n/a	n/a	C14 H27 N2 O2

Figure vi: ESI-Q-TOF

Compound 3: 2-aminotridecanoic acid

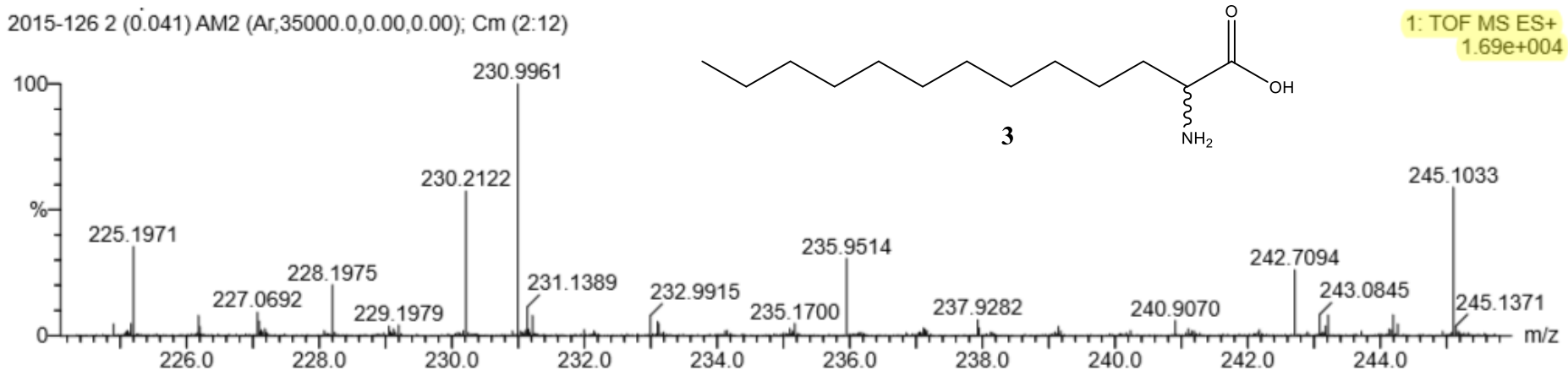

Minimum:				-1.5				
Maximum:		5.0	2.0	50.0				
Mass	Calc. Mass	mDa	PPM	DBE	i-FIT	Norm	Conf(%)	Formula
230.2122	230.2120	0.2	0.9	0.5	834.8	n/a	n/a	C13 H28 N O2 Ion observed [M+H]+

Figure vii: ESI-Q-TOF

Compound 4: 8’-apo-β-caroten-8’-al

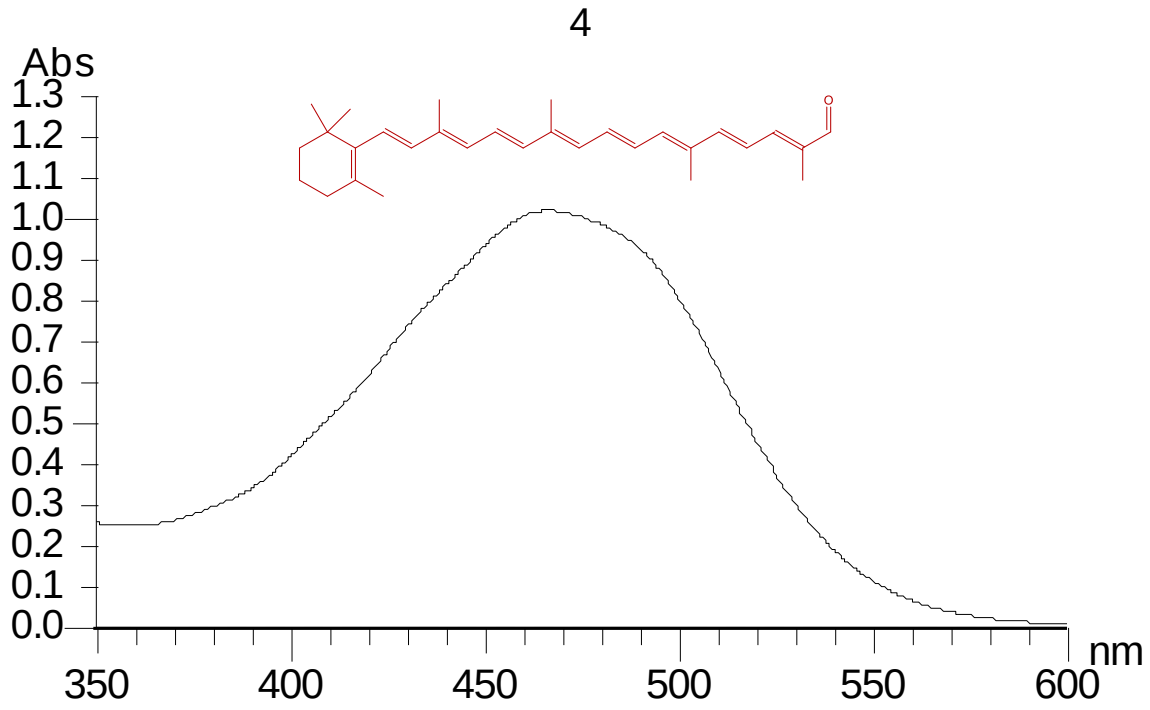

Figure 0.1: UV/vis absorption spectre (DCM)

Peak #	Start (nm)	Apex (nm)	End (nm)	Height (Abs)	Valley (nm)	Valley (Abs)
1	650.0	464.5	362.0	1.271	362.0	0.441
2	362.0	276.0	257.0	0.816	257.0	0.722

Table ii: UV/vis absorption data

Compound 10: dibenzyl N,N-dibenzyl-L-glutamate

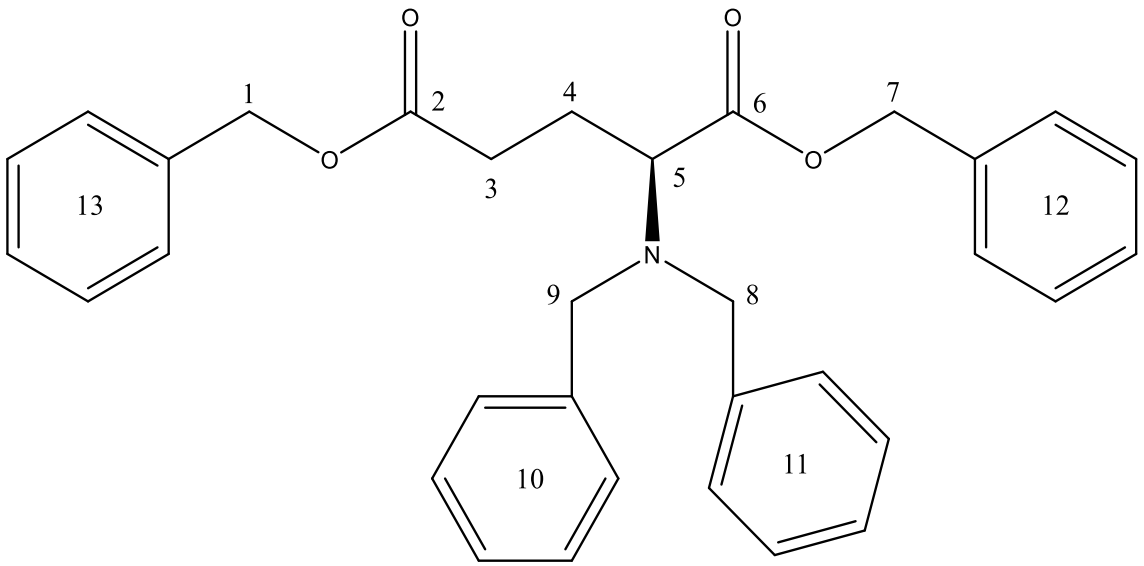

	Proton shift (ppm)	Carbon shift (ppm)
1	5.18	66.3
2	-	173.0
3	2.05	24.3
4	2.40	30.7
5	3.40	54.5
6	-	172.3
7	4.95	65.2
8	3.87	59.9
9	3.49	59.9
10-13	7.18-7.40	127.0-129.0, 136.0, 139.3

Table iii: NMR data

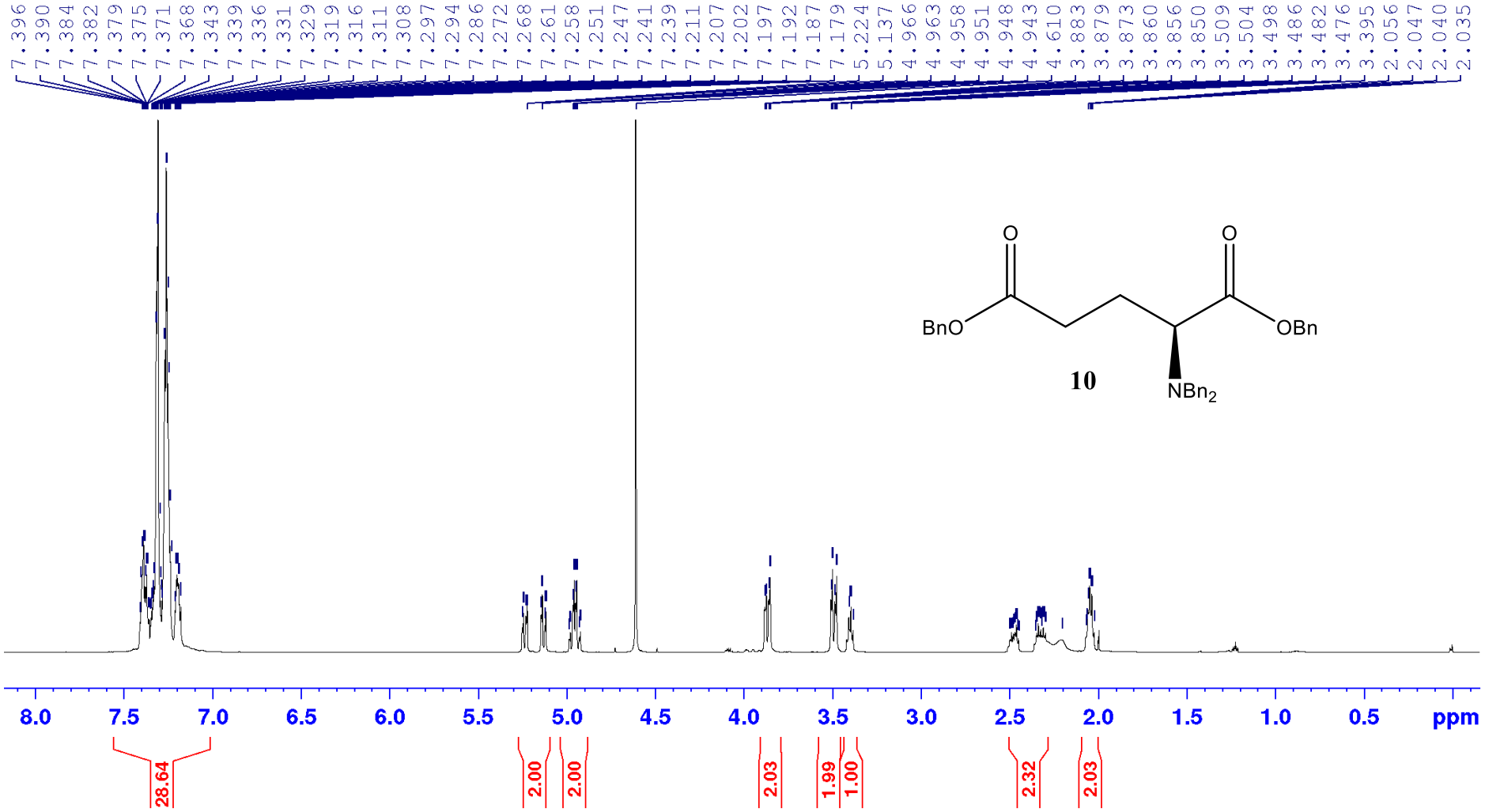

Figure viii: ^{1}H-NMR (600 MHz, $CDCl_3$), contamination of BnBr, δ = 4.61, 7.18-7.40

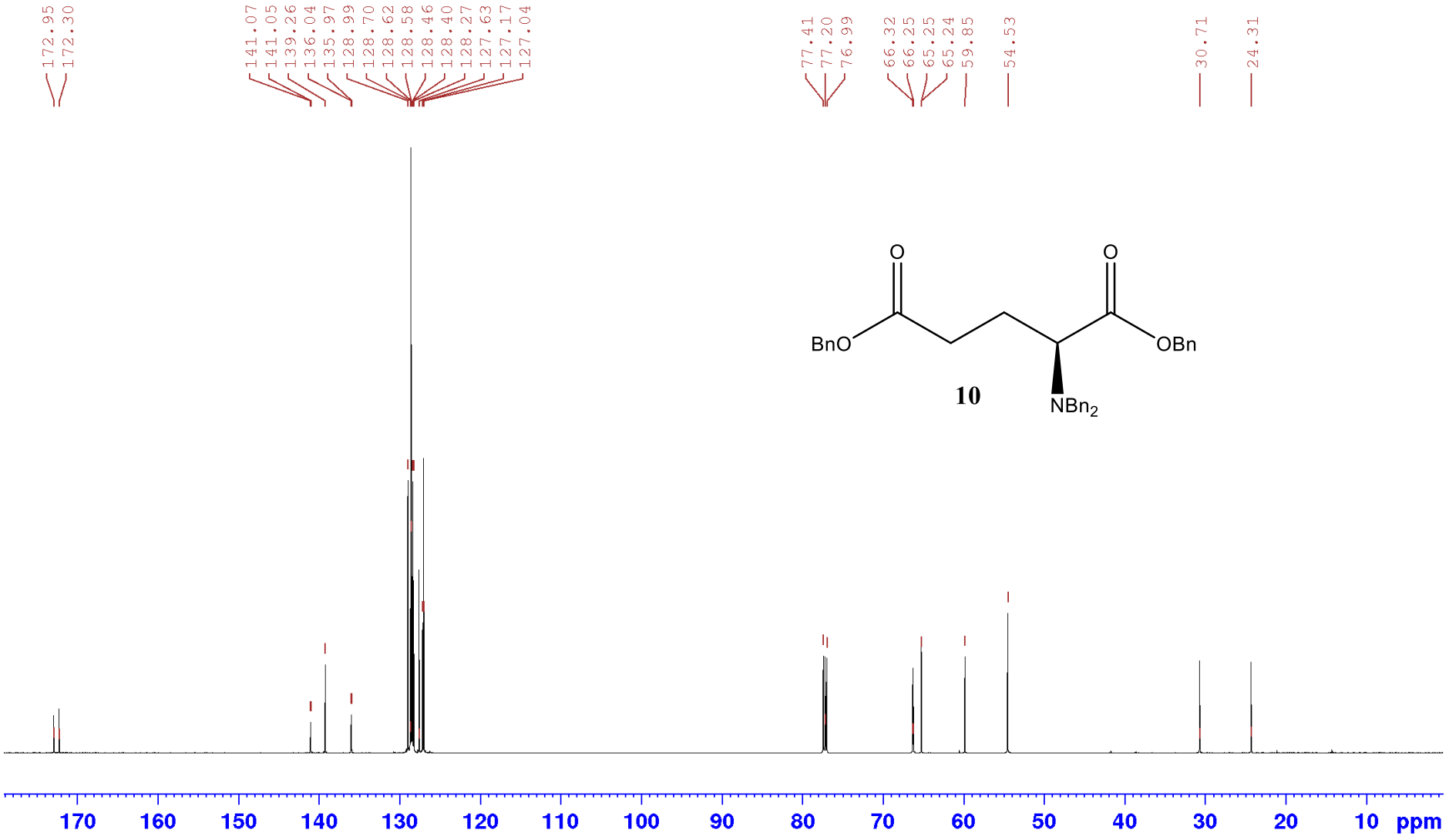

Figure ix: ^{13}C-NMR (600 MHz, $CDCl_3$), contamination of BnBr, δ = 65, 127-129

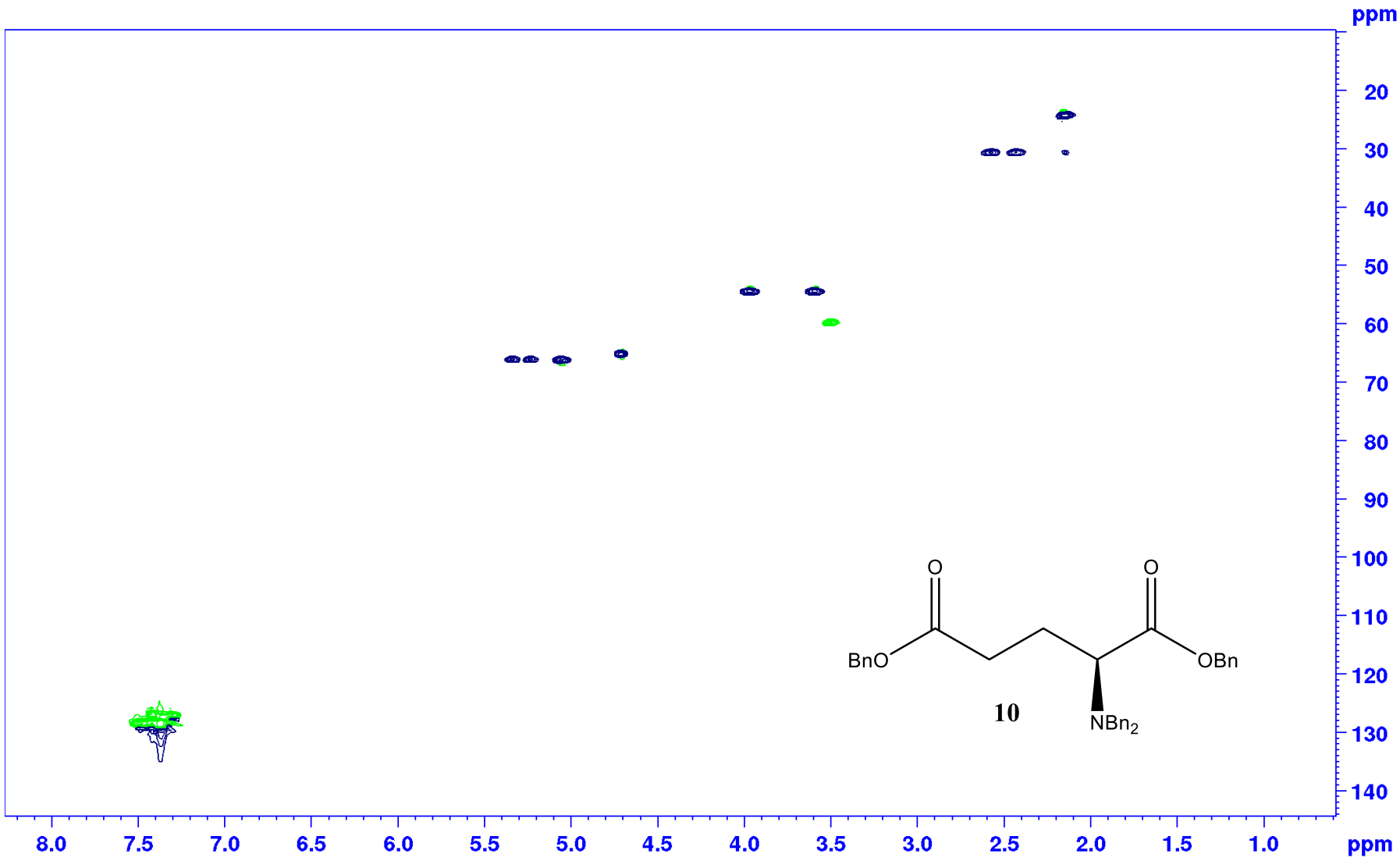

Figure x: HSQC (600 MHz, $CDCl_3$)

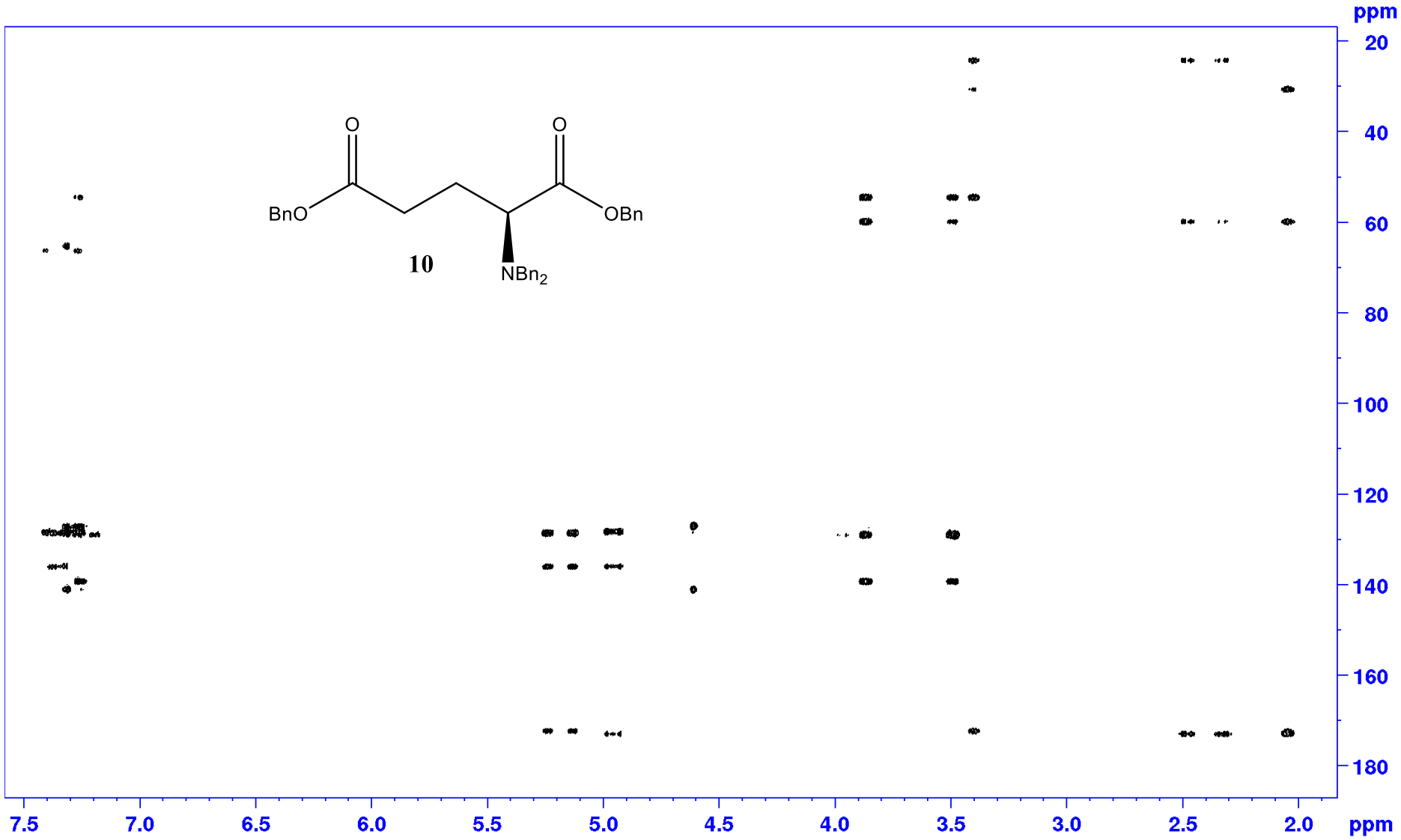

Figure xi: HMBC (600 MHz, $CDCl_3$)

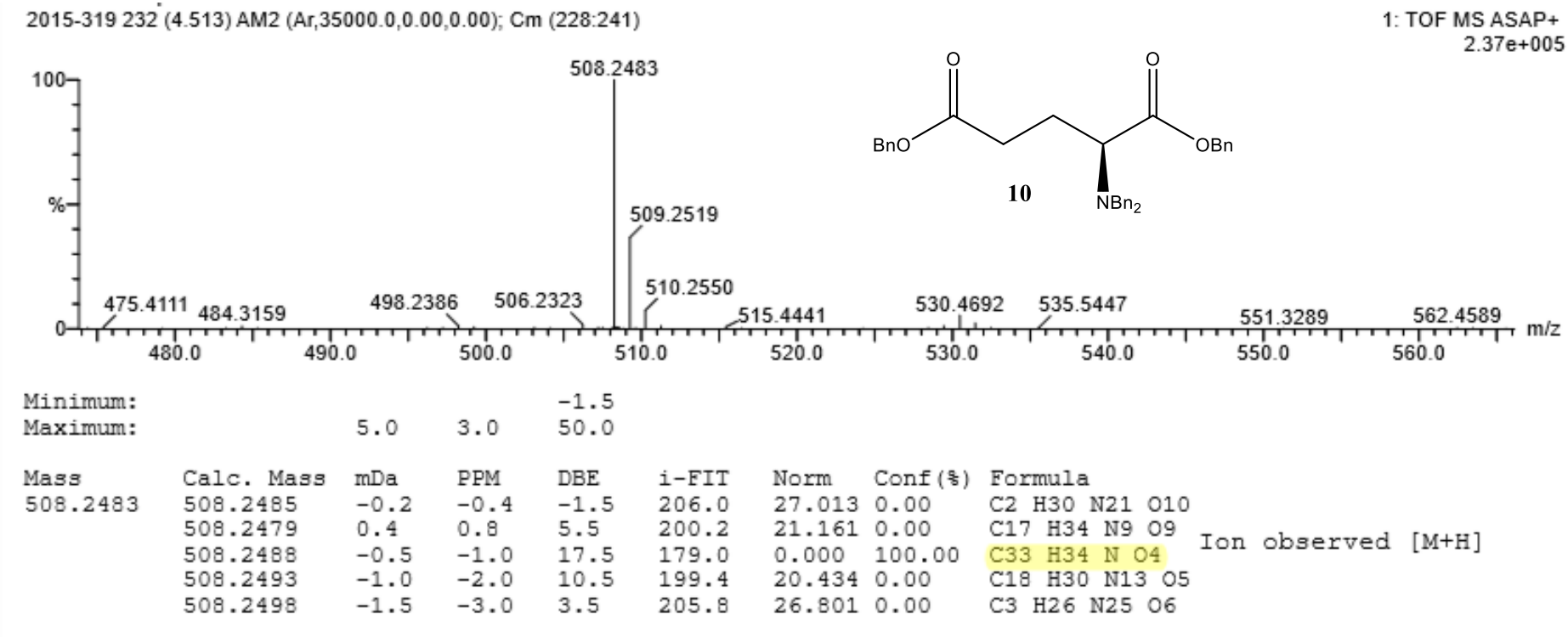

Figure xii: ASAP^{+}-Q-TOF

Compound 13: dimethyl (*tert*-butoxycarbonyl)-L-glutamate

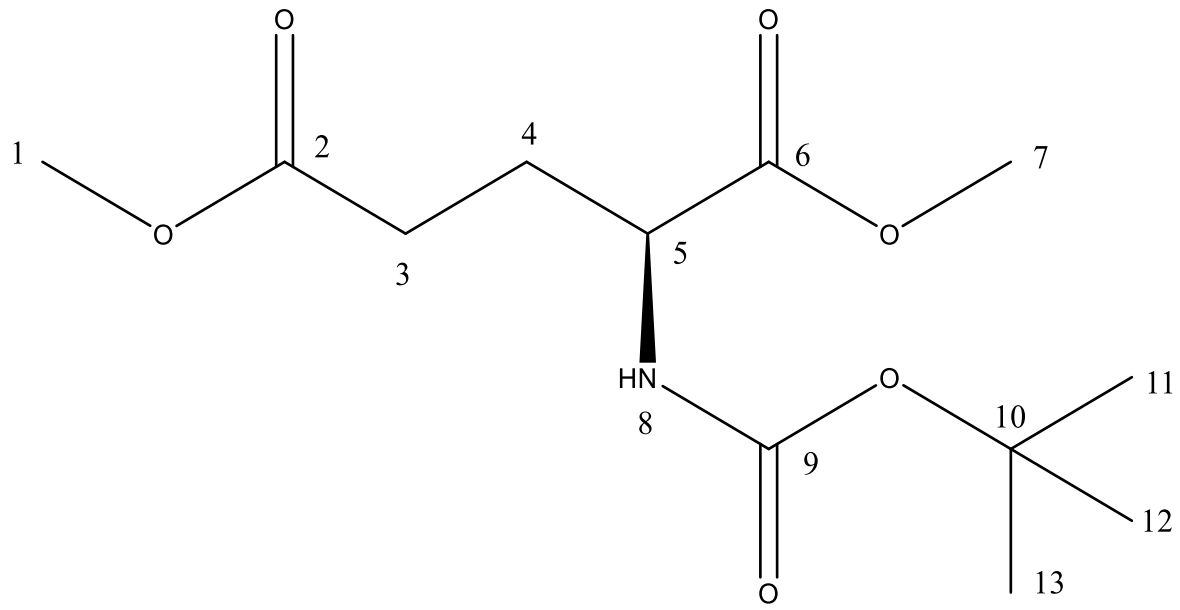

	Proton shift (ppm)	Carbon shift (ppm)
1	3.68	51.8
2	-	173.2
3	2.41	30.0
4	1.97, 2.18	27.7
5	4.34	52.8
6	-	172.7
7	3.75	52,4
8	5.17	-
9	-	155.3
10	-	80.0
11-13	1.44	28.3

Table iv: NMR data

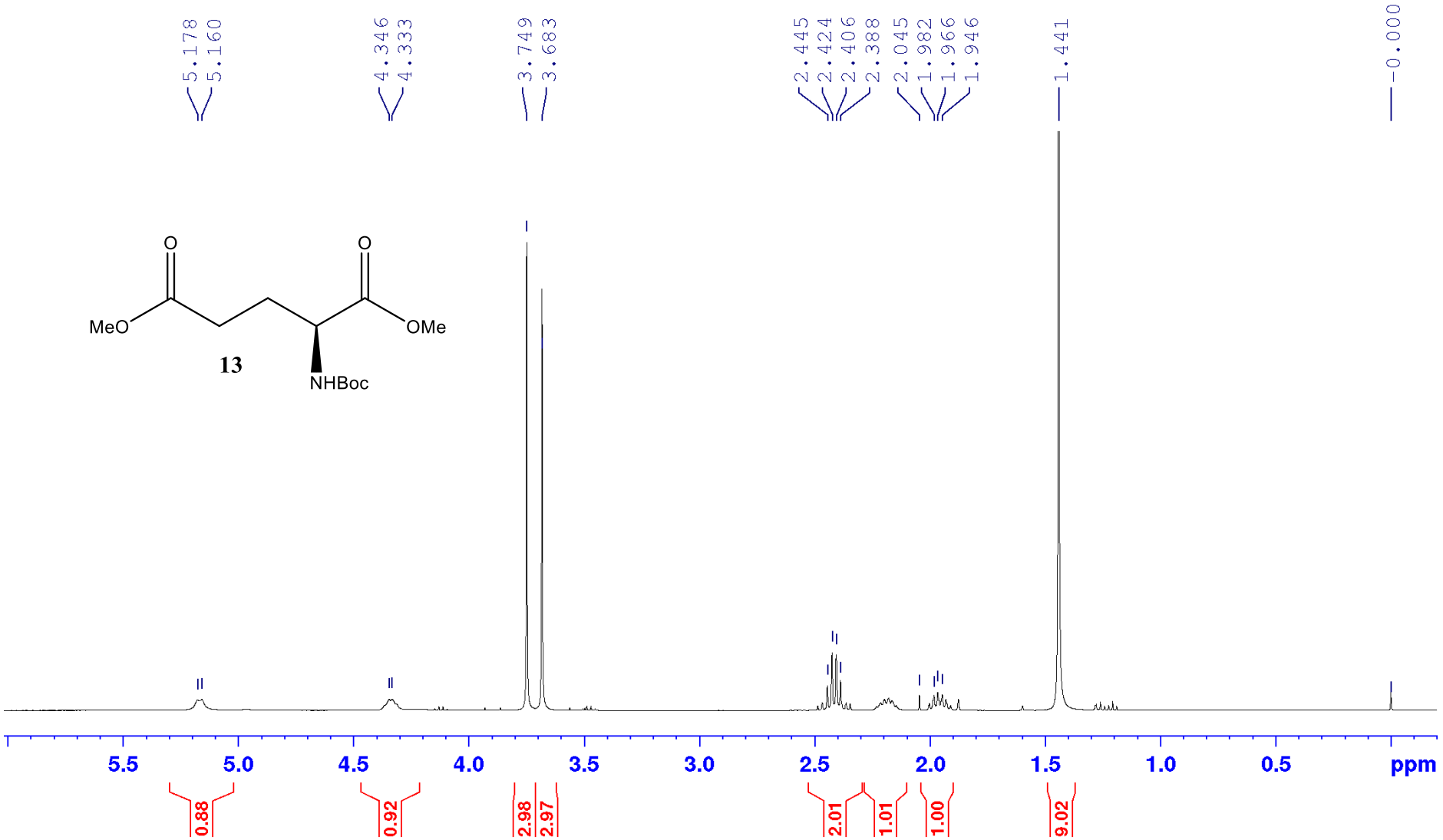

Figure xiii: ^{1}H-NMR (400 MHz, $CDCl_3$)

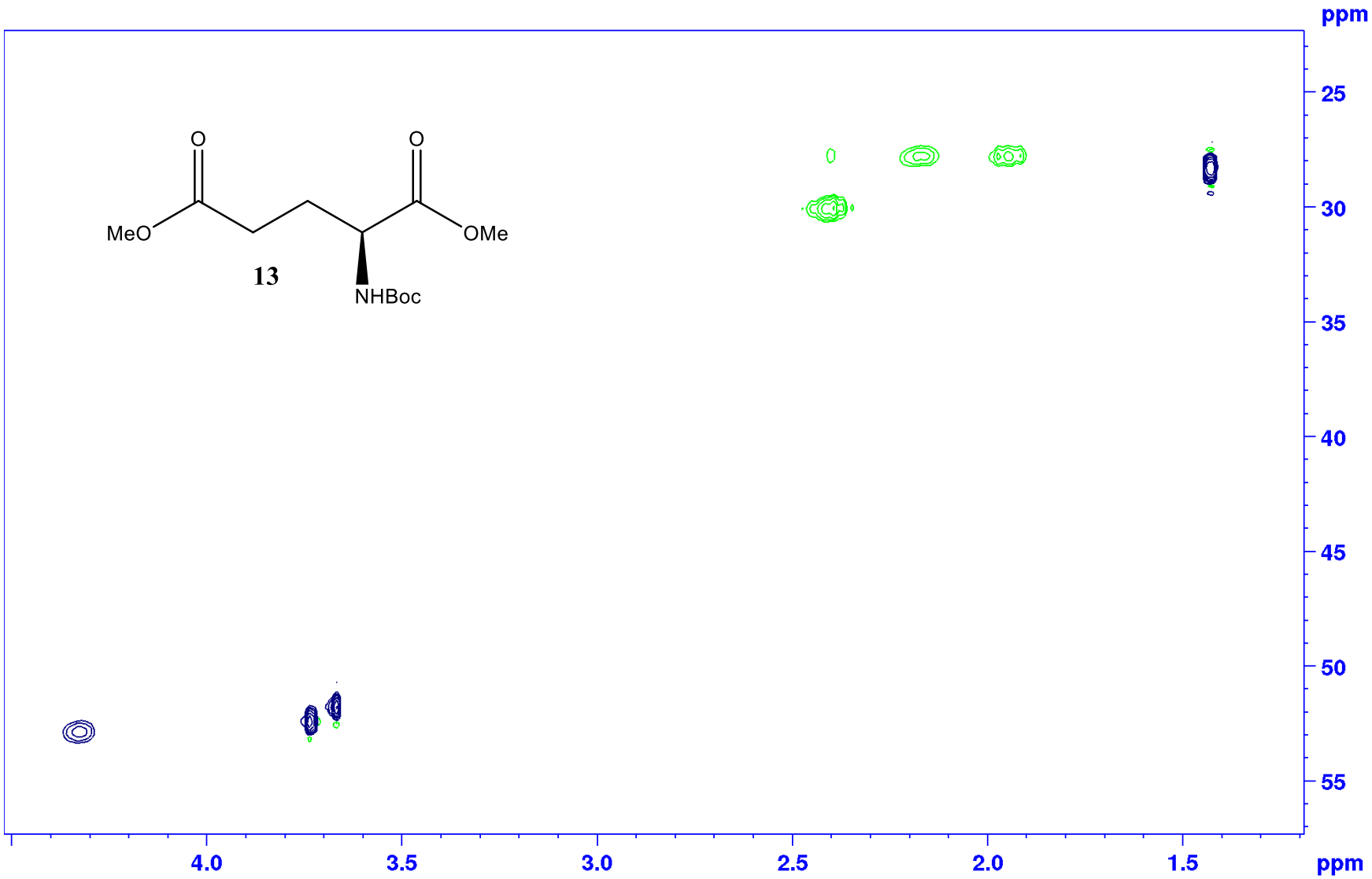

Figure xiv: HSQC (400 MHz, $CDCl_3$)

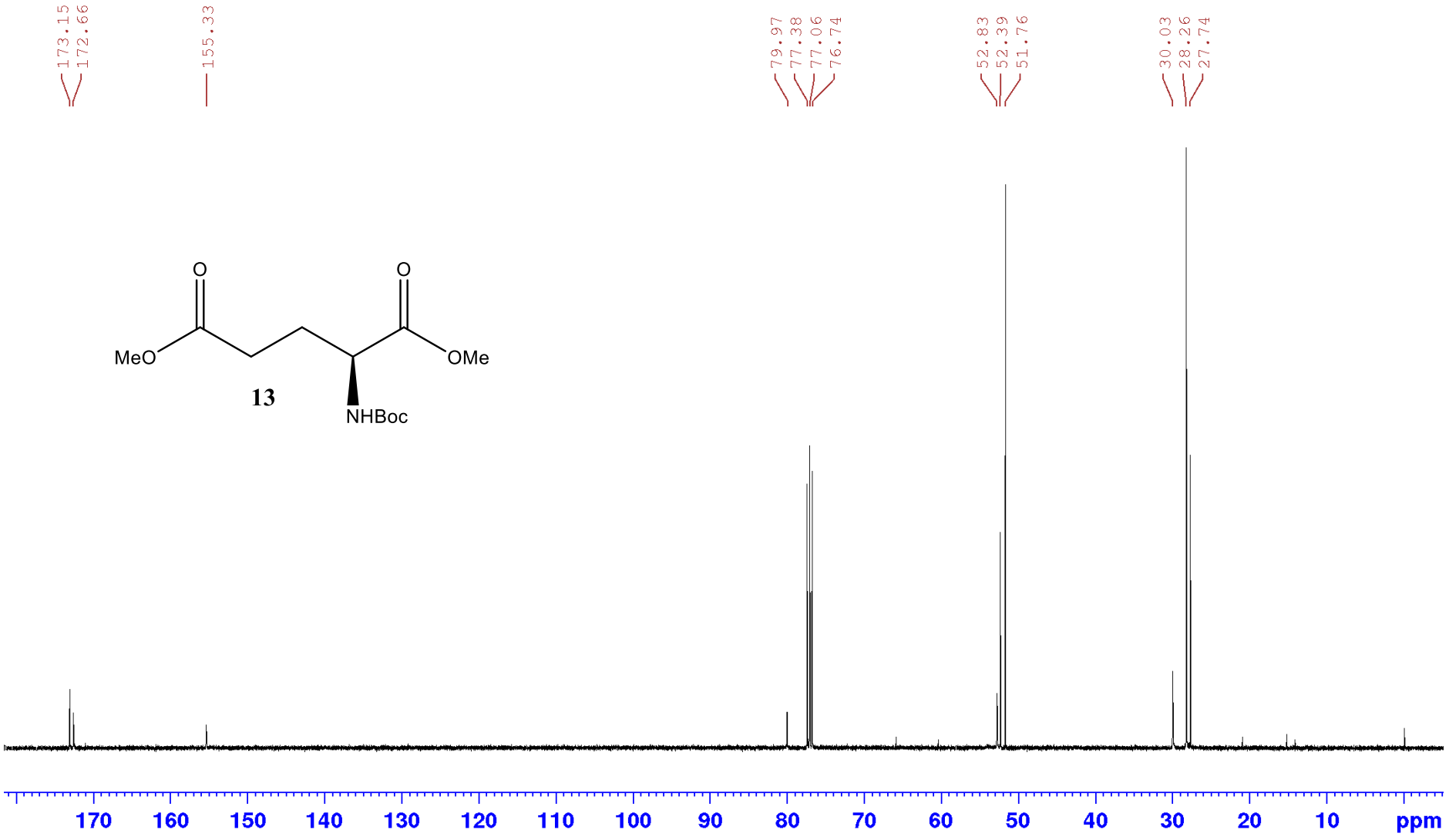

Figure xv: ^{13}C-NMR (400 MHz, $CDCl_3$)

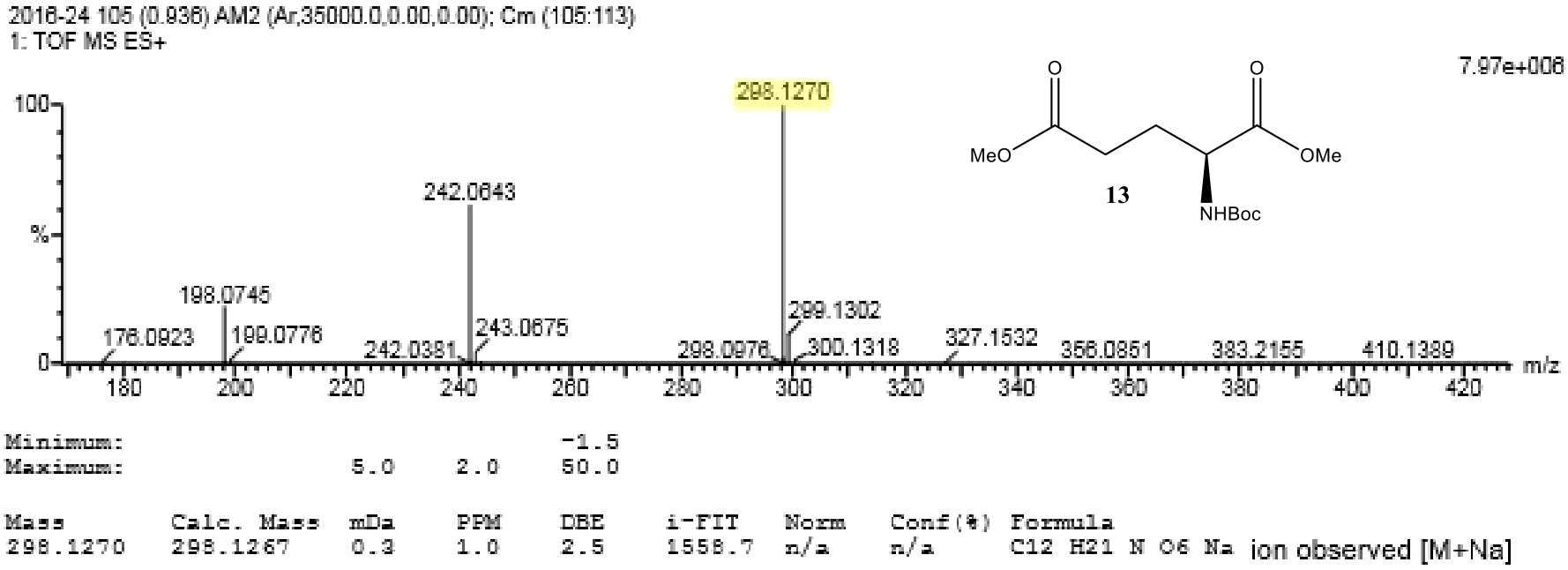

Figure xvi: ESI-Q-TOF

Compound 14: dimethyl di(tert-butoxycarbonyl)-L-glutamate

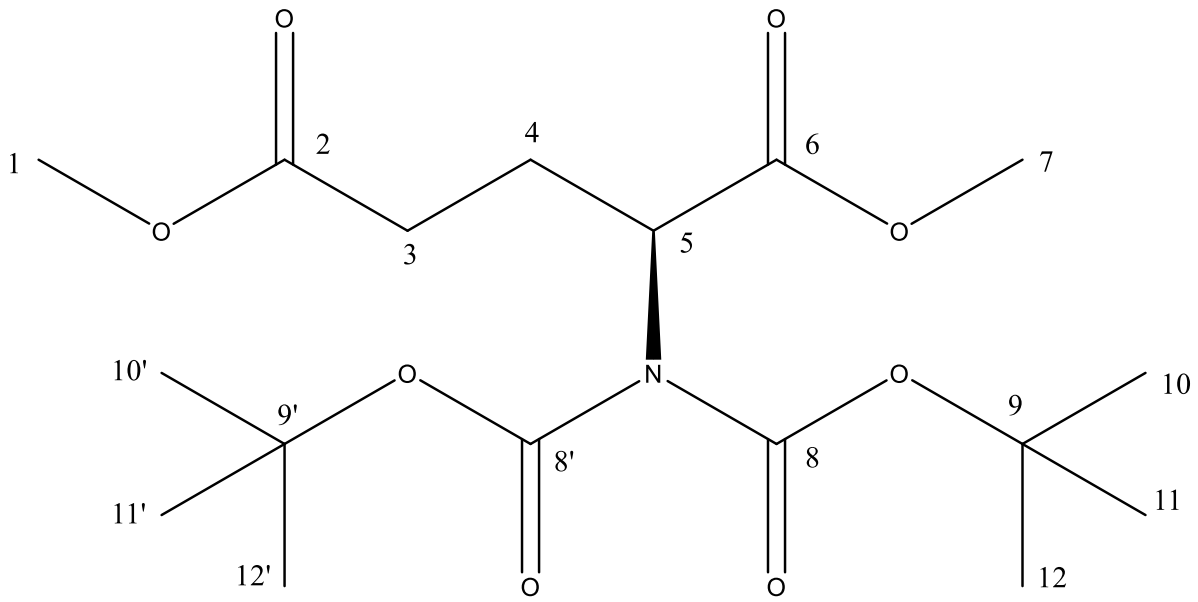

	Proton shift (ppm)	Carbon shift (ppm)
1	3.68	51.7
2	-	173.1
3	2.20, 2.52	25.2
4	2.46	30.6
5	4.95	57.3
6	-	170.8
7	3.73	52,2
8, 8’	-	151.9
9, 9’	-	83.3
10-12, 10’-12’	1.50	28.0

Table v: NMR data

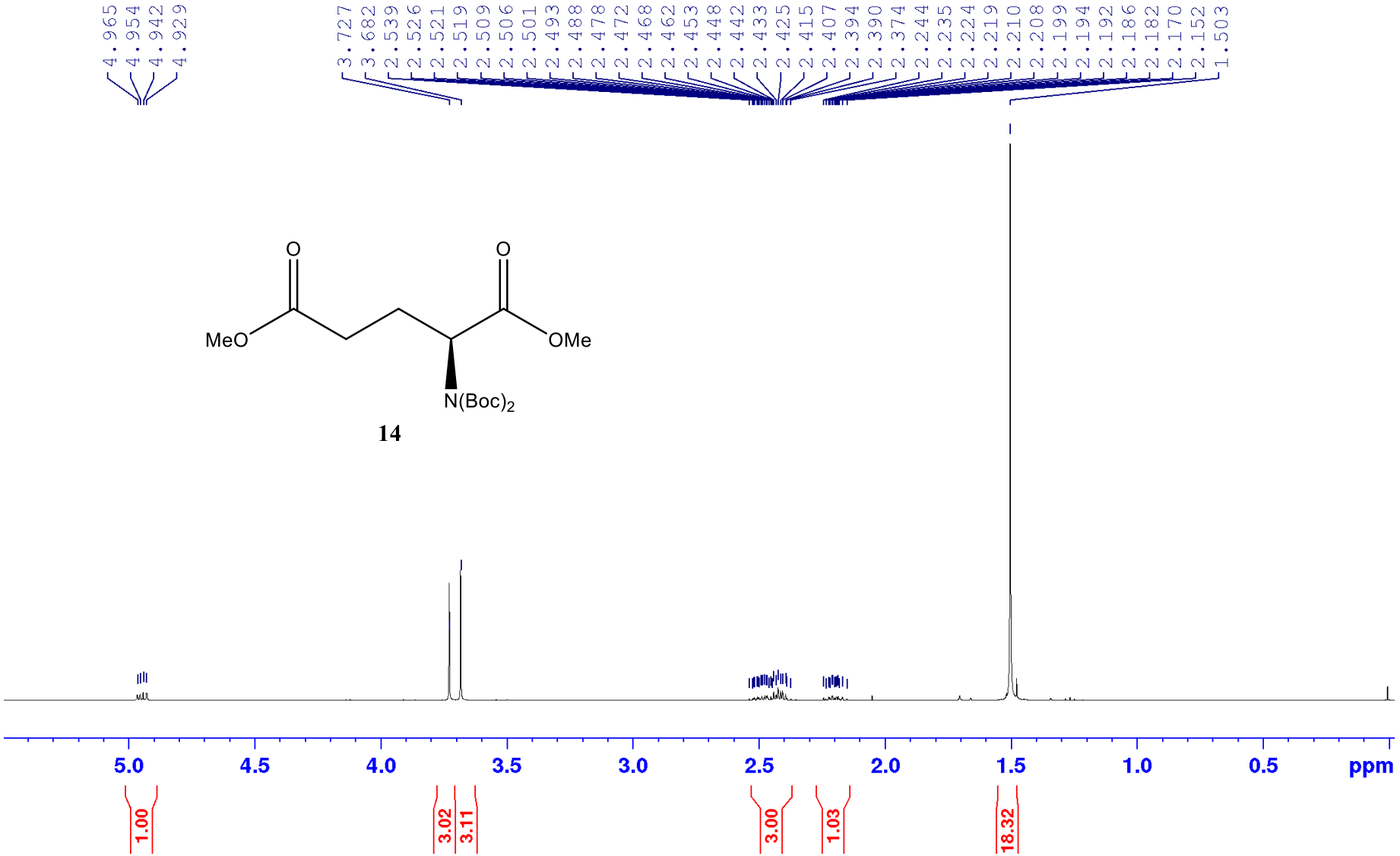

14

Figure xvii: ^{1}H-NMR (400 MHz, $CDCl_3$)

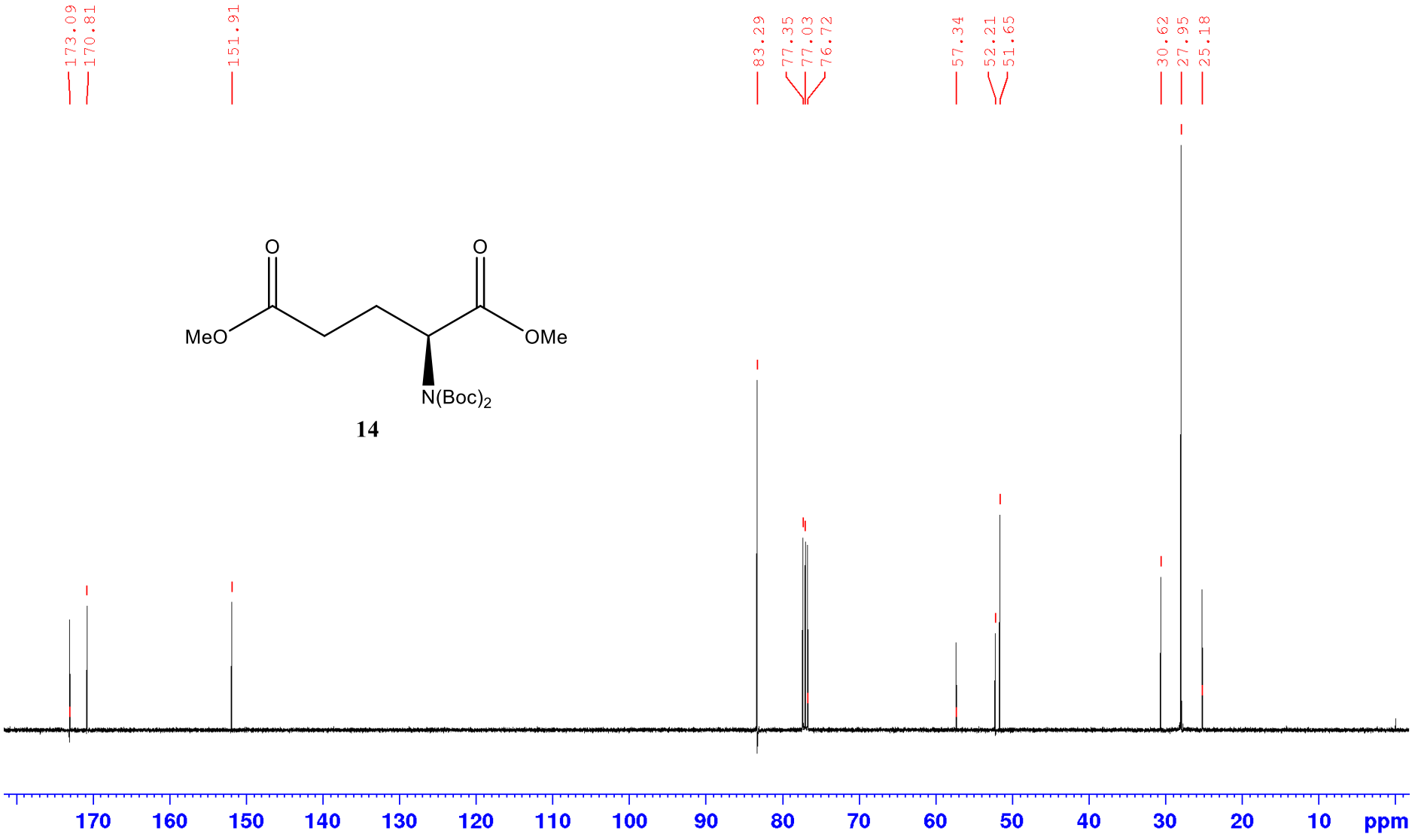

Figure xviii: ^{13}C-NMR (400 MHz, $CDCl_3$)

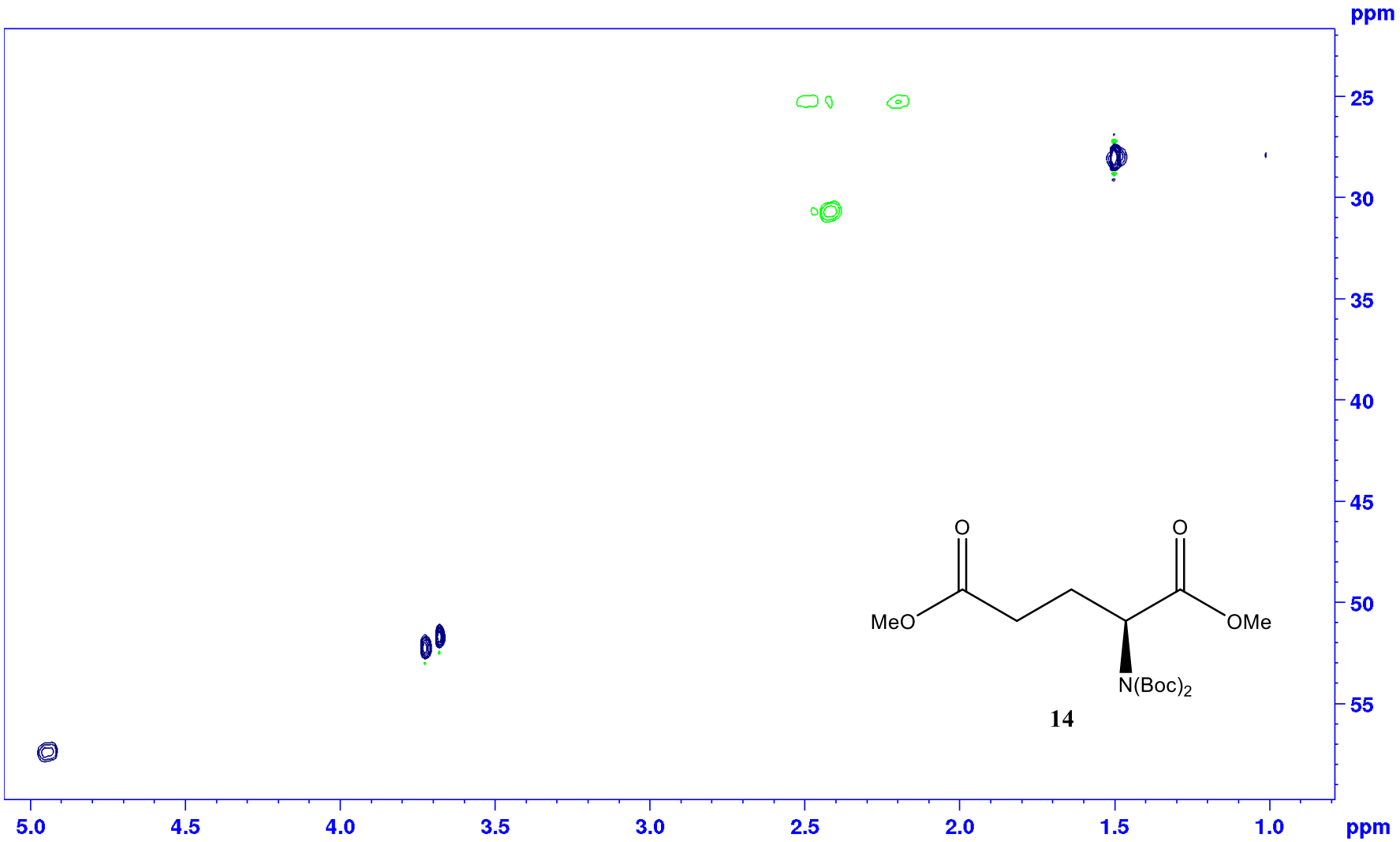

Figure xix: HSQC (400 MHz, $CDCl_3$)

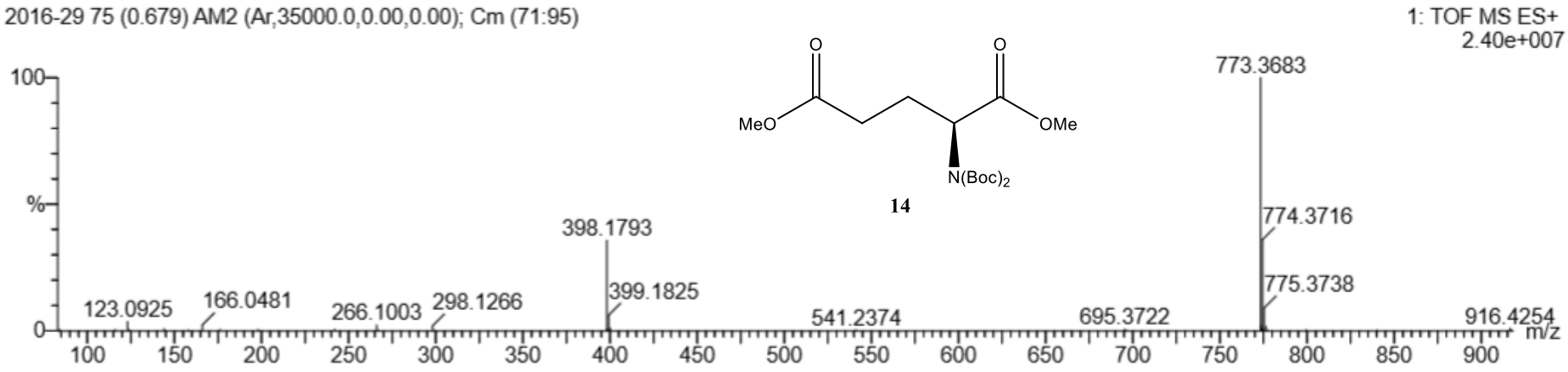

Minimum:				-1.5				
Maximum:		5.0	3.0	50.0				
Mass	Calc. Mass	mDa	PPM	DBE	i-FIT	Norm	Conf(%)	Formula
398.1793	398.1791	0.2	0.5	3.5	97.9	0.325	72.22	C17 H29 N O8 Na Ion Observed[M+Na]
	398.1788	0.5	1.3	7.5	98.9	1.382	25.10	C15 H24 N7 O6
	398.1801	-0.8	-2.0	12.5	101.5	3.924	1.98	C16 H20 N11 O2
	398.1804	-1.1	-2.8	8.5	102.5	4.962	0.70	C18 H25 N5 O4 Na

Figure xx: ESI-Q-TOF

Compound 15: methyl (2*S*)-2-[bis(*tert*-butoxycarbonyl)amino]-5-oxopentanoate

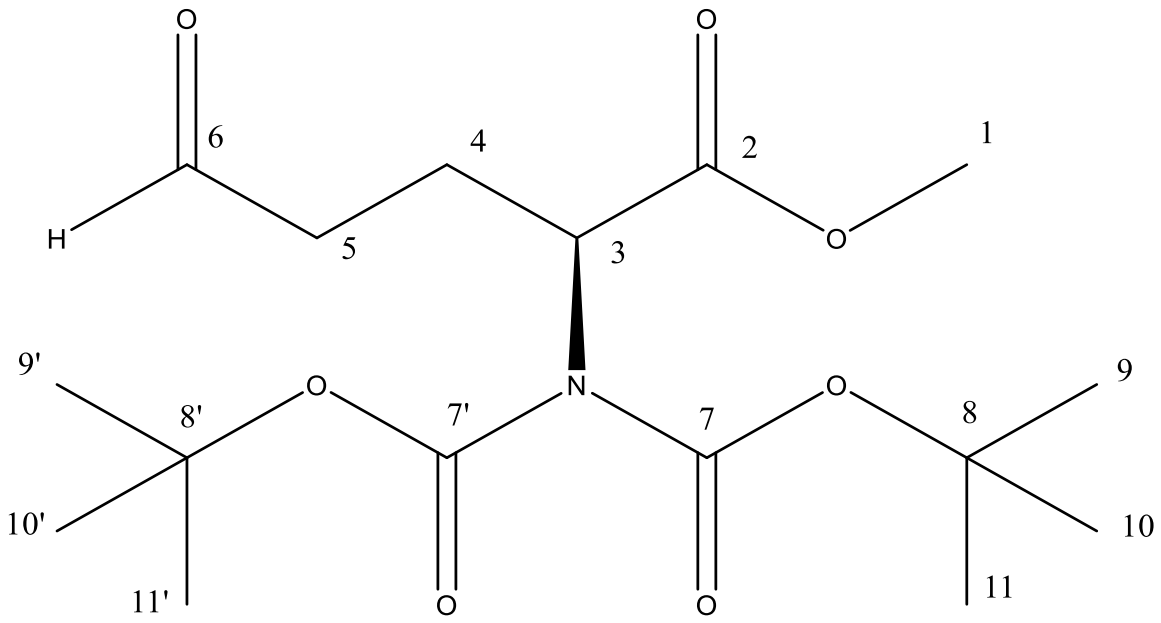

	Proton shift (ppm)	Carbon shift (ppm)
1	3.74	52.3
2		170.8
3	4.90	57.3
4	2.15-2.61	22.5
5		40.5
6	9.78	201.0
7		152.0
8, 8’		83.5
9-11, 9’-11’	1.50	28.0

Table vi: NMR data

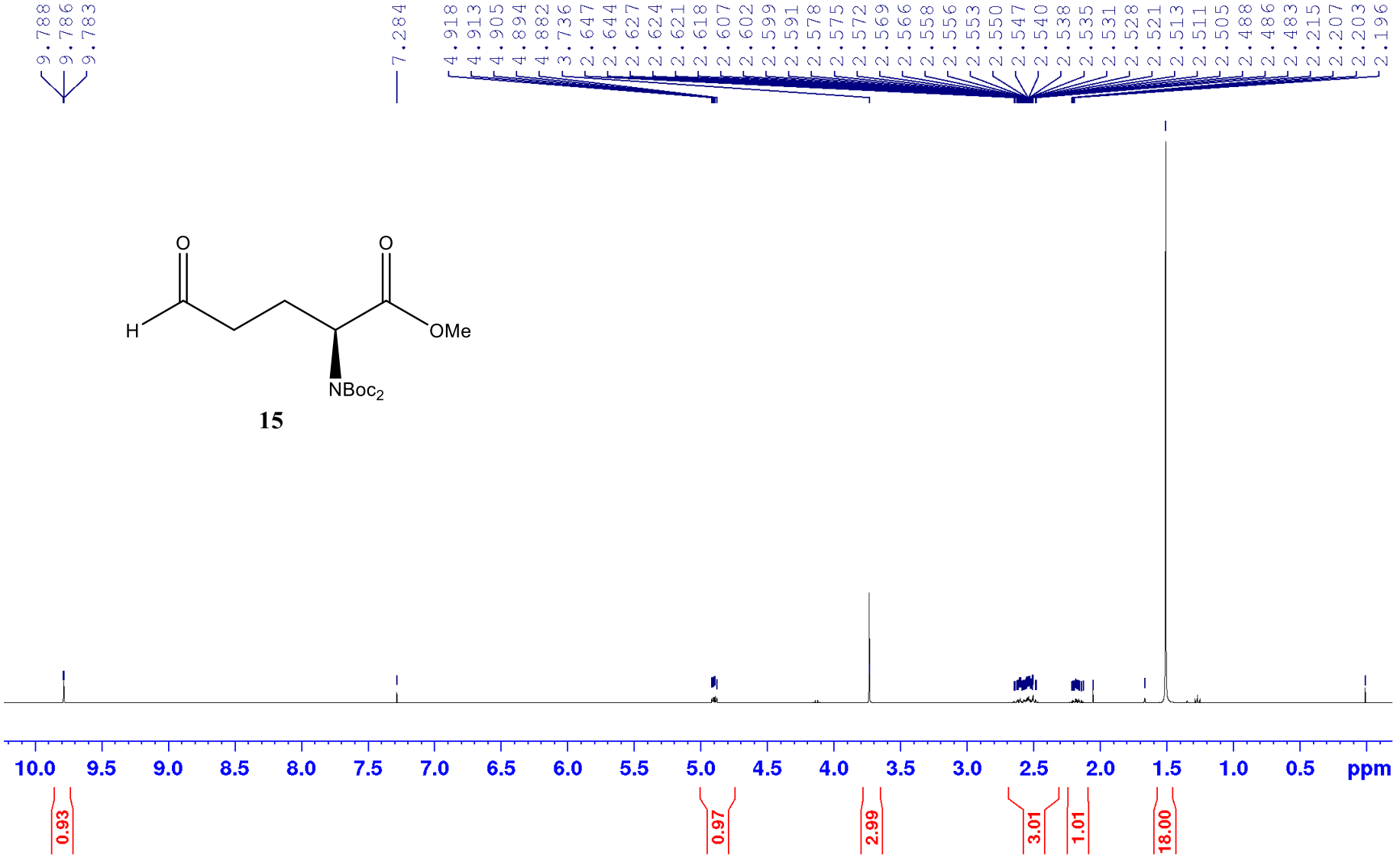

15

Figure xxi: ^{1}H-NMR (400 MHz, $CDCl_3$)

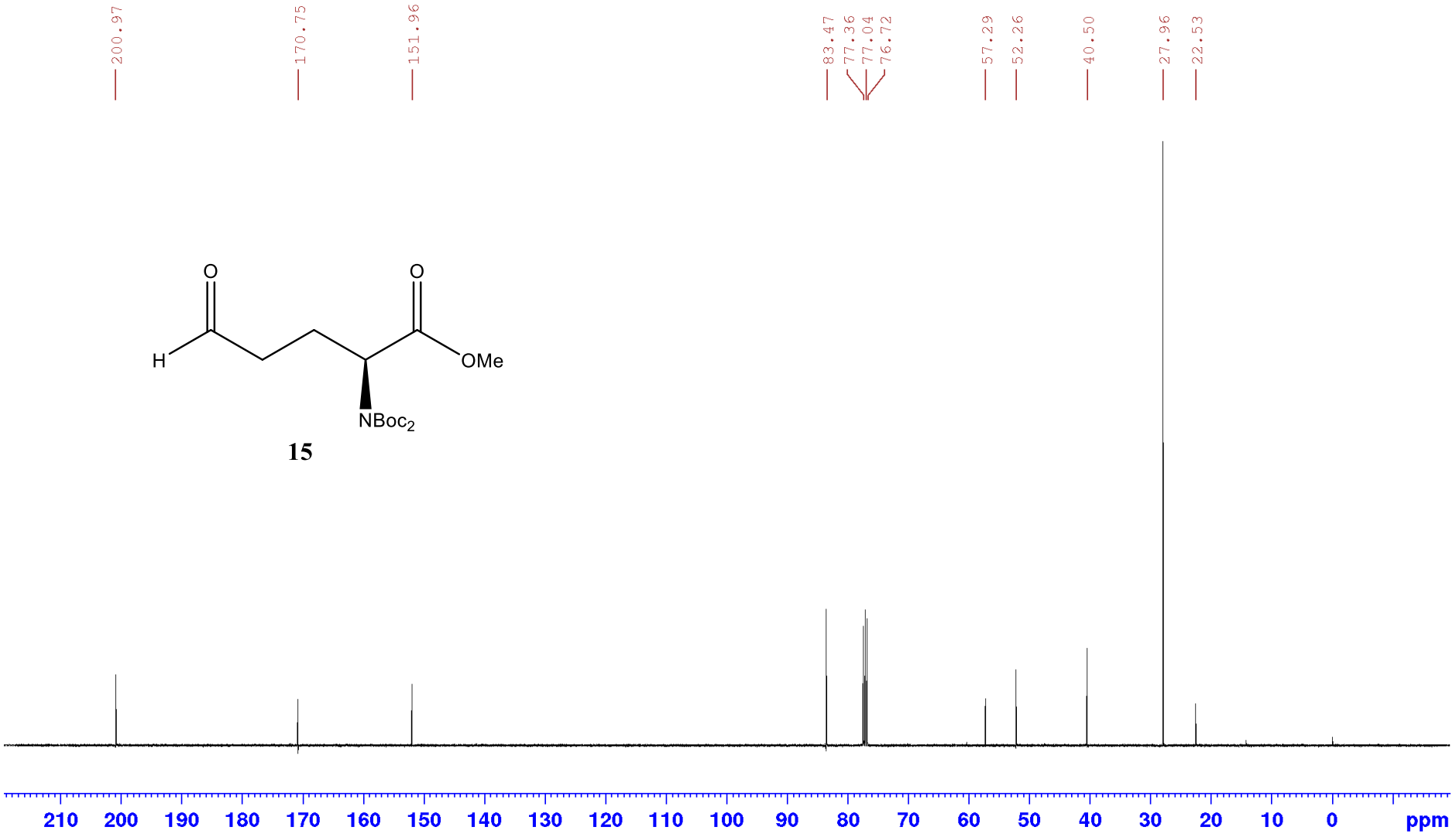

Figure xxii: ^{13}C-NMR (400 MHz, $CDCl_3$)

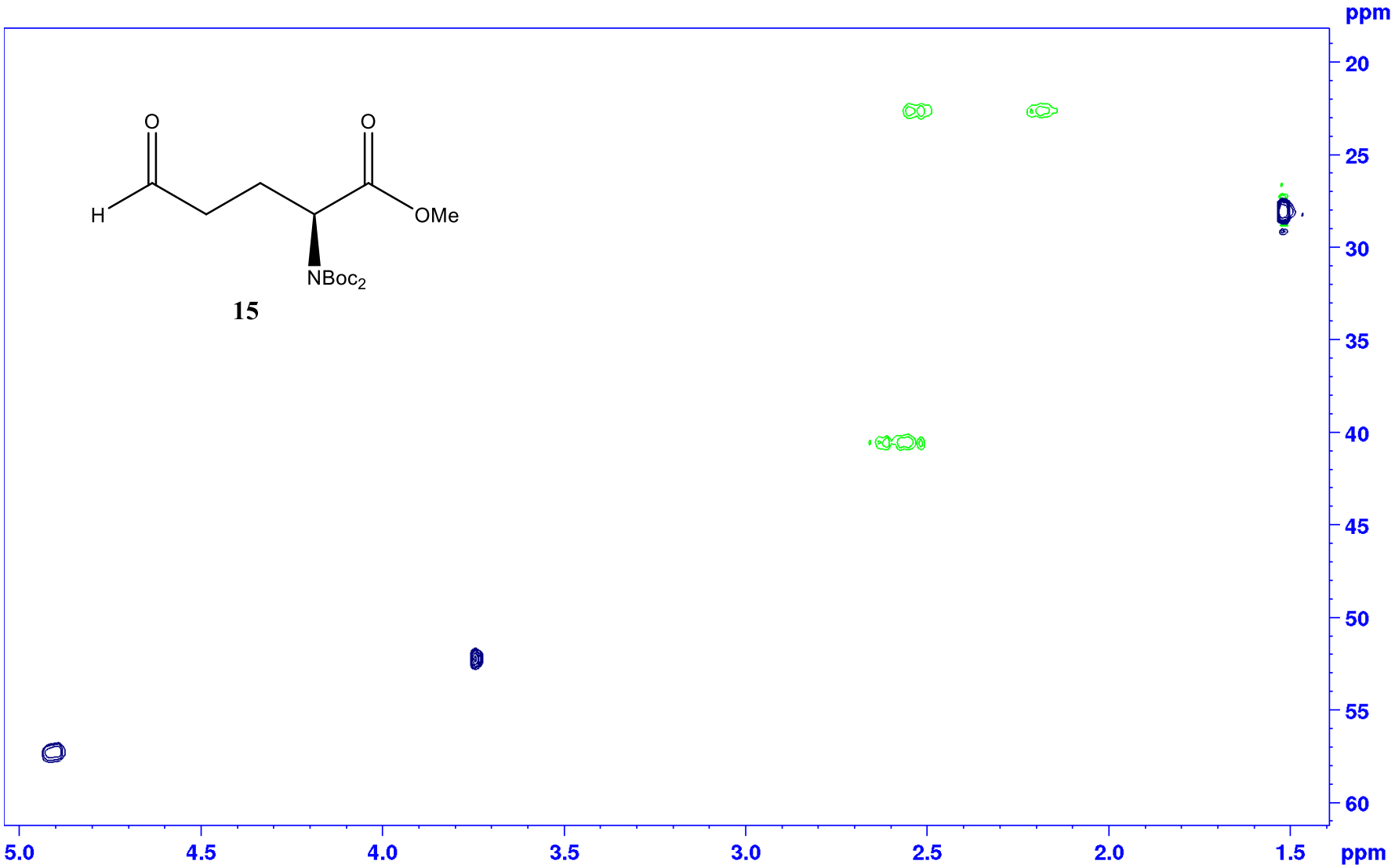

Figure xxiii: Excerpt from HSQC (400 MHz, $CDCl_3$)

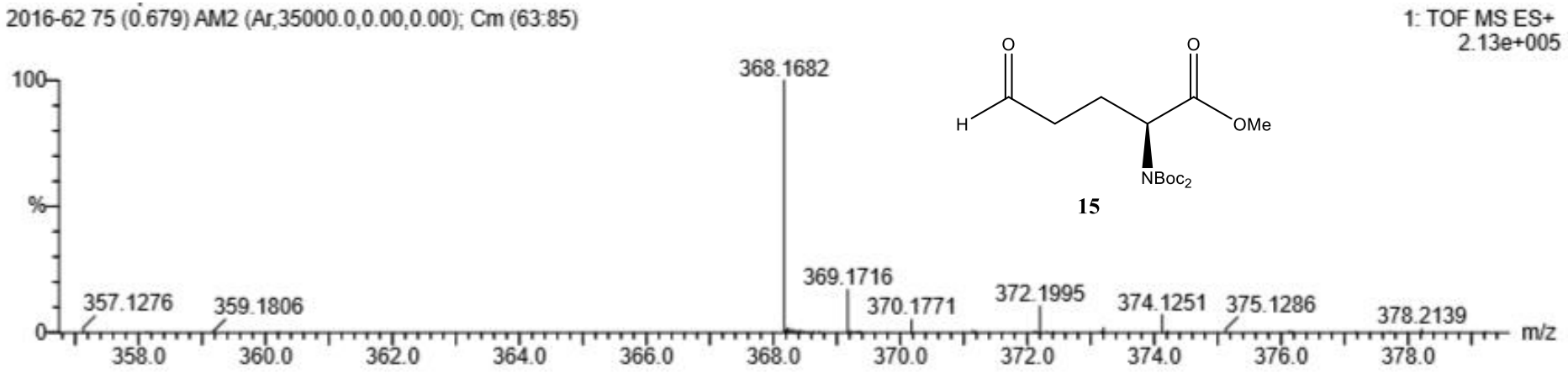

Minimum:				-1.5					
Maximum:		5.0	2.0	50.0					
Mass	Calc. Mass	mDa	PPM	DBE	i-FIT	Norm	Conf(%)	Formula	Ion observed M+Na
368.1682	368.1685	-0.3	-0.8	3.5	278.3	0.214	80.76	C16 H27 N O7 Na	
	368.1682	0.0	0.0	7.5	279.7	1.648	19.24	C14 H22 N7 O5	

Figure xxiv: ESI-Q-TOF

Compound 16: Methyl (2*S*)-2-[bis(*tert*-butoxycarbonyl)amino]-5-hydroxypentanoate

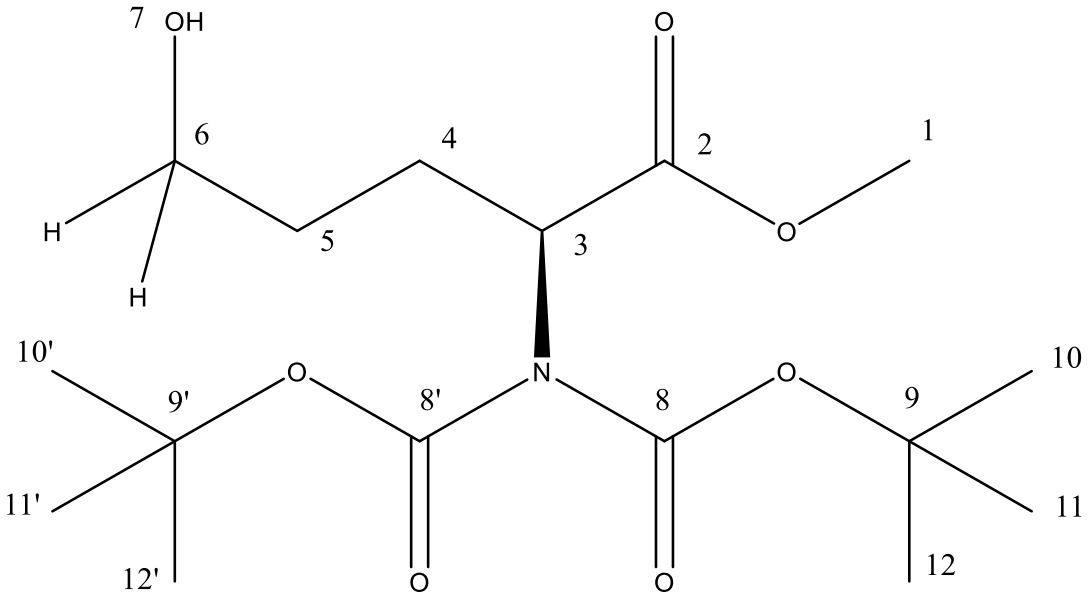

	Proton shift (ppm)	Carbon shift (ppm)
1	3.72	52.2
2	-	171.4
3	4.89	57.9
4	1.94, 2.25	26.4
5	1.65	29.4
6	3.69	65.9
7	1.52	-
8, 8’	-	152.2
9, 9’	-	83.2
10-12, 10’-12’	1.50	28.0

Table vii: NMR data

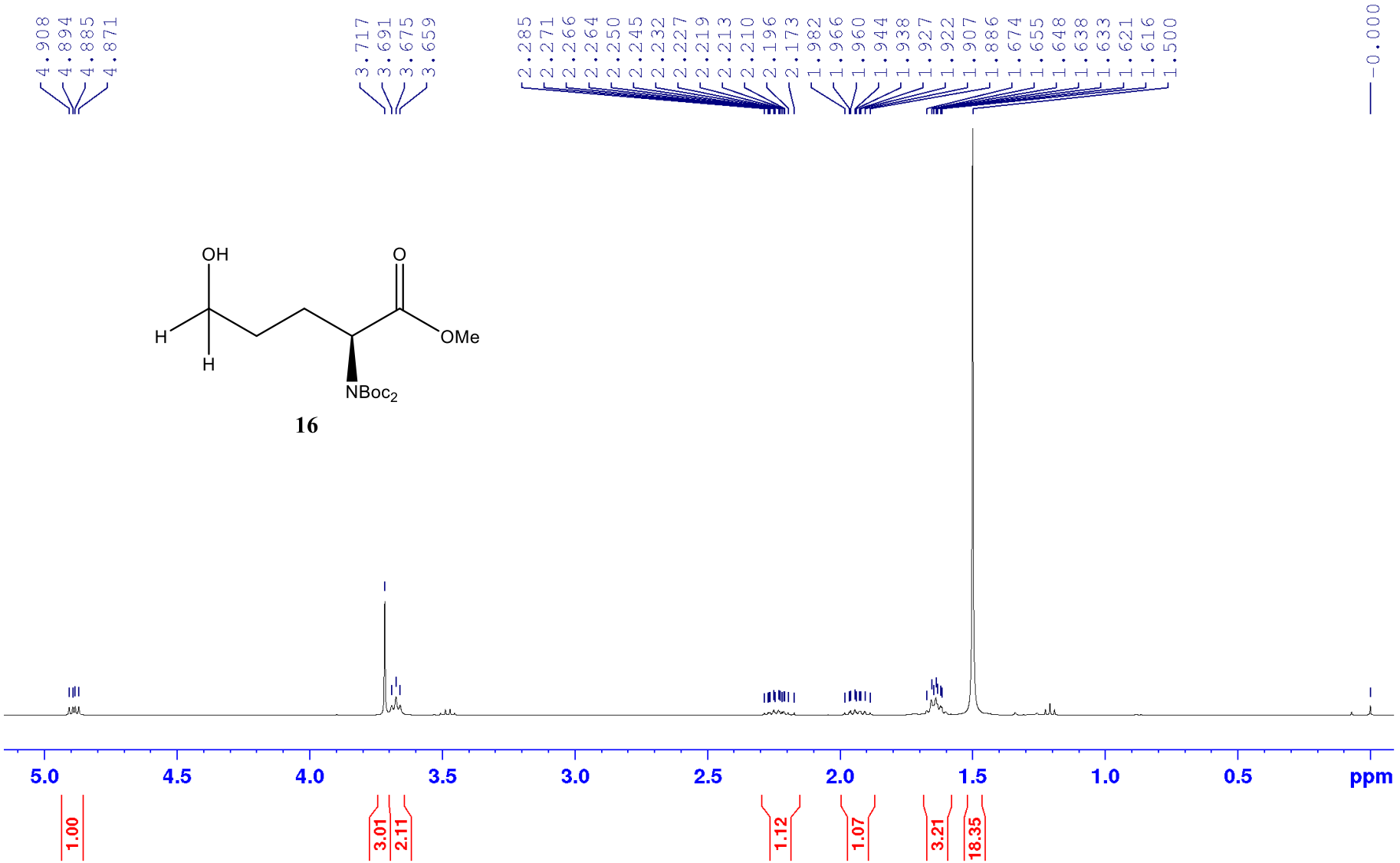

Figure xxv: ^{1}H-NMR (400 MHz, $CDCl_3$)

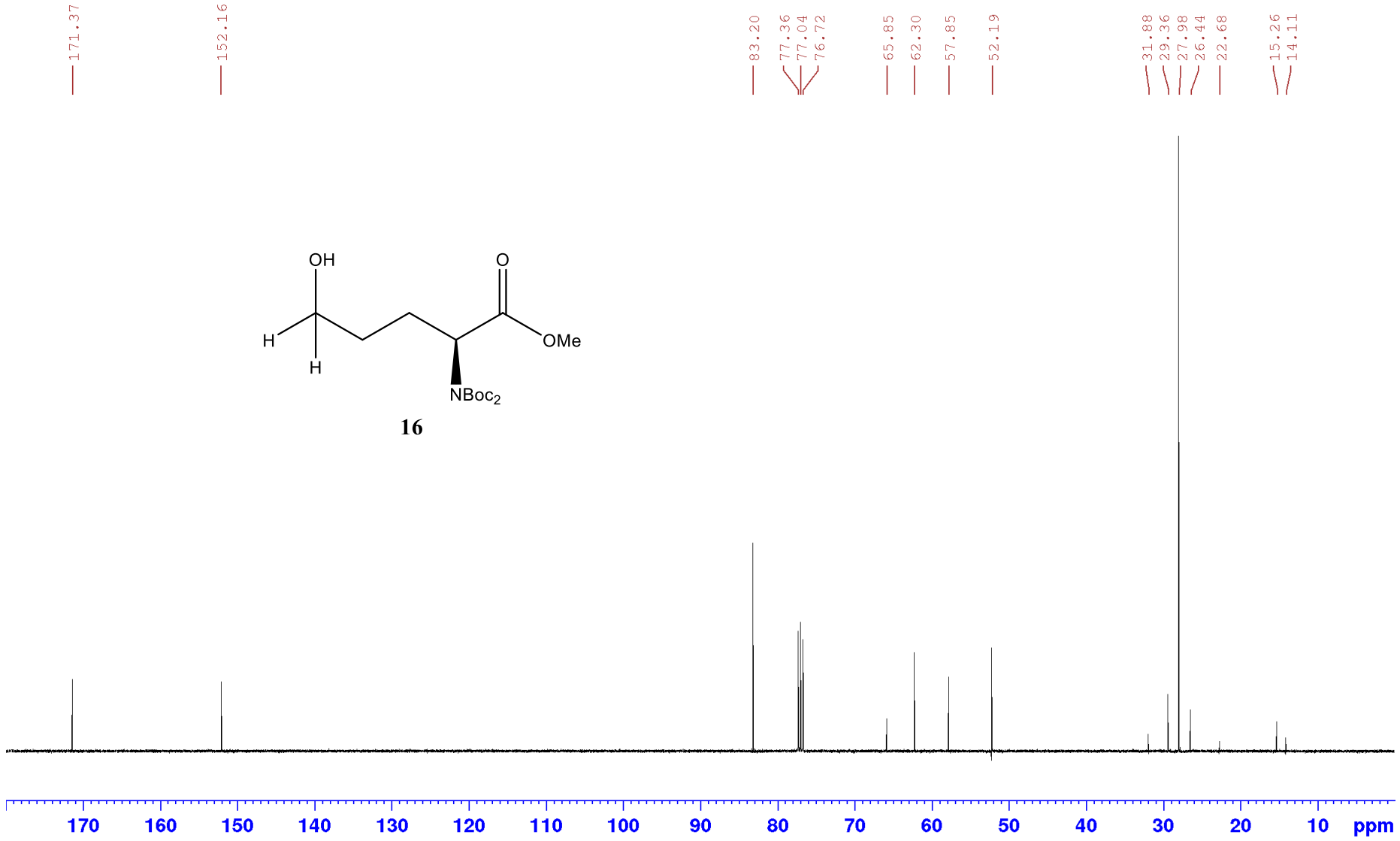

Figure xxvi: ^{13}C-NMR (400 MHz, $CDCl_3$)

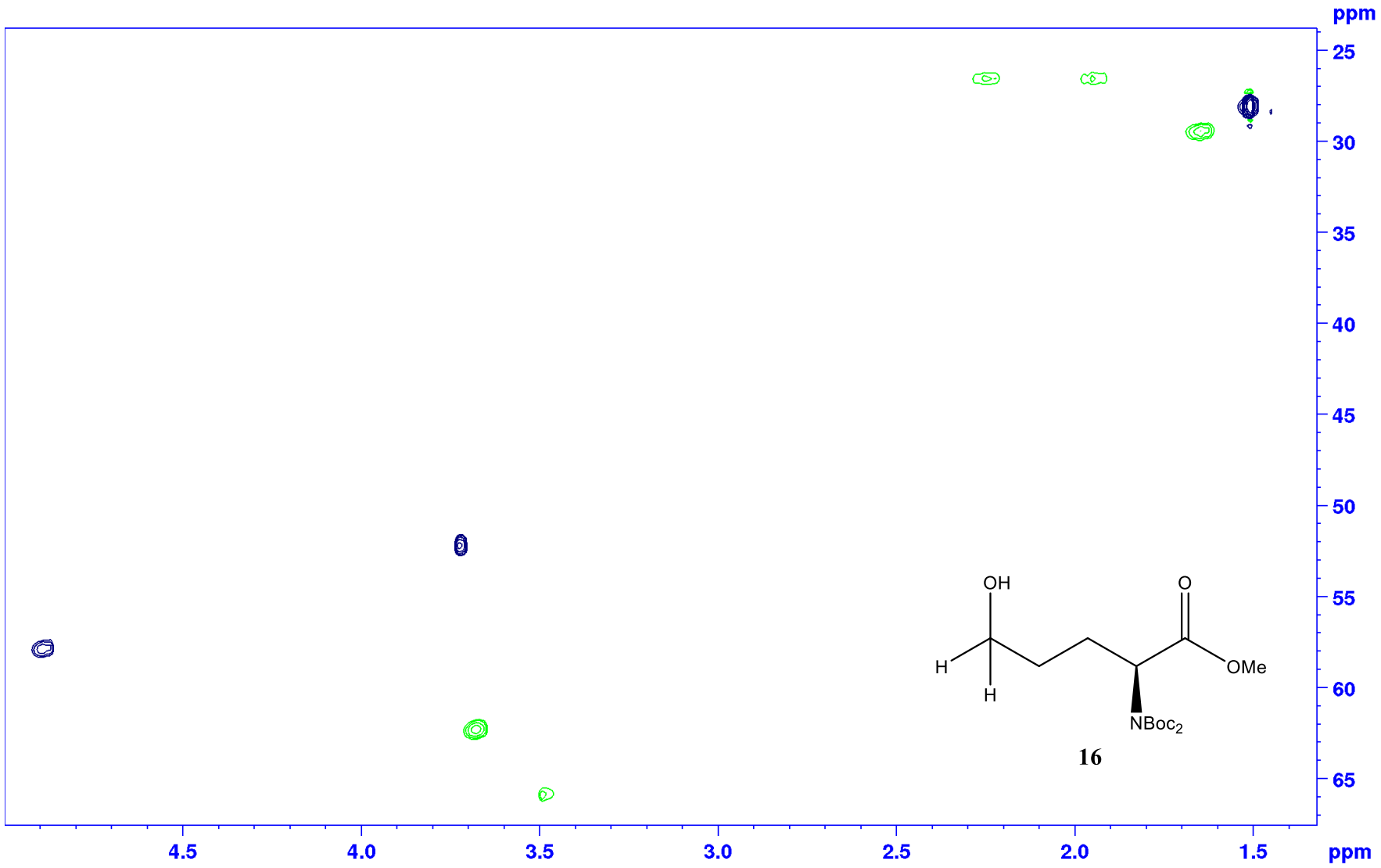

Figure xxvii: Excerpt from HSQC (400 MHz, 25 °C, $CDCl_3$)

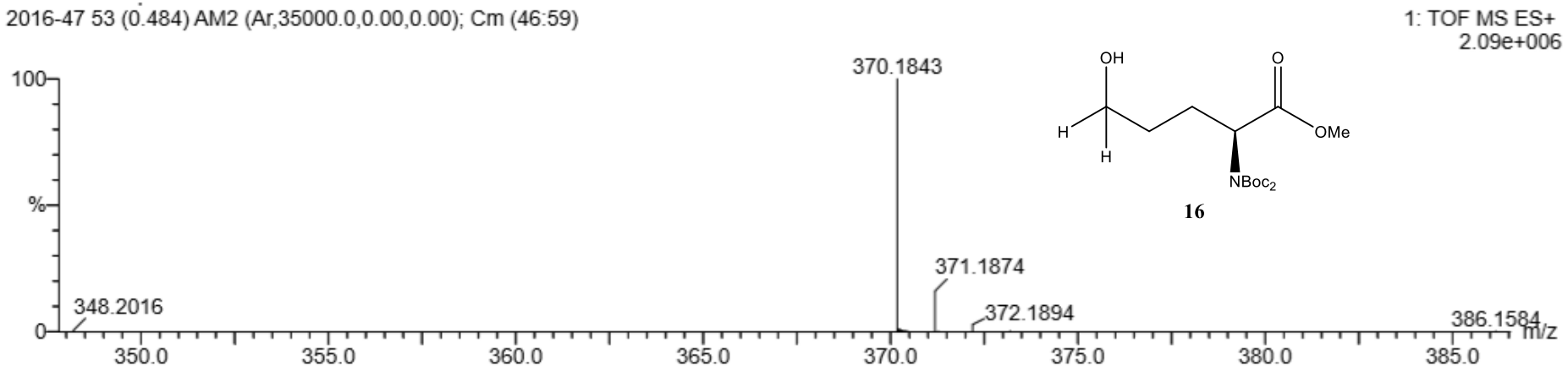

Minimum:				-1.5				
Maximum:		5.0	3.0	50.0				
Mass	Calc. Mass	mDa	PPM	DBE	i-FIT	Norm	Conf(%)	Formula
370.1843	370.1842	0.1	0.3	2.5	223.7	0.164	84.89	C16 H29 N O7 Na
	370.1839	0.4	1.1	6.5	225.4	1.924	14.61	C14 H24 N7 O5
	370.1852	-0.9	-2.4	11.5	228.8	5.297	0.50	C15 H20 N11 O

Ion observed [M+Na]

Figure xxviii: ESI-Q-TOF

Compound 17: 8’-apo-β-caroten-8’-ol

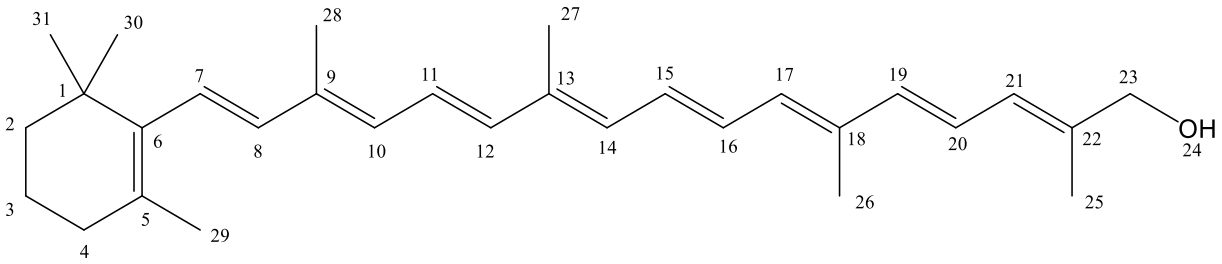

	Proton shift (ppm)
2-4	1.61, 1.76, 1.80, 2.02
7-8, 10-12, 14-17, 19-21	6.01-6.71
23	4.12
24	-
25-28	1.72, 1.86, 1.96, 1.97
29	1.47
30-31	1.03

Table viii: NMR-data

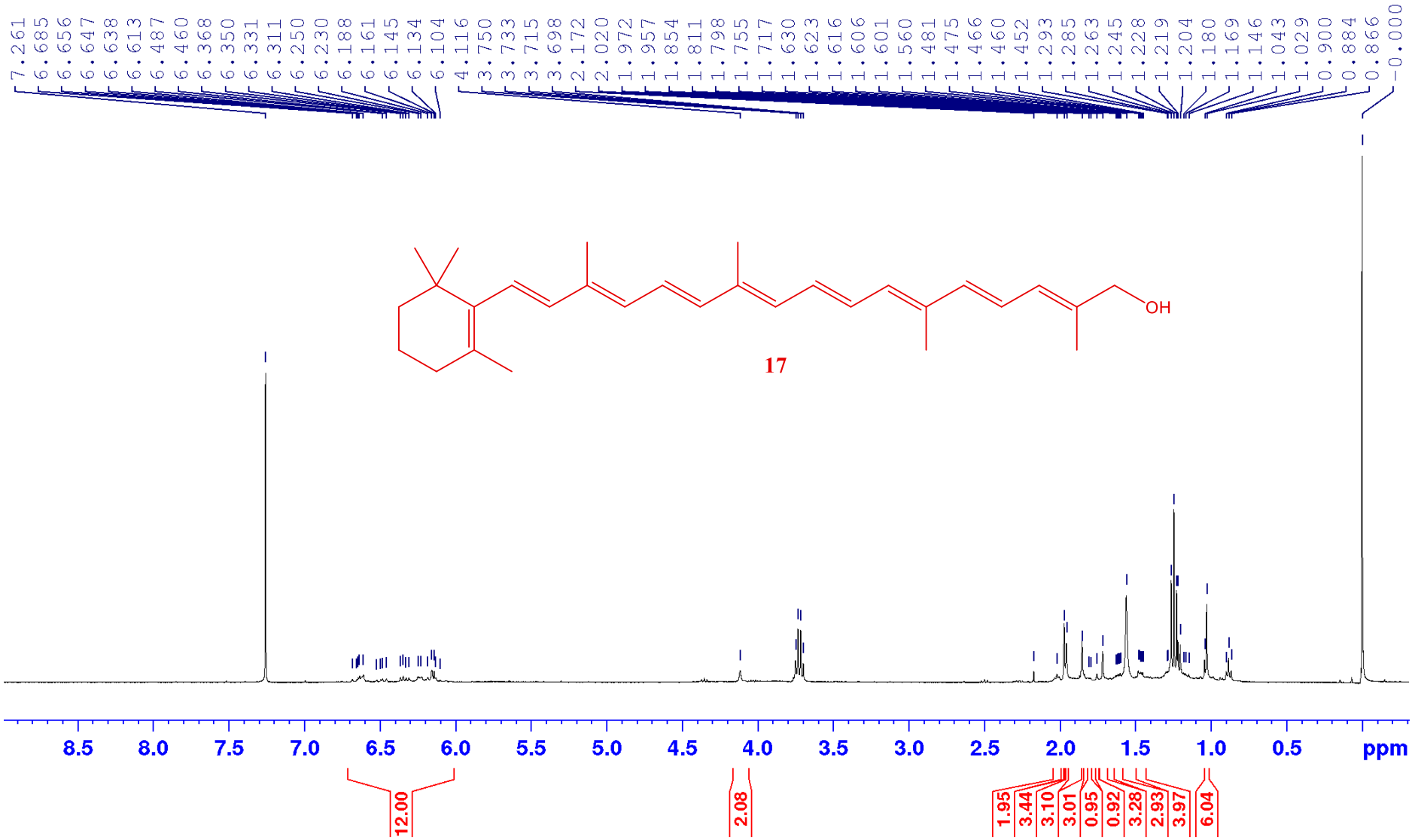

Figure xxix: ^{1}H-NMR (400 MHz, $CDCl_3$)

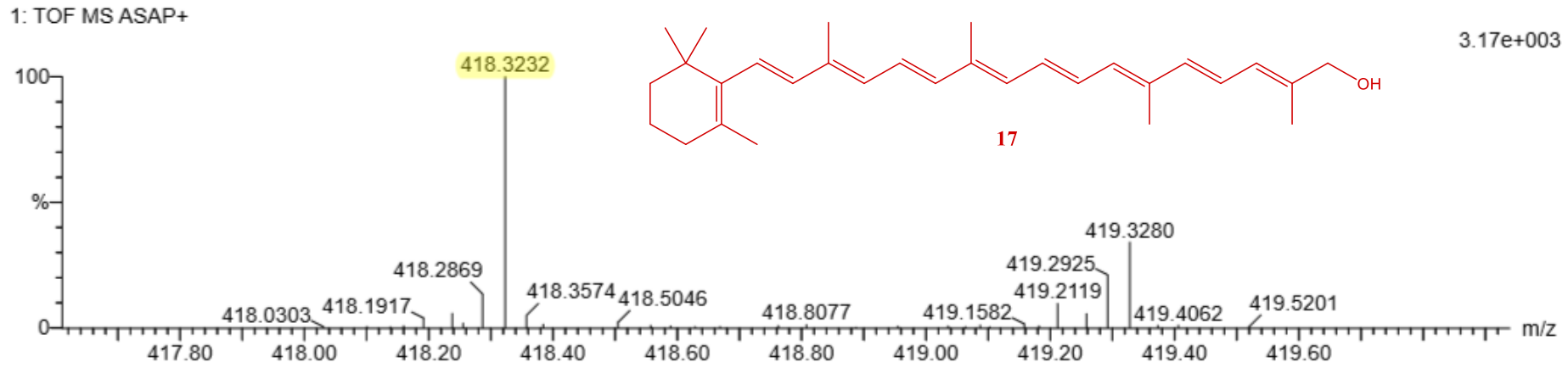

Minimum:				-1.5				
Maximum:		5.0	5.0	50.0				
Mass	Calc. Mass	mDa	PPM	DBE	i-FIT	Norm	Conf(%)	Formula
418.3232	418.3236	-0.4	-1.0	10.0	194.4	n/a	n/a	C30 H42 O ion observed M*+

Figure xxx: ASAP^{+}-Q-TOF

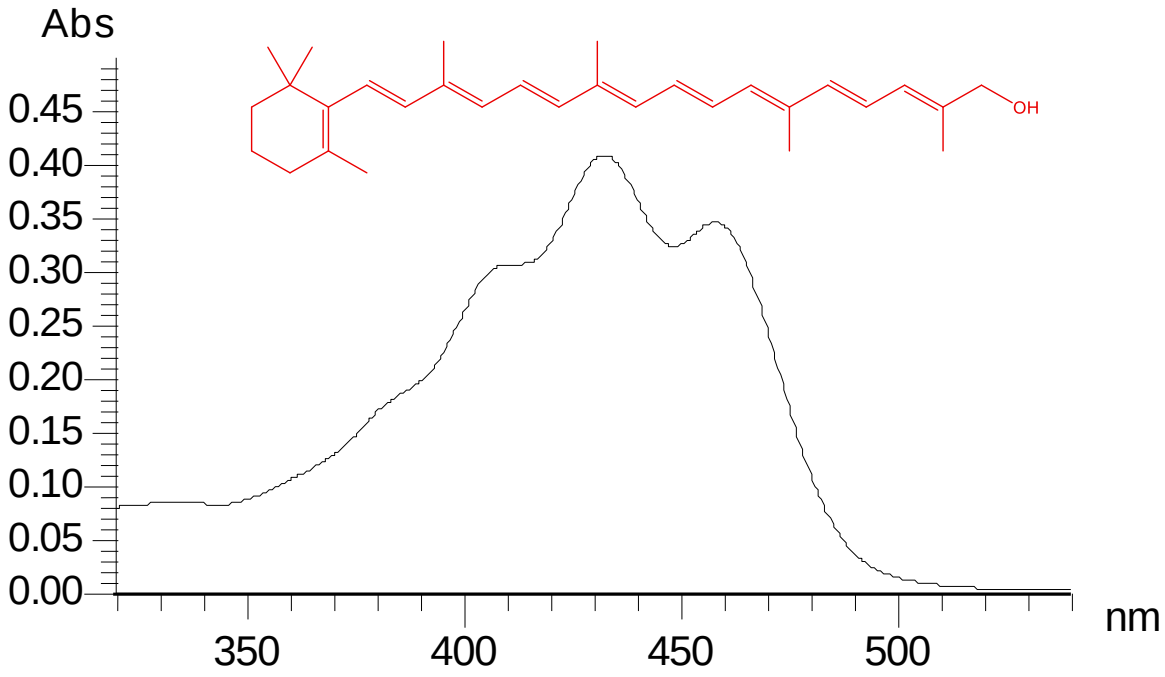

Figure xxxi: UV/vis absorption spectre (DCM)

Peak #	Start (nm)	Apex (nm)	End (nm)	Height (Abs)	Valley (nm)	Valley (Abs)
1	650.0	458.0	448.5	0.345	448.5	0.323
2	448.5	432.5	289.0	.408	289.0	0.064

Table ix: UV/vis absorption data (DCM)

Compound 18a: 8’-apo-β-caroten-8’-bromide

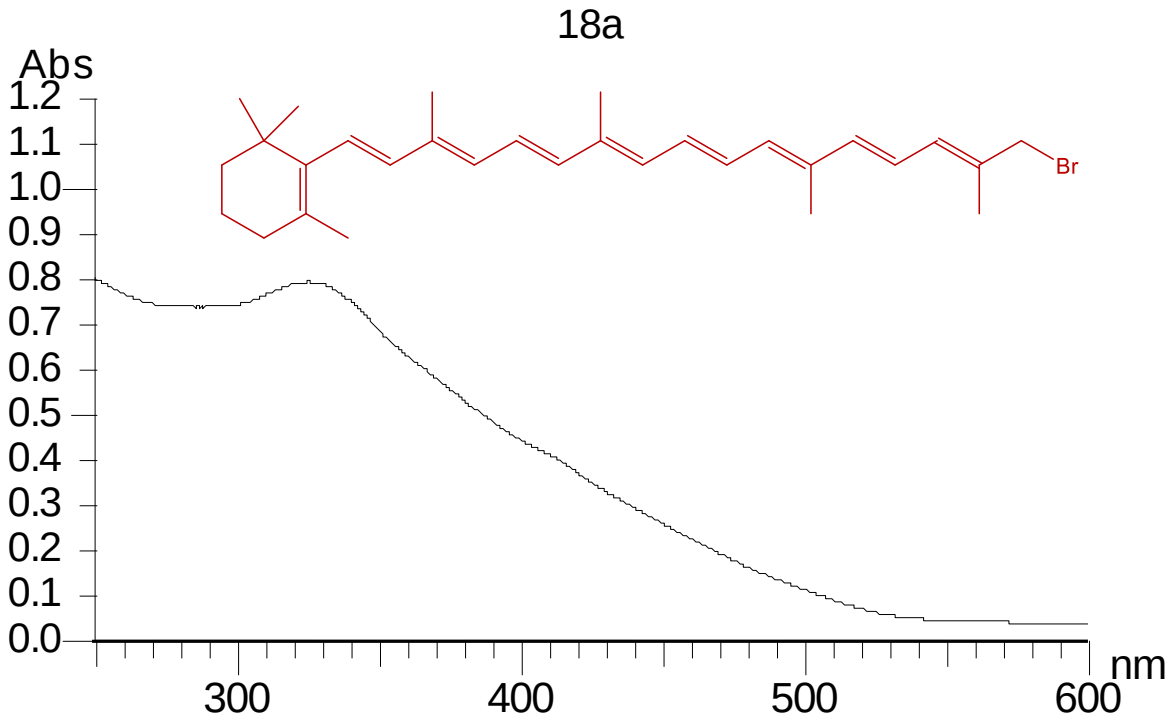

Figure xxxii: UV/vis absorption spectre (DCM)

Peak #	Start (nm)	Apex (nm)	End (nm)	Height (Abs)	Valley (nm)	Valley (Abs)
1	650.0	325.0	287.0	0.792	287.0	0.736

Table x: UV/vis absorption data (DCM)

Compound 18b: 8’-apo-β-caroten-8’-bromide

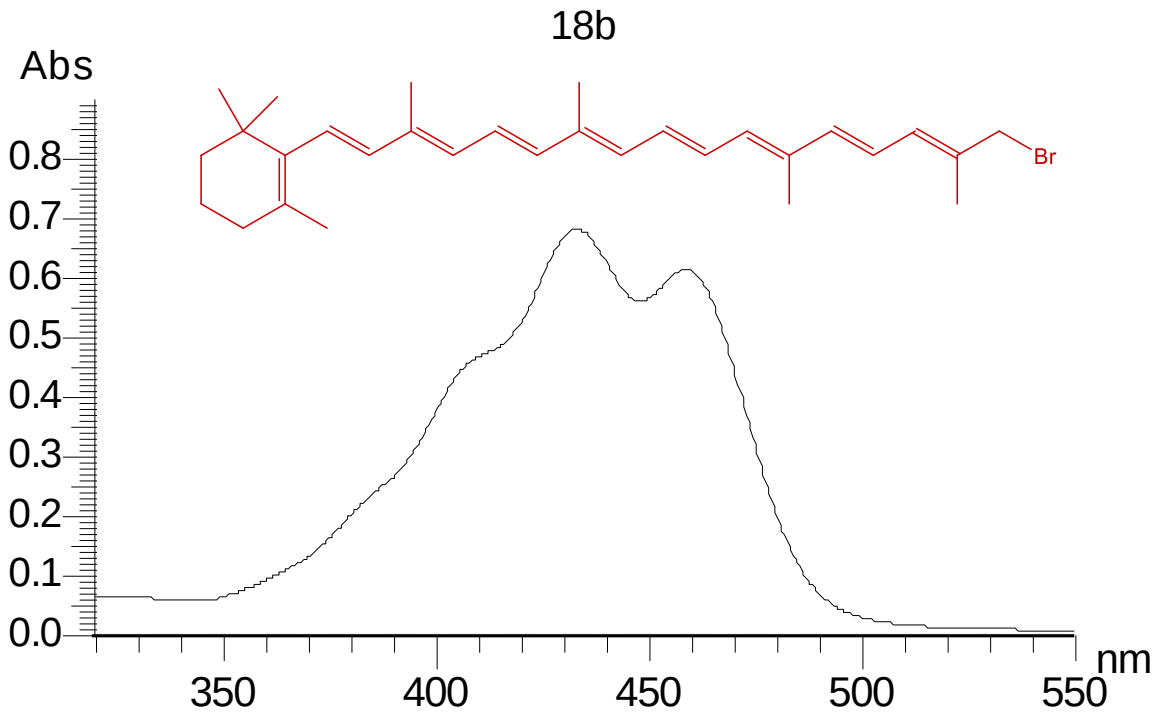

Figure xxxiii: UV/vis absorption spectre (DCM)

Peak #	Start (nm)	Apex (nm)	End (nm)	Height (Abs)	Valley (nm)	Valley (Abs)
1	650.0	458.5	448.0	0.613	448.0	0.558
2	448.0	433.0	292.0	0.680	292.0	0.047

Table xi: UV/vis absorption data (DCM)

Compound 19: 8'-apo-β-caroten-8'-triphenylphosphine bromide

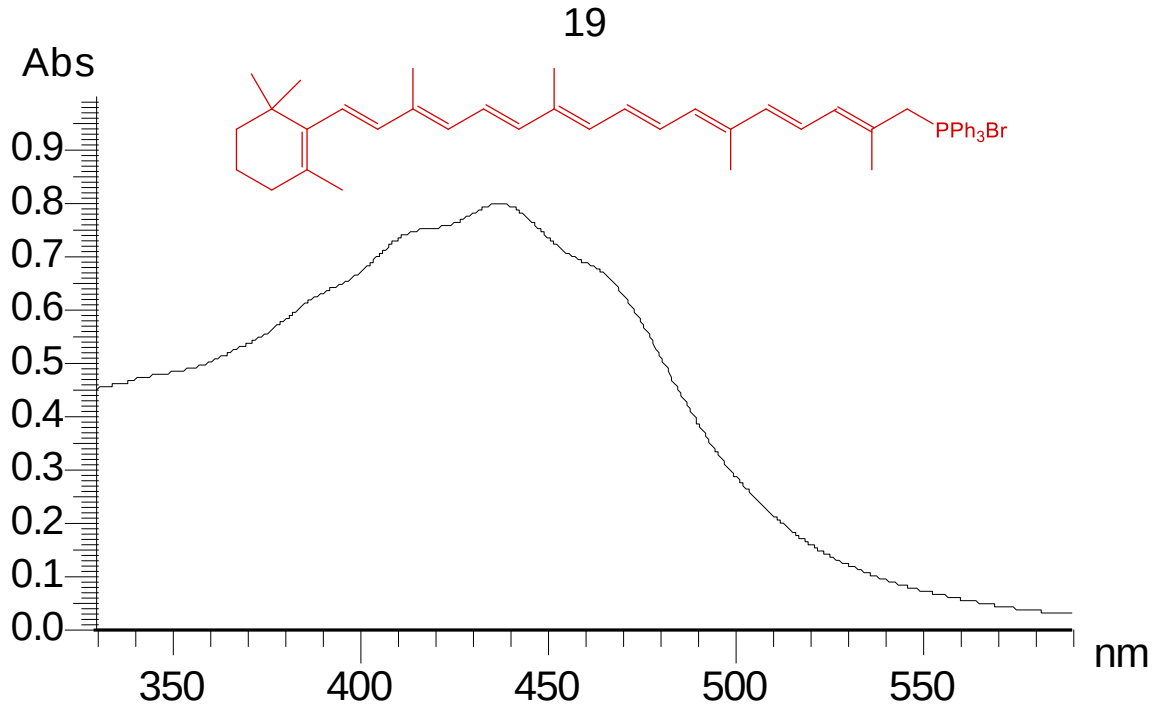

Figure xxxiv: UV/vis absorption spectre (DCM)

Peak #	Start (nm)	Apex (nm)	End (nm)	Height (Abs)	Valley (nm)	Valley (Abs)
1	650.0	441.0	292.0	0.850	292.0	0.272
2	292.0	268.0	250.0	0.394	250.0	0.356

Table xii: UV/vis absorption data (DCM)

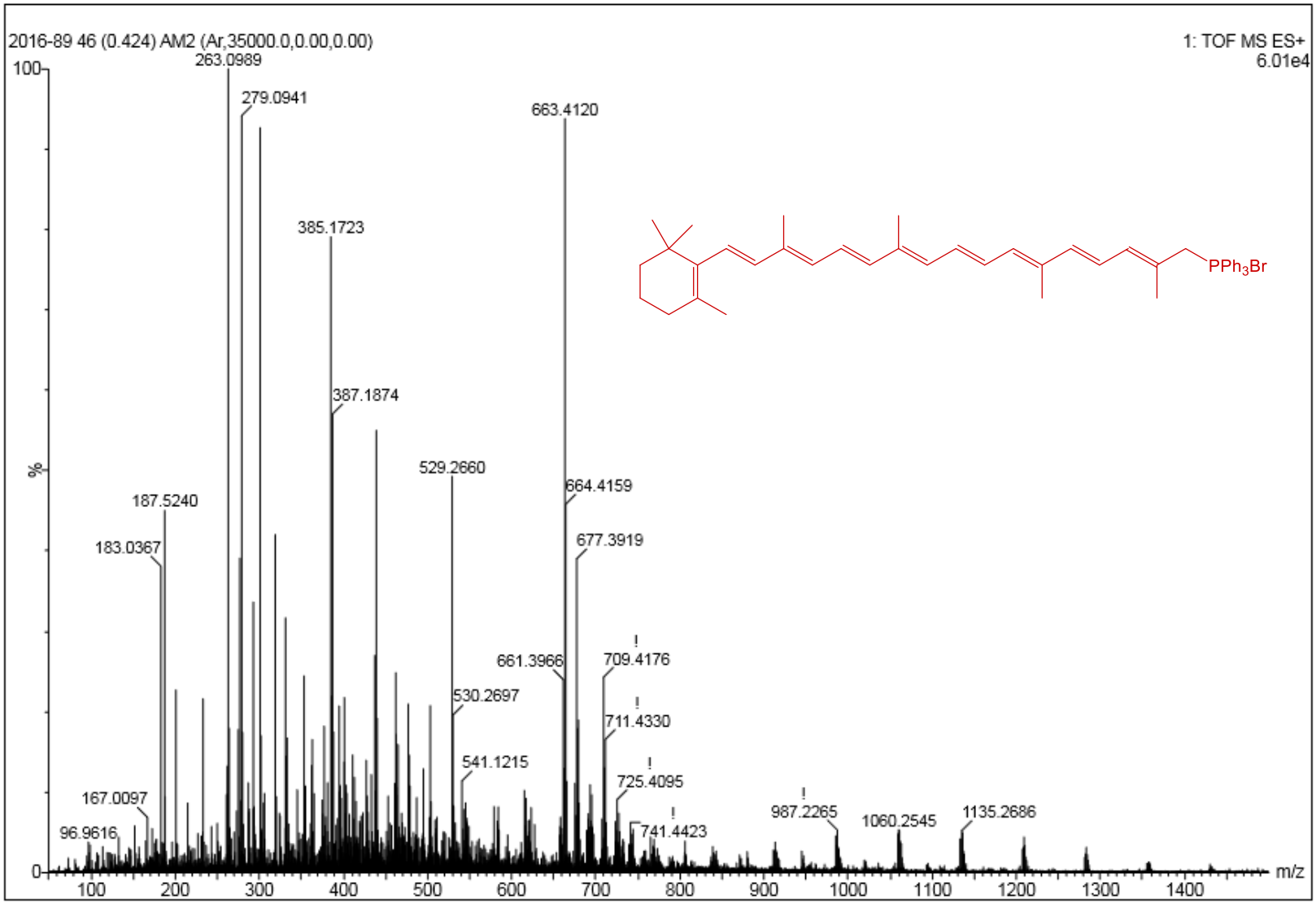

Figure xxxv: ESI-Q-TOF

Compound 22: C15Zea-P

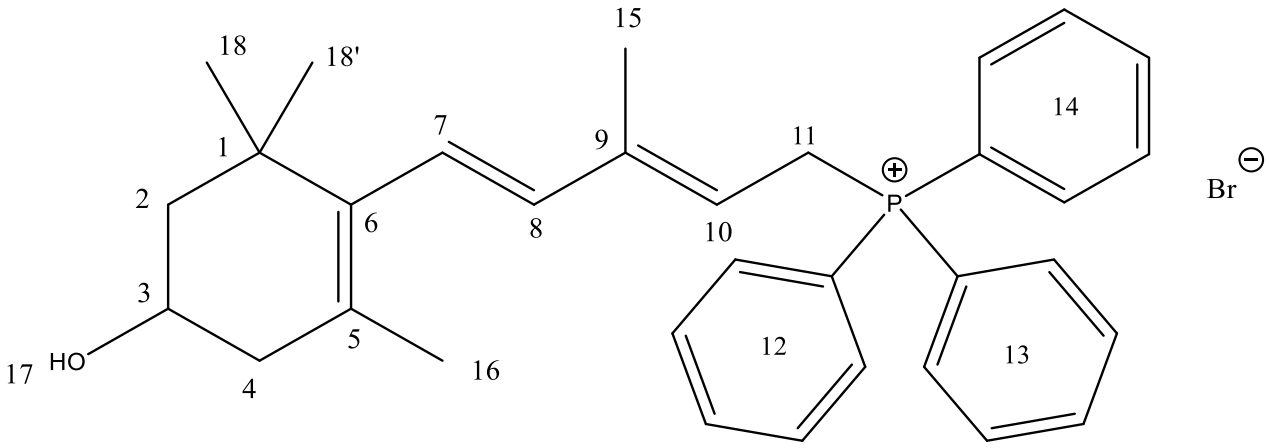

	Proton shift (ppm)	Carbon shift (ppm)
1	-	36.8
2	1.27, 1.64	48.7
3	3.71	63.1
4	1.87, 2.18	42.9
5	-	118.5-136.9
6	-	
7	5.97	
8	5.42	
9	-	
10	6.03	
11	4.63	22.8
12 - 14	7.74 - 7.93	118.5-138.9
15	1.40	12.7
16	1.60	21.8
17	4.57	-
18, 18’	0.94, 0.97	28.9, 30.6

Table xiii: NMR-data

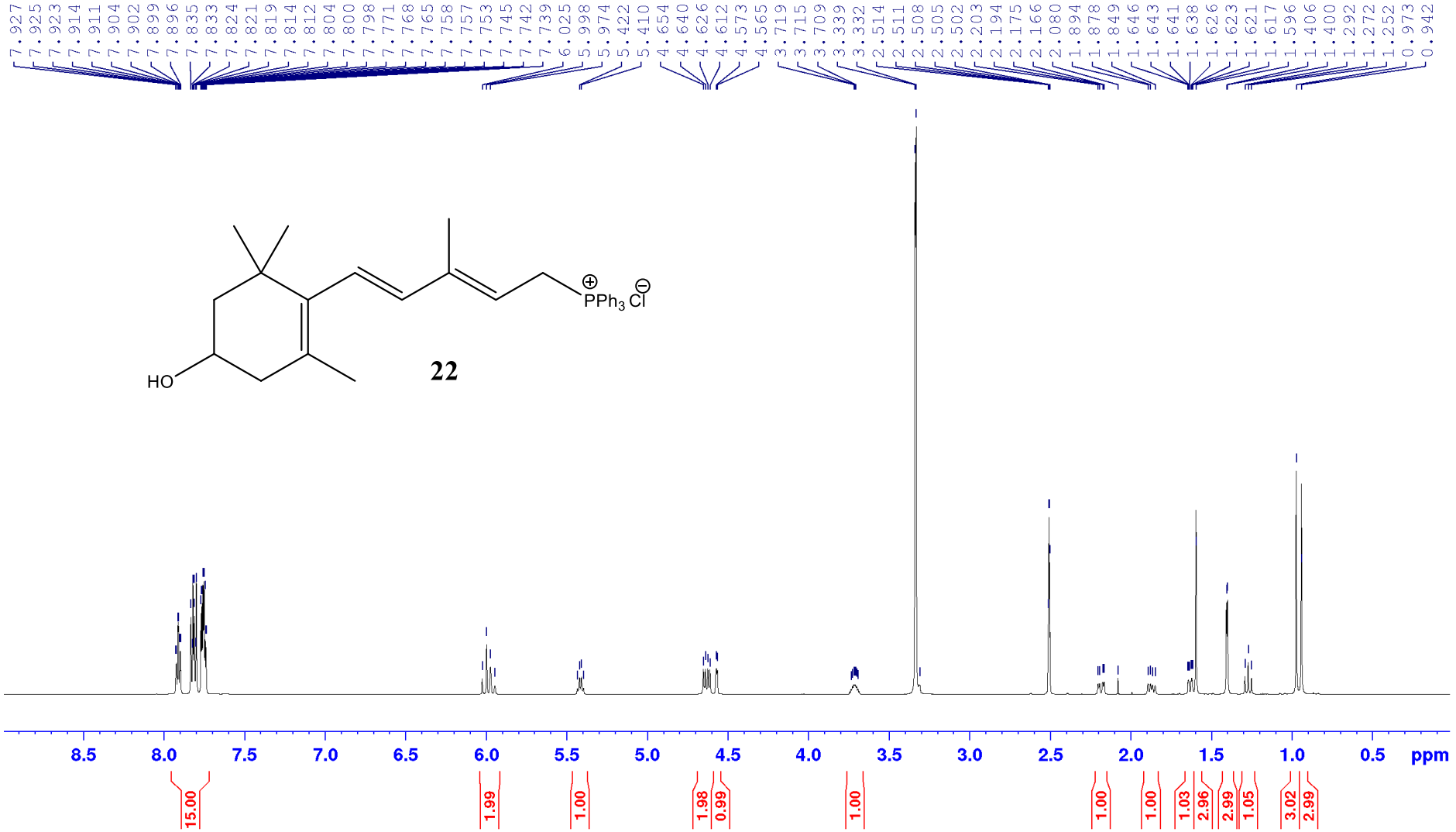

Figure xxxvi: ^{1}H-NMR (600 MHz, d_6-DMSO)

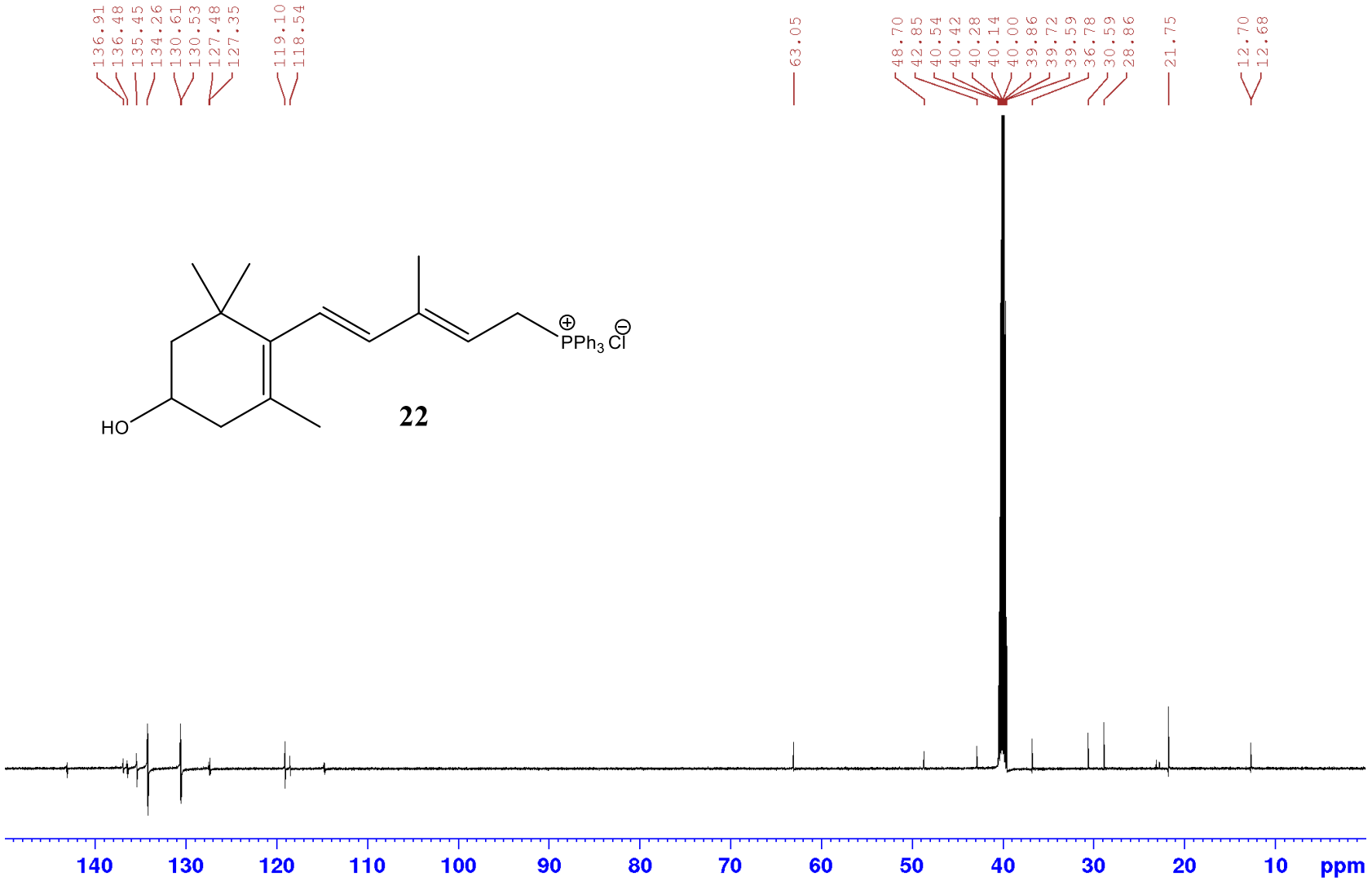

Figure xxxvii: ^{13}C-NMR (600 MHz, d_6-DMSO)

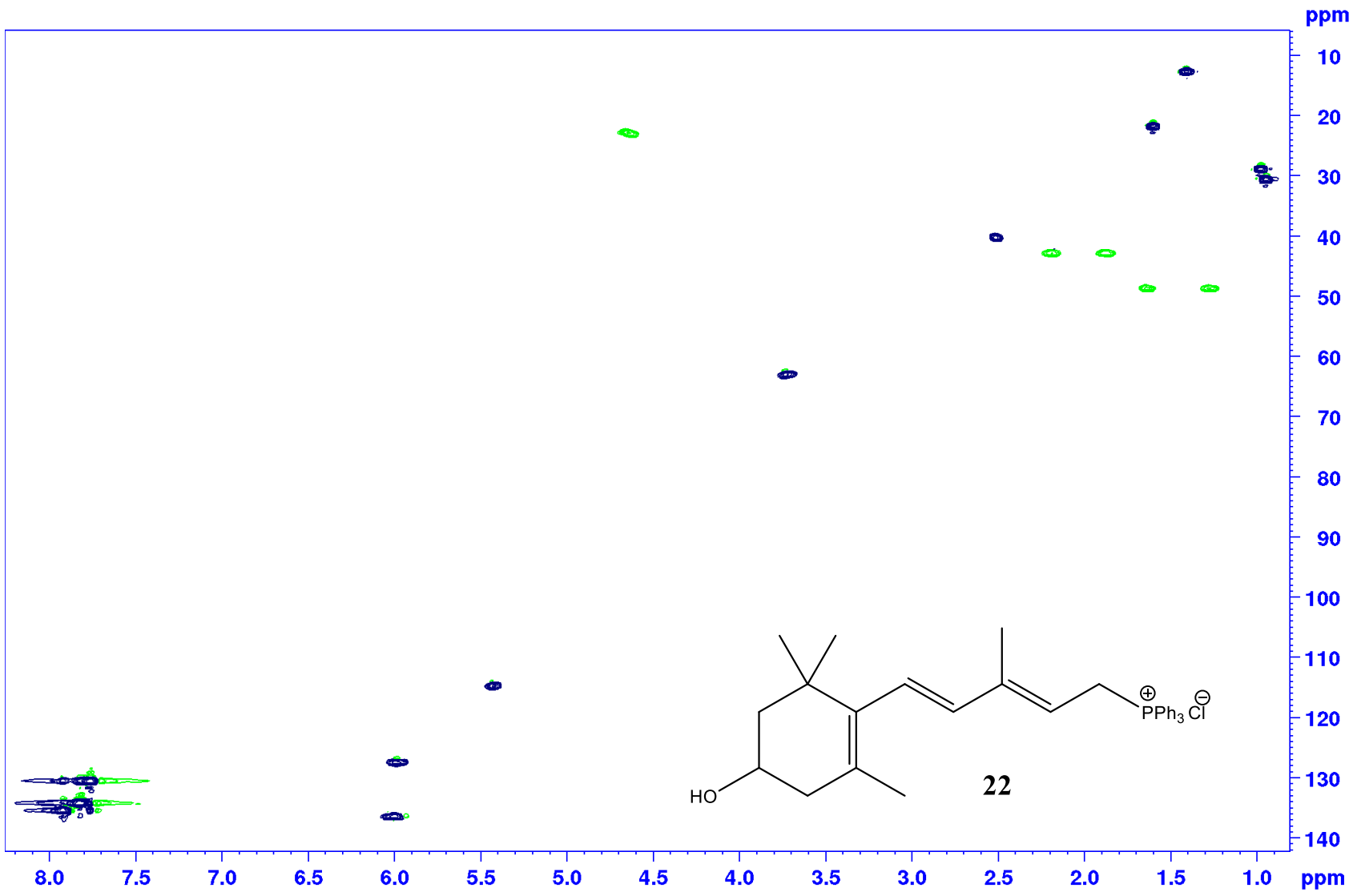

Figure xxxviii: Excerpt from HSQC (600 MHz, d_6-DMSO)

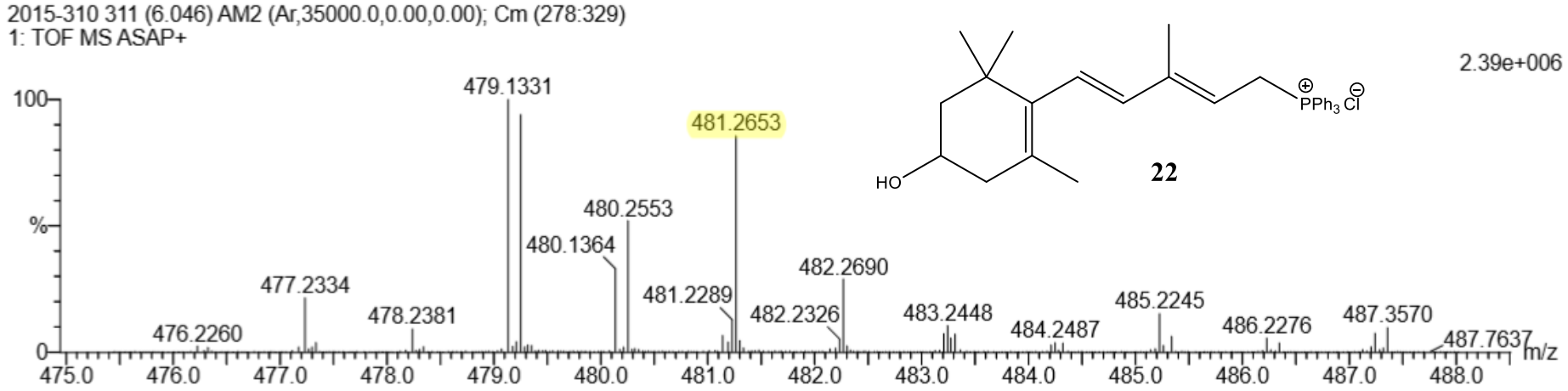

Minimum:				-1.5				
Maximum:		5.0	2.0	50.0				
Mass	Calc. Mass	mDa	PPM	DBE	i-FIT	Norm	Conf(%)	Formula
481.2653	481.2660	-0.7	-1.5	15.5	1275.4	0.001	99.95	C33 H38 O P
	481.2649	0.4	0.8	2.5	1283.0	7.576	0.05	C22 H41 O11

ion observed M*+

Figure xxxix: ASAP^{+}-Q-TOF

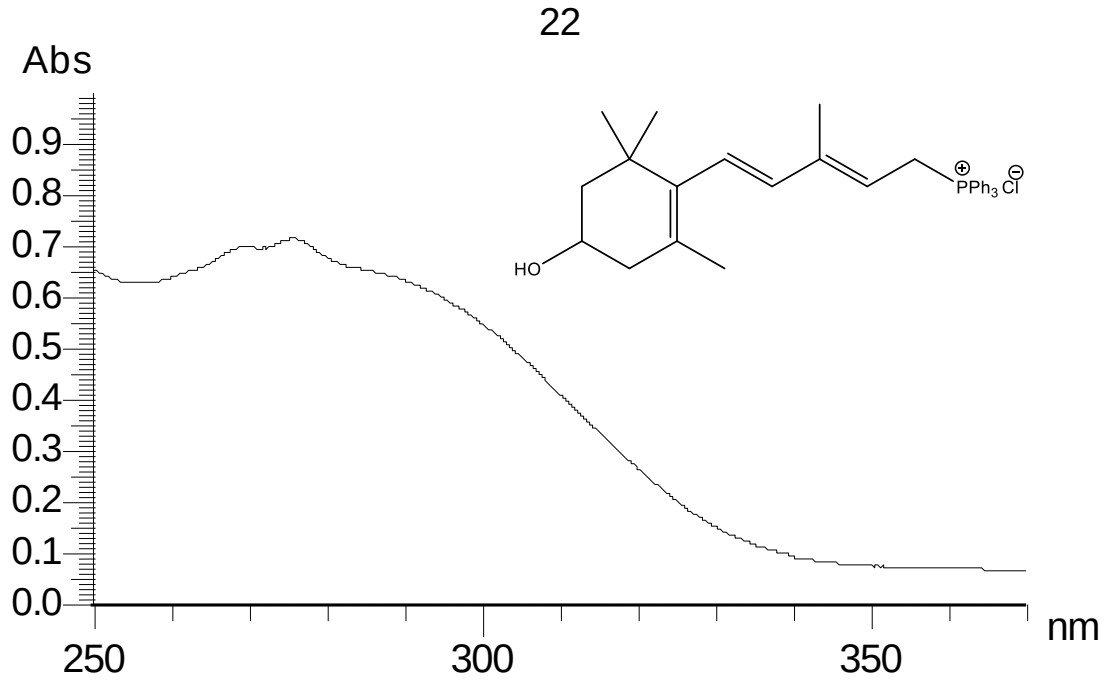

Figure xl: UV/vis absorption spectre (DCM)

‘

Peak #	Start (nm)	Apex (nm)	End (nm)	Height (Abs)	Valley (nm)	Valley (Abs)
1	400.0	275.6	256.0	0.713	256.0	0.626
2	256.0	225.4	216.0	1.768	216.0	-1.470
3	216.0	205.0	201.6	1.864	201.6	0.408

Table xiv: UV/vis absorption data (DCM)

Compound 23: C20:4-N-diBoc-methylester

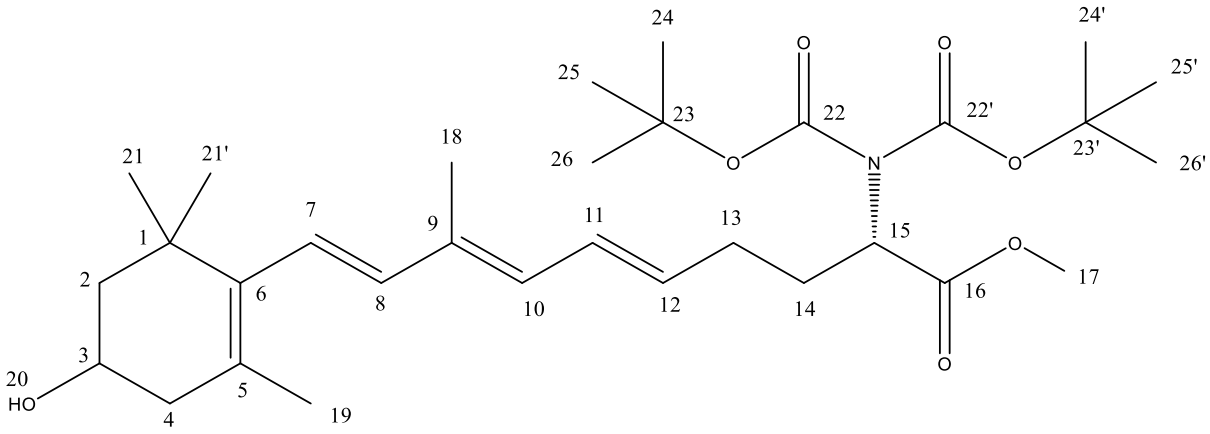

	Proton shift (ppm)	Carbon shift (ppm)
1	-	37.1
2	2.05, 2.38	42.5
3	4.02	65.1
4	1.47, 1.78	48.4
5, 6, 9	-	125.1 – 138.7
7, 8, 10-12	5.39 – 6.38	
13	1.98 – 2.22	24.5
14	2.29	30.2
15	4.89	57.6
16	-	171.3
17	3.71	52.2
18	1.89	12.4
19	1.71	21.5
20		-
21, 21’	1.05, 1.06	29.9
22, 22’	-	152.1
23, 23’	-	83.1
24-26, 24’-26’	1.49, 1.50	28.0

Table xv: NMR-data

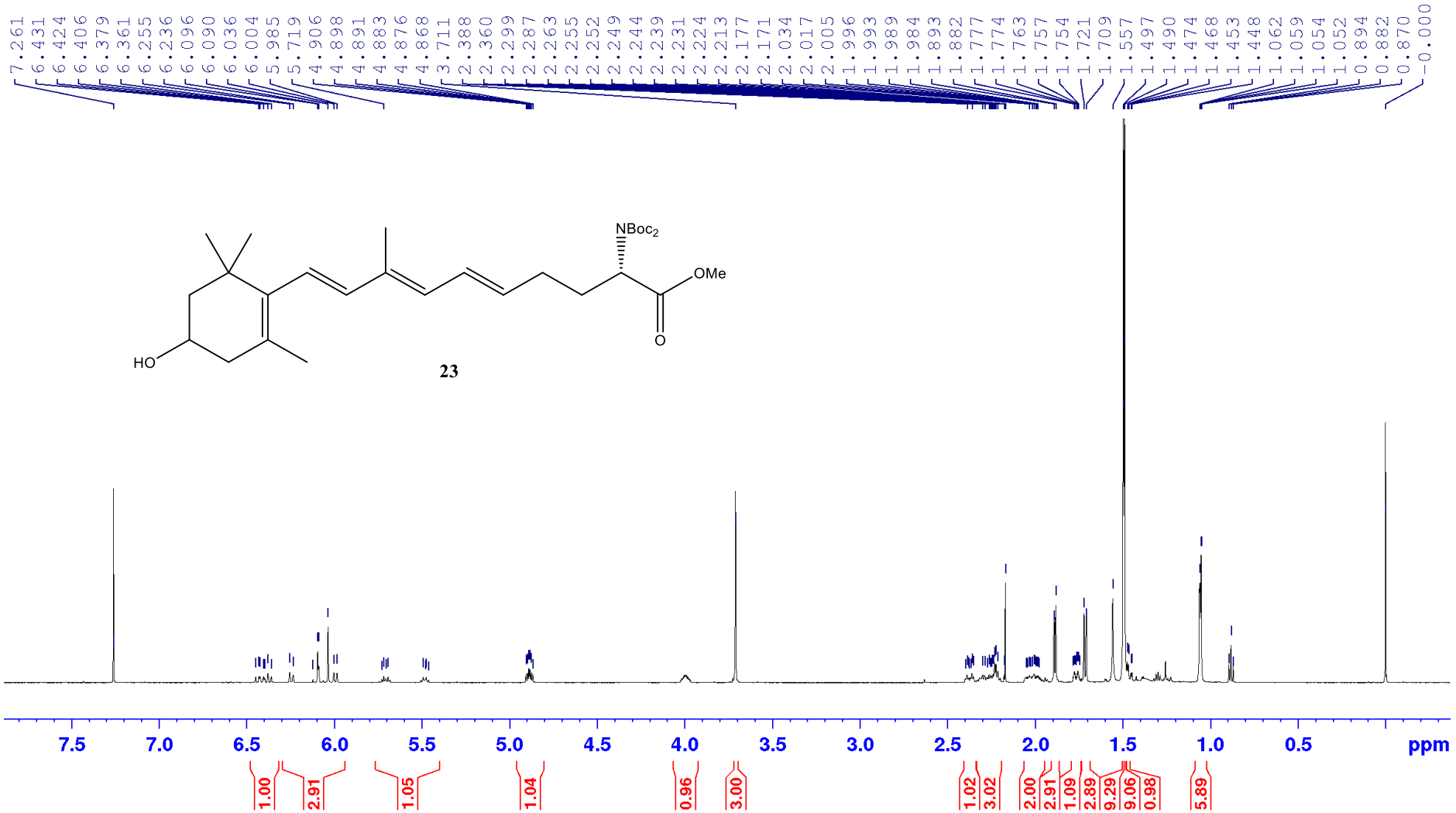

Figure xli: ^{1}H-NMR (600 MHz, $CDCl_3$)

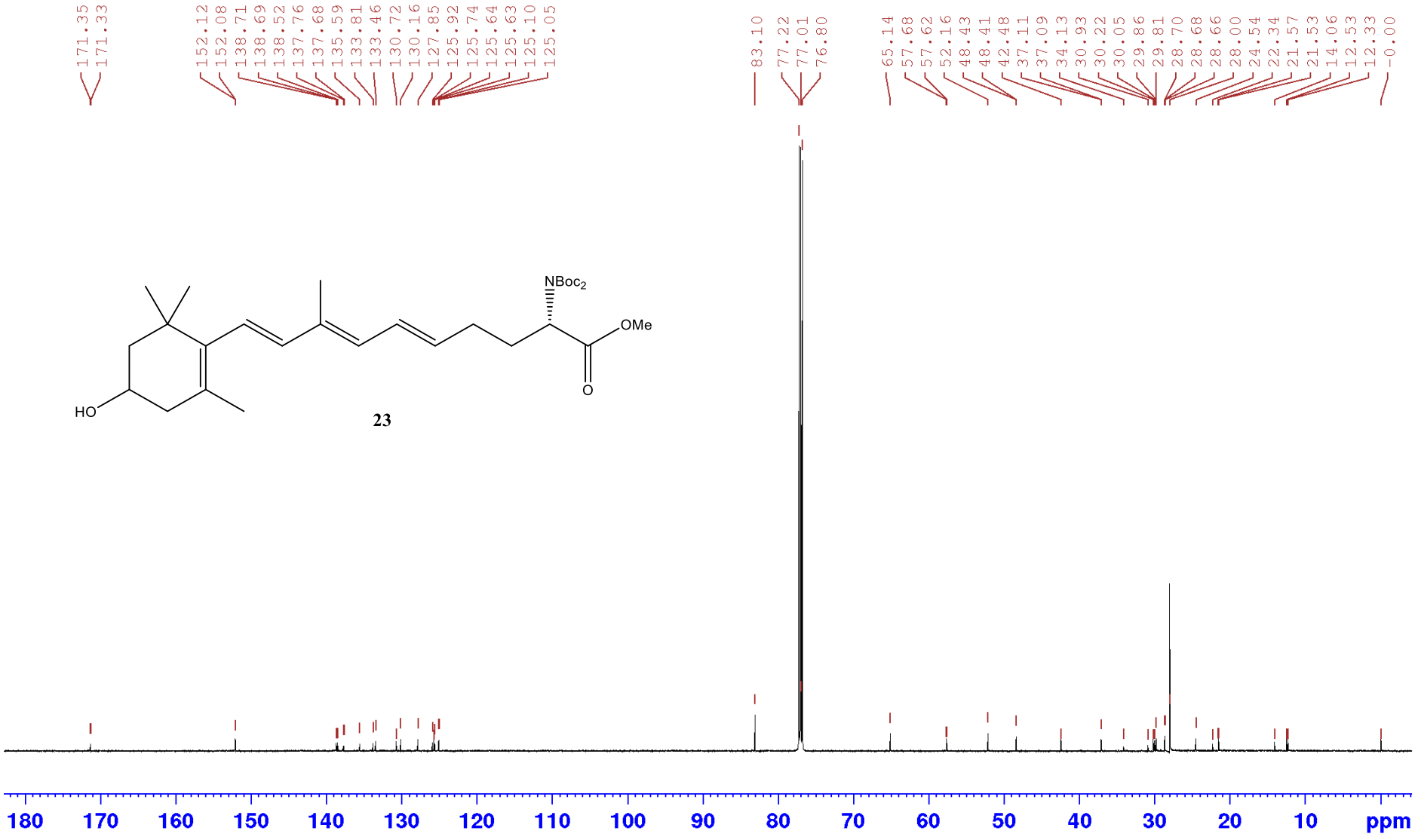

Figure xlii: ^{13}C-NMR (600 MHz, $CDCl_3$)

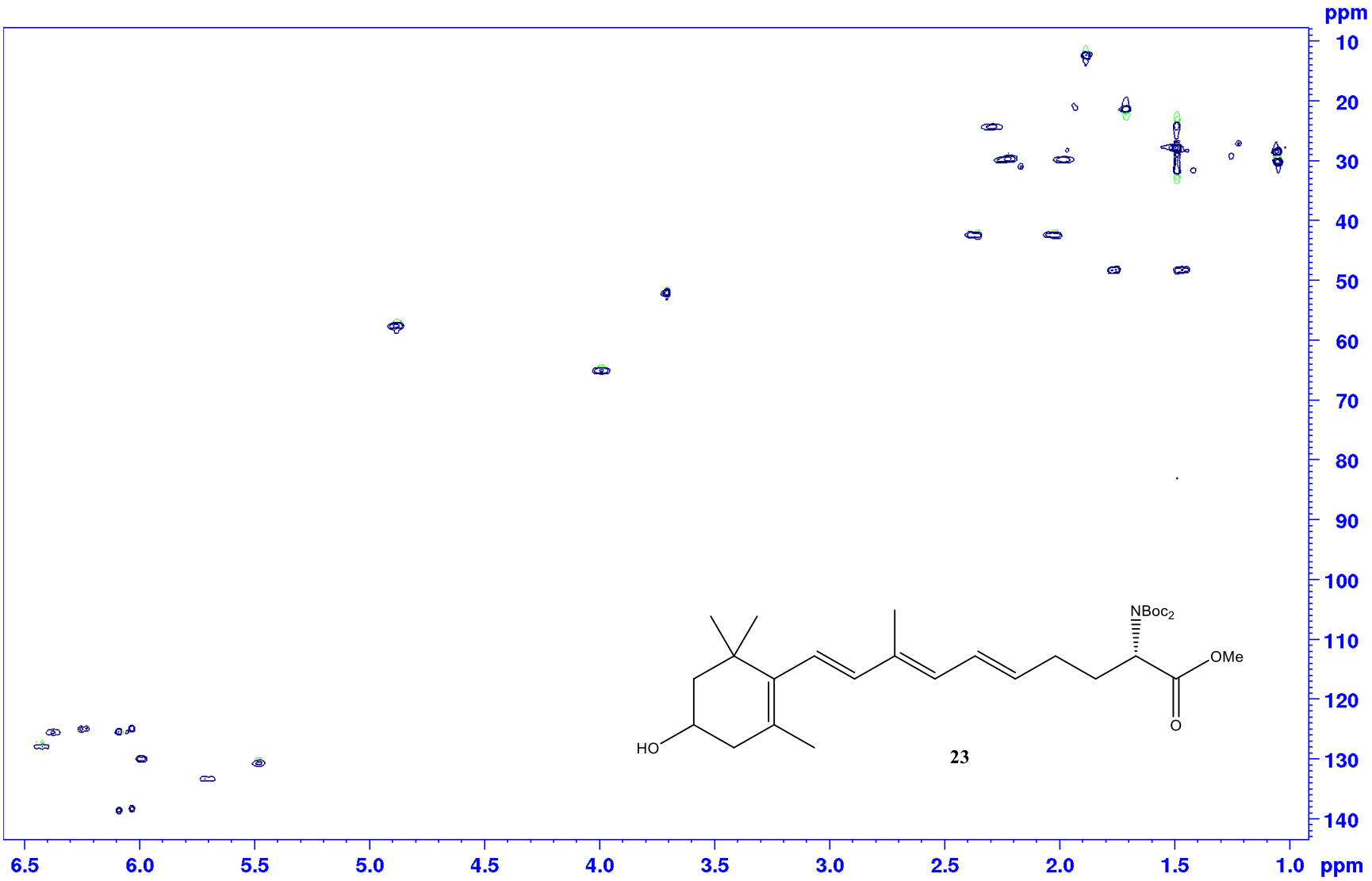

Figure xliii: HSQC (600 MHz, $CDCl_3$)

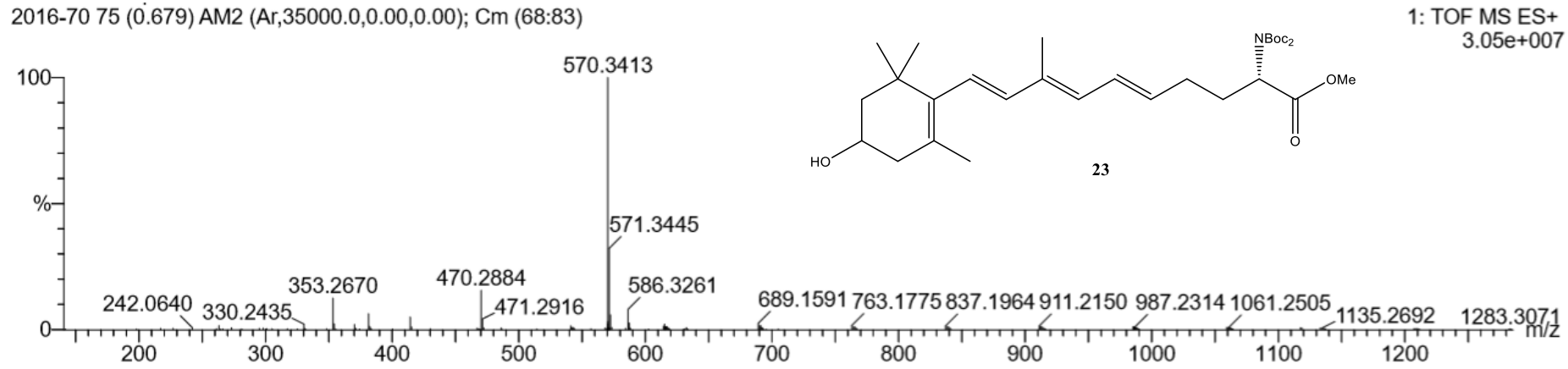

Minimum:				-1.5				
Maximum:		5.0	2.0	50.0				
Mass	Calc. Mass	mDa	PPM	DBE	i-FIT	Norm	Conf(%)	Formula
570.3413	570.3407	0.6	1.1	7.5	274.7	1.007	36.54	C31 H49 N O7 Na Ion observed [M+Na]
	570.3404	0.9	1.6	11.5	274.8	1.093	33.51	C29 H44 N7 O5
	570.3417	-0.4	-0.7	16.5	275.2	1.446	23.55	C30 H40 N11 O
	570.3420	-0.7	-1.2	12.5	276.6	2.865	5.70	C32 H45 N5 O3 Na
	570.3422	-0.9	-1.6	-1.5	278.9	5.162	0.57	C17 H48 N9 O12
	570.3412	0.1	0.2	0.5	280.7	6.975	0.09	C16 H45 N13 O8 Na
	570.3422	-0.9	-1.6	9.5	282.2	8.485	0.02	C15 H36 N23 O2
	570.3409	0.4	0.7	4.5	283.1	9.312	0.01	C14 H40 N19 O6

Figure xliv: ESI-Q-TOF

Compound 25: C20N:4

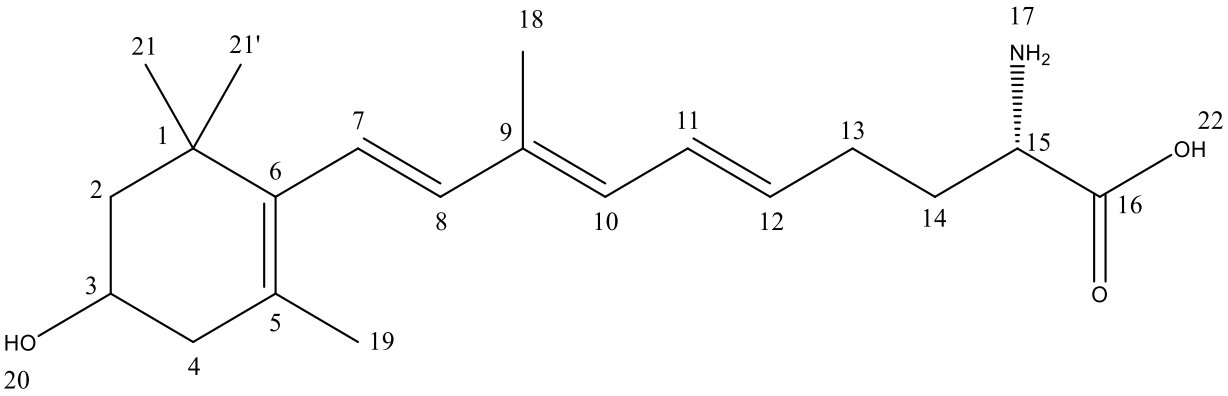

	Proton shift (ppm)	Carbon shift (ppm)
1	-	
2	1.33, 1.65	48.0
3	3.81	62.6
4	1.87, 2.20	41.2
5	-	
6	-	
7, 8, 10-12	5.75 – 7.24	126.9 - 131.2
9	-	
13	1.42	28.9
14	1.75	30.1
15	3.58/3.62	51.1/51.6
16	-	
17	7.28	-
18	1.97	15.7
19	1.34	20.6
20		-
21, 21’	1.04	29.1
22	8.41	-

Table xvi: NMR-data

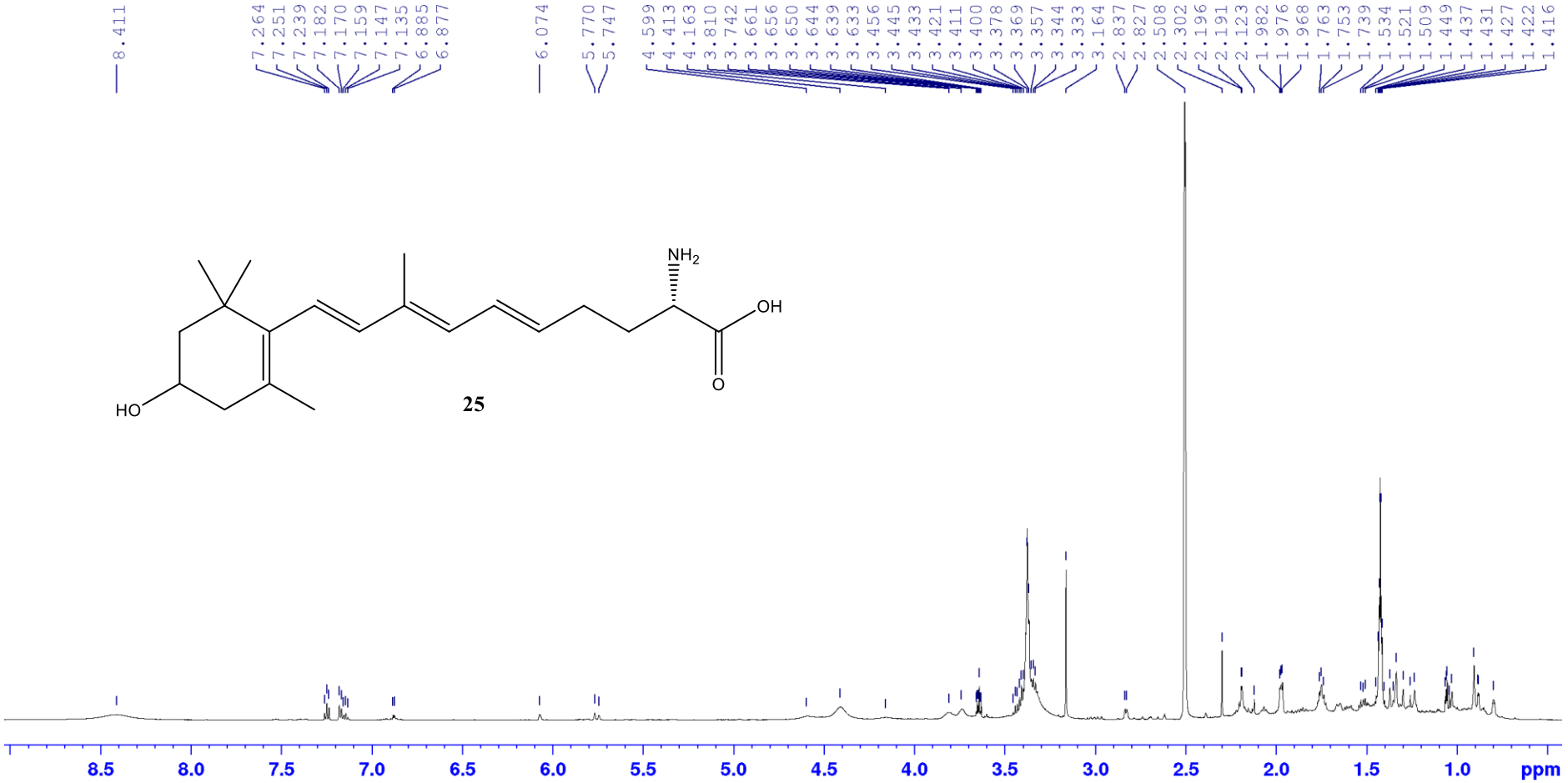

Figure xlv: ^{1}H-NMR (600 MHz, d_6-DMSO) without solvent suppression

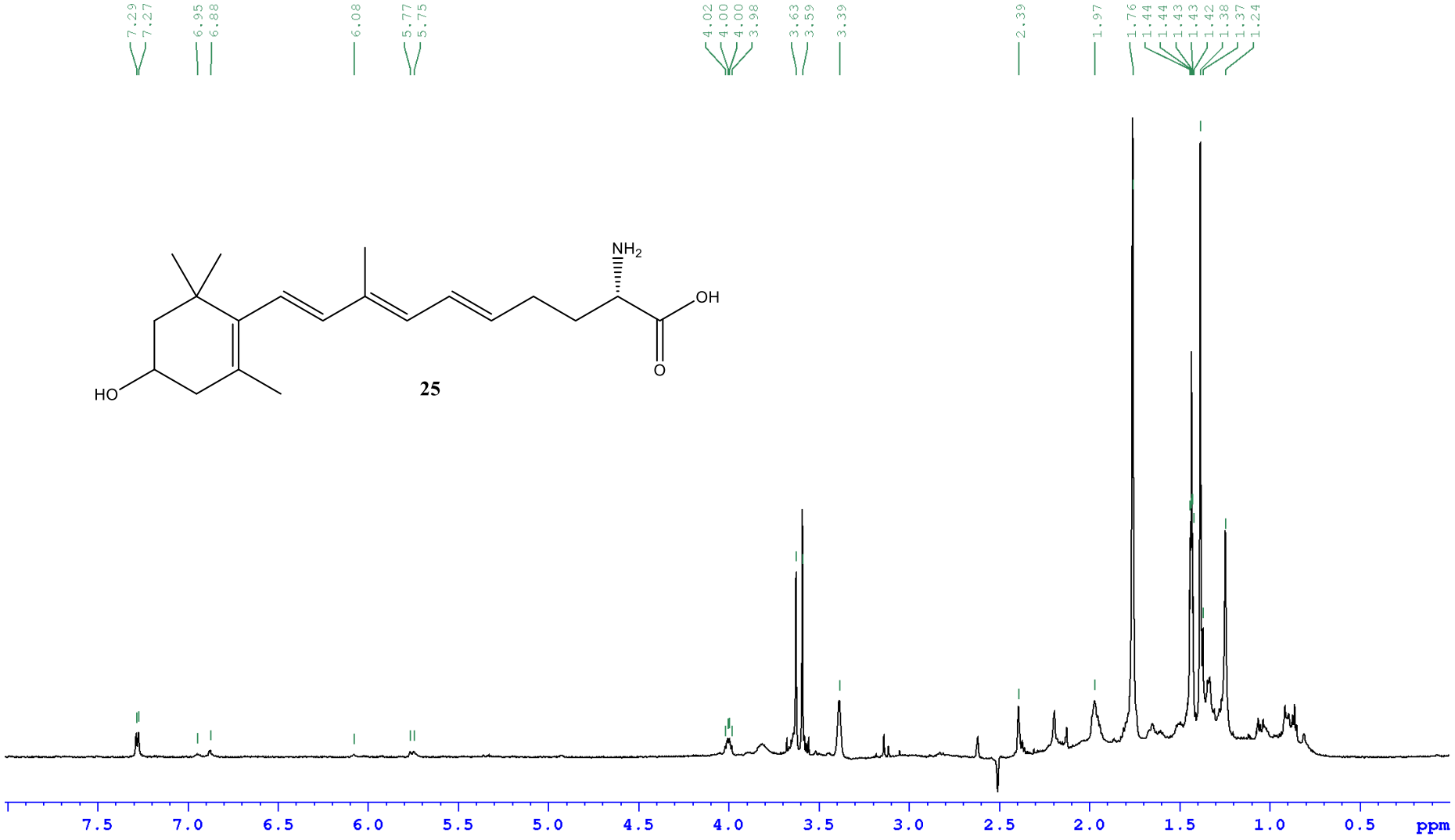

Figure xlvi: ^{1}H-NMR (600 MHz, d_6-DMSO) with solvent suppression of DMSO and H_2O

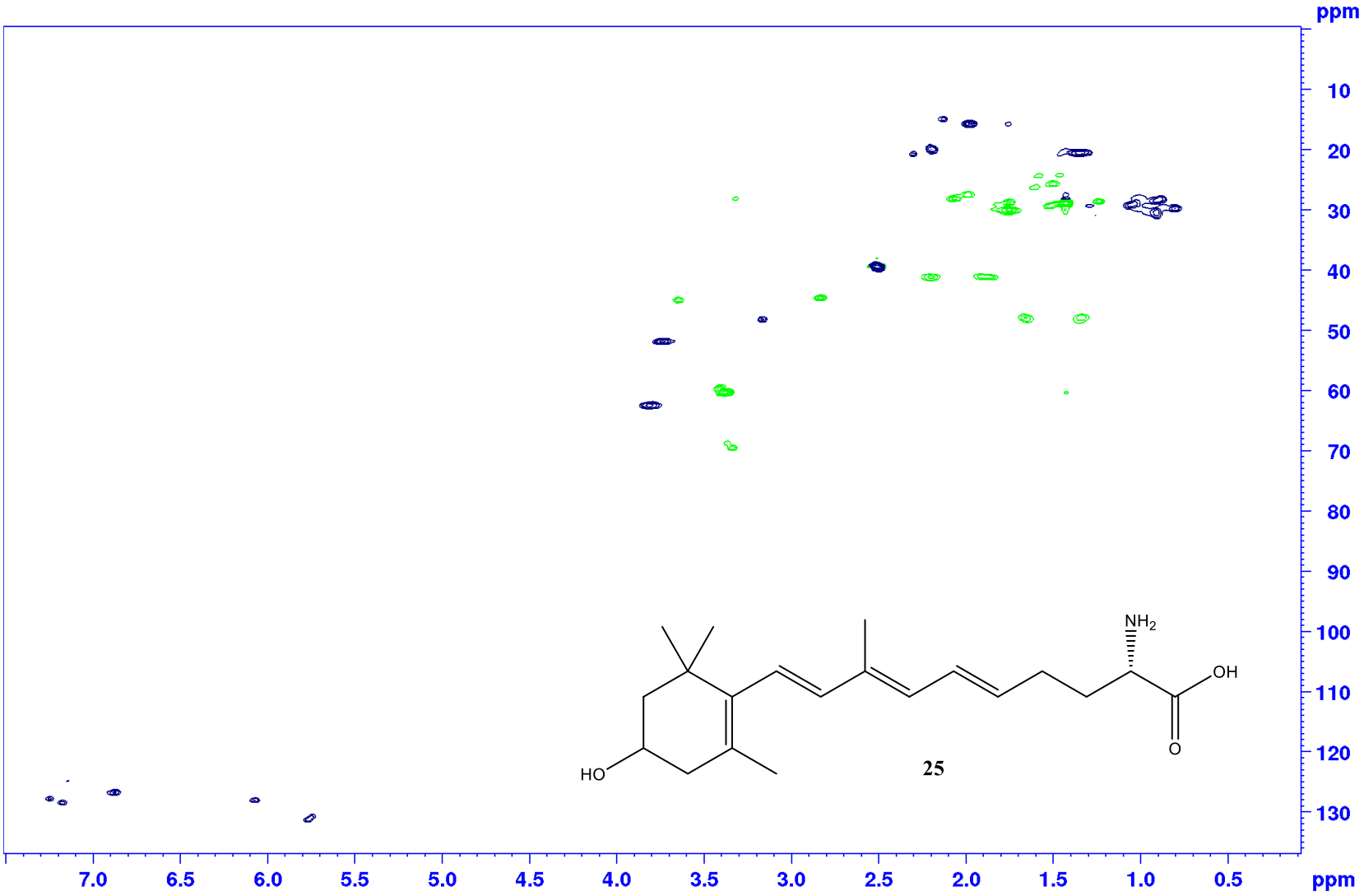

Figure xlvii: HSQC (600 MHz, d_6-DMSO)

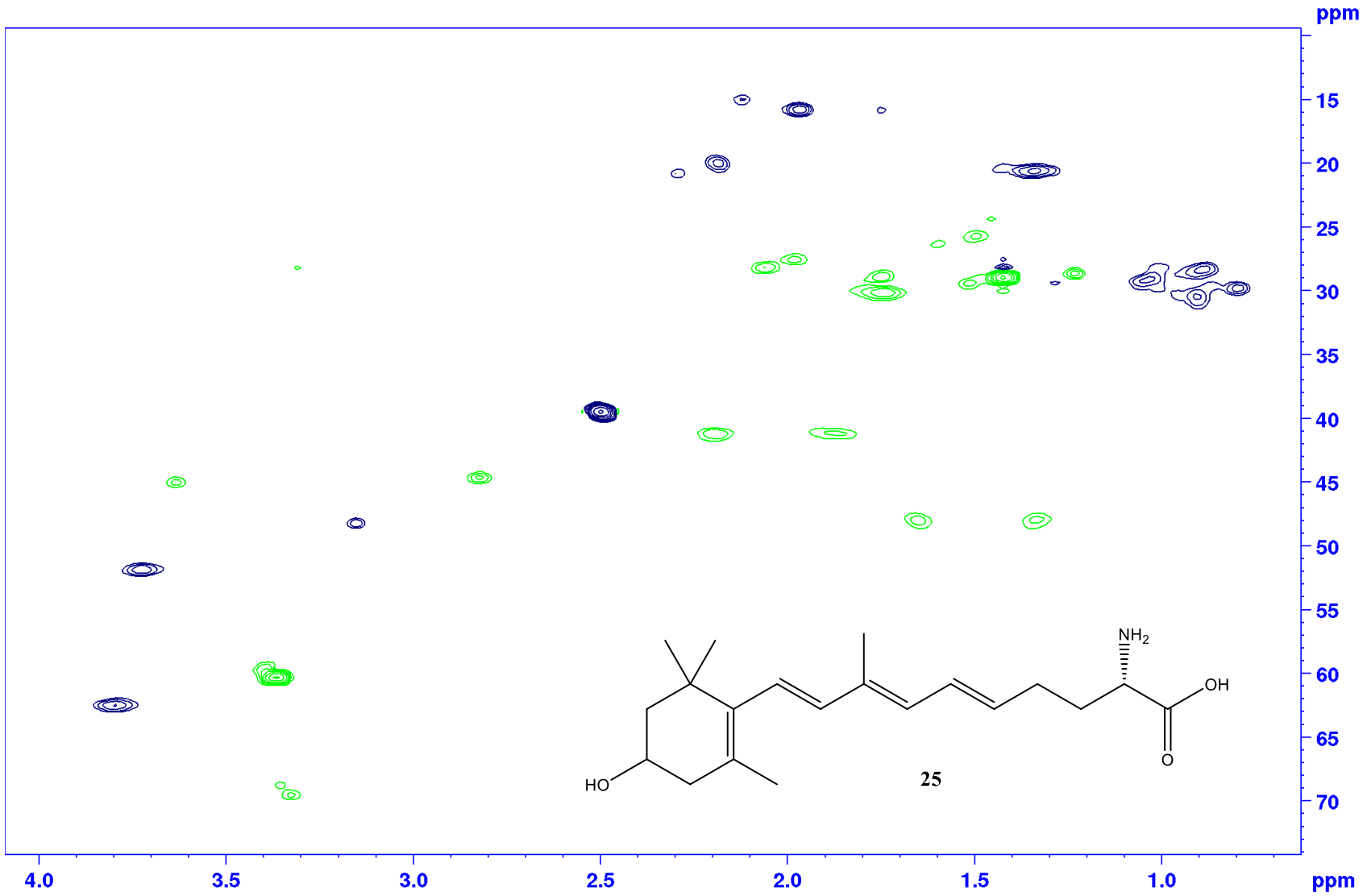

Figure xlviii: Excerpt of HSQC(600 MHz, d_6-DMSO)

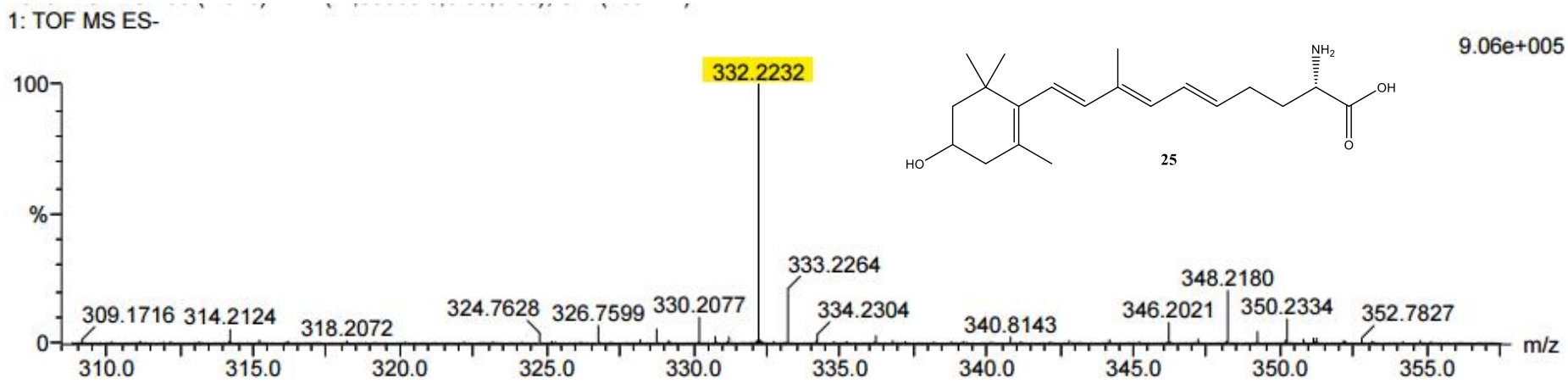

Minimum:				-1.5				
Maximum:		5.0	2.0	50.0				
Mass	Calc. Mass	mDa	PPM	DBE	i-FIT	Norm	Conf(%)	Formula
332.2232	332.2226	0.6	1.8	6.5	1347.6	0.000	100.00	C20 H30 N O3 ion observed [M-H]
	332.2231	0.1	0.3	-0.5	1360.1	12.463	0.00	C5 H26 N13 O4

Figure xlix: ESI-Q-TOF

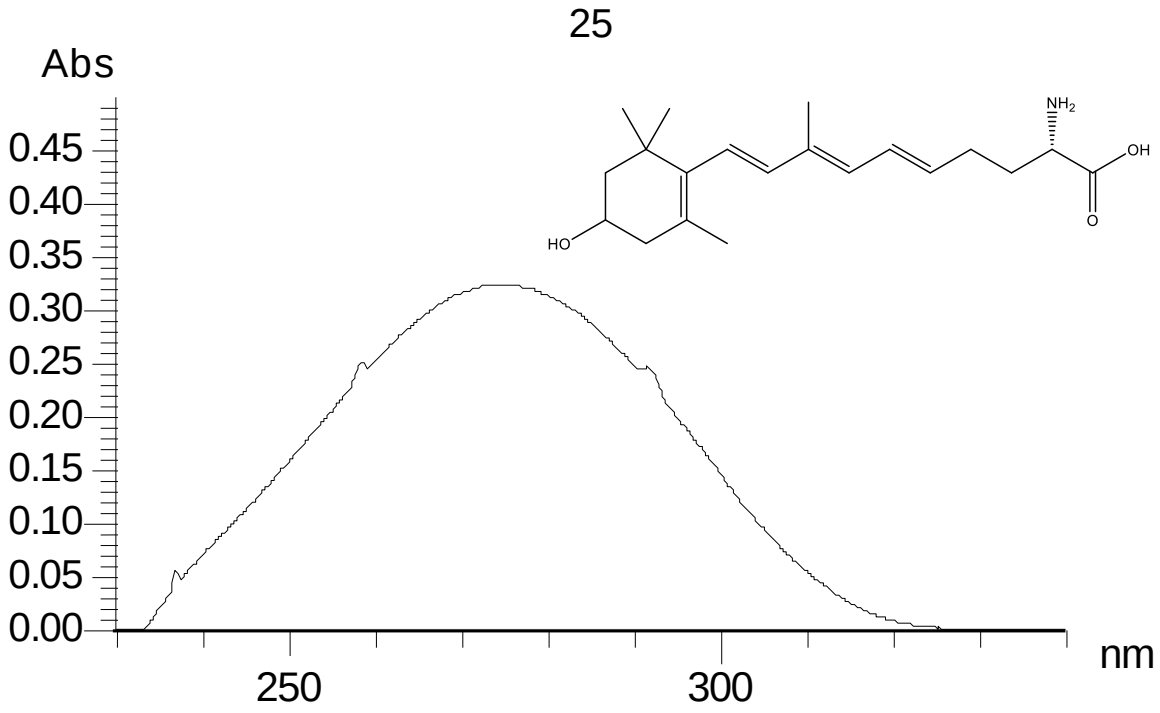

Figure l: UV/vis absorption spectre (DCM)

Peak #	Start (nm)	Apex (nm)	End (nm)	Height (Abs)	Valley (nm)	Valley (Abs)
1	400.0	275.0	219.0	0.323	219.0	-29.040

Table xvii: UV/vis absorption data (DCM)